AD-A050 214 NAVAL POSTGRADUATE SCHOOL MONTEREY CALIF F/G 1/3
THE FEASIBILITY OF THE JET-FLAP ROTOR AS A LIFT GENERATOR FOR V--ETC(U)
DEC 77 J C BALL

UNCLASSIFIED NL

1 OF 2
AD
A050 214

AD A050214

AD No. ____
DDC FILE COPY

NAVAL POSTGRADUATE SCHOOL
Monterey, California

DDC
RECEIVED
FEB 22 1978
D

(9) Master's THESIS

(6) THE FEASIBILITY OF THE JET-FLAP ROTOR AS A LIFT GENERATOR FOR VERTICAL TAKEOFF AND LANDING AIRCRAFT.

by

(10) John Charles Ball

(12) 132 p.

(11) December 1977

Thesis Advisor: M.F. Platzer

Approved for public release; distribution unlimited.

151450

SECURITY CLASSIFICATION OF THIS PAGE (When Data Entered)

REPORT DOCUMENTATION PAGE

READ INSTRUCTIONS BEFORE COMPLETING FORM

1. REPORT NUMBER	2. GOVT ACCESSION NO. / 3. RECIPIENT'S CATALOG NUMBER
4. TITLE (and Subtitle): The Feasibility of the Jet-Flap Rotor as a Lift Generator for Vertical Takeoff and Landing Aircraft	5. TYPE OF REPORT & PERIOD COVERED: Master's Thesis; December 1977
	6. PERFORMING ORG. REPORT NUMBER
7. AUTHOR(s): John Charles Ball	8. CONTRACT OR GRANT NUMBER(s)
9. PERFORMING ORGANIZATION NAME AND ADDRESS: Naval Postgraduate School, Monterey, California 93940	10. PROGRAM ELEMENT, PROJECT, TASK AREA & WORK UNIT NUMBERS
11. CONTROLLING OFFICE NAME AND ADDRESS: Naval Postgraduate School, Monterey, California 93940	12. REPORT DATE: December 1977
	13. NUMBER OF PAGES: 133
14. MONITORING AGENCY NAME & ADDRESS(if different from Controlling Office)	15. SECURITY CLASS. (of this report): Unclassified
	15a. DECLASSIFICATION/DOWNGRADING SCHEDULE

16. DISTRIBUTION STATEMENT (of this Report)

Approved for public release; distribution unlimited.

17. DISTRIBUTION STATEMENT (of the abstract entered in Block 20, if different from Report)

18. SUPPLEMENTARY NOTES

19. KEY WORDS (Continue on reverse side if necessary and identify by block number)

Jet Flap
Jet-Flap Rotor
Lift Generator
Rotor

20. ABSTRACT (Continue on reverse side if necessary and identify by block number)

The objectives of this study were first to determine the effectiveness of the jet-flap rotor relative to other lift generators, and second to examine the potential effectiveness of the jet-flap rotor in a tactical VTOL aircraft.

It was found that the jet-flap rotor has a high theoretical potential, but at present is the least-developed of the lift generators considered. The jet-flap rotor was

DD FORM 1 JAN 73 1473 (Page 1) EDITION OF 1 NOV 65 IS OBSOLETE S/N 0102-014-6601

SECURITY CLASSIFICATION OF THIS PAGE (When Data Entered)

(20. ABSTRACT continued)

found to be unattractive as a means of providing vertical lift, except when a long hover duration is necessary.

With regard to weight considerations alone, the jet-flap rotor was found to be inadvisable for use in a tactical VTOL aircraft. However, its benign downwash characteristics could make the jet-flap rotor advantageous if high downwash velocities and temperatures could not be tolerated.

Approved for public release; distribution unlimited.

The Feasibility of the Jet-Flap Rotor as a Lift Generator for Vertical Takeoff and Landing Aircraft

by

John Charles Ball
Lieutenant, United States Navy
B.S.A.E., United States Naval Academy, 1971

Submitted in partial fulfillment of the requirements for the degree of

MASTER OF SCIENCE IN AERONAUTICAL ENGINEERING

from the

NAVAL POSTGRADUATE SCHOOL
December 1977

DDC
RECEIVED
FEB 22 1978
D

Author John C Ball

Approved by: M. F. Platzer
Thesis Advisor

Second Reader

Chairman, Department of Aeronautics

George J. Haltiner
Dean of Science and Engineering

ACCESSION for
NTIS White Section
DDC Buff Section
UNANNOUNCED
JUSTIFICATION
BY
DISTRIBUTION/AVAILABILITY CODES
Dist. AVAIL. and/or SPECIAL
A

ABSTRACT

The objectives of this study were first to determine the effectiveness of the jet-flap rotor relative to other lift generators, and second to examine the potential effectiveness of the jet-flap rotor in a tactical VTOL aircraft.

It was found that the jet-flap rotor has a high theoretical potential, but at present is the least-developed of the lift generators considered. The jet-flap rotor was found to be unattractive as a means of providing vertical lift, except when a long hover duration is necessary.

With regard to weight considerations alone, the jet-flap rotor was found to be inadvisable for use in a tactical VTOL aircraft. However, its benign downwash characteristics could make the jet-flap rotor advantageous if high downwash velocities and temperatures could not be tolerated.

TABLE OF CONTENTS

I. INTRODUCTION ---------- 15

II. VTOL CONCEPTS AND AIRCRAFT ---------- 17

A. BASIC RELATIONS ---------- 17

B. LIFT AMPLIFICATION ---------- 23

C. VTOL AIRCRAFT CONFIGURATIONS ---------- 31

D. TRANSITION FLIGHT ---------- 31

E. CRUISE FLIGHT ---------- 37

F. CONTROL SYSTEMS ---------- 39

G. INTERACTION PROBLEMS ---------- 41

1. Interactions Out of Ground Effect -------- 41

2. Ground Intereference Effects ---------- 42

a. Ground Effect ---------- 42

b. Fountain Effect ---------- 42

c. Recirculation ---------- 44

d. Ground Erosion ---------- 44

e. Reingestion ---------- 44

III. THE JET FLAP ---------- 46

A. BOUNDARY LAYER CONTROL ---------- 46

B. SUPERCIRCULATION ---------- 46

C. JET FLAP BASICS ---------- 48

1. Description ---------- 48

2. Principle of the Jet Flap ---------- 48

3. Configurations ---------- 51

4. Characteristics ---------- 51

IV. THE JET-FLAP ROTOR ---------- 56

A. INTRODUCTION ---------- 56

B. DESCRIPTION ---------- 56

C. CHARACTERISTICS ---------- 58

D. PROPULSION REQUIREMENTS ---------- 58

E. PROPULSIVE EFFICIENCY ---------- 59

1. Hot Cycle ---------- 59

2. Cold Cycle ---------- 62

3. Overall Comparison ---------- 62
F. TIP-JET PROPULSION ---------- 62
G. JET-FLAP ROTOR EXPERIMENTS ---------- 63
V. STOWABLE ROTOR AIRCRAFT ---------- 67
A. GENERAL ---------- 67
B. A JET-FLAP STOWABLE ROTOR AIRCRAFT ---------- 69
VI. JET-FLAP ROTOR HOVER ANALYSIS ---------- 75
A. BACKGROUND ---------- 75
B. GENERAL DESCRIPTION ---------- 75
C. ASSUMPTIONS ---------- 76
D. PROGRAM VALIDATION ---------- 78
VII. LIFT GENERATOR COMPARISONS ---------- 79
A. LIFT GENERATOR TYPES ---------- 79
1. Lift Engines ---------- 79
a. Description ---------- 79
b. Examples ---------- 79
c. Development ---------- 80
d. Advantages and Disadvantages ---------- 80
2. Lift Fans ---------- 82
a. Description ---------- 82
b. Examples ---------- 82
c. Development ---------- 82
d. Advantages and Disadvantages ---------- 83
3. Rotors ---------- 83
a. Description ---------- 83
b. Examples ---------- 83
c. Development ---------- 83
d. Advantages and Disadvantages ---------- 85
4. Ejectors ---------- 85
a. Description ---------- 85
b. Examples ---------- 87
c. Development ---------- 89
d. Advantages and Disadvantages ---------- 89
B. LIFT GENERATORS AS AUXILIARY LIFT DEVICES ---- 90
1. Introduction ---------- 90
2. Assumptions ---------- 91
3. Computations ---------- 91

a. Lift Engines ---------- 91
b. Lift Fans ---------- 92
c. Jet-Flap Rotor ---------- 92
4. Fuel Consumption Analysis ---------- 93
5. Weight Analysis ---------- 95
6. Summary ---------- 98
C. LIFT GENERATORS AS PRIMARY LIFT DEVICES ------ 98
1. Introduction ---------- 98
2. Assumptions ---------- 98
3. Computations ---------- 99
a. Lift Engines ---------- 99
b. Lift Fans (Integral) ---------- 99
c. Lift Fans (Tip-Driven) ---------- 99
d. Ejectors ---------- 100
e. Vectored Thrust ---------- 100
f. Jet-Flap Rotor ---------- 100
4. Fuel Consumption Analysis ---------- 100
5. Weight Analysis ---------- 100
6. Summary ---------- 104
D. DISCUSSION ---------- 104
VIII. CONCLUSIONS ---------- 108
APPENDIX A JET-FLAP ROTOR THEORY ---------- 109
APPENDIX B COMPUTER PROGRAM DESCRIPTION ---------- 119
APPENDIX C SAMPLE CALCULATIONS ---------- 123
COMPUTER OUTPUT ---------- 126
COMPUTER PROGRAM ---------- 127
LIST OF REFERENCES ---------- 131
INITIAL DISTRIBUTION LIST ---------- 133

LIST OF FIGURES

1. The hovering rotor ---------- 18
2. Downwash velocity as a function of disc loading -- 21
3. Lift efficiency as a function of downwash velocity ---------- 22
4. Thrust generators for hovering ---------- 24
5. Thrust augmentation as a function of slipstream velocity and bypass ratio ---------- 26
6. Specific fuel consumption and engine thrust/weight ratios as a function of slipstream velocity ---------- 28
7. Hovering and cruise performance of VTOL systems -- 29
8. Relative component weights of VTOL aircraft ------ 30
9. VTOL configurations ---------- 32
10. Typical VTOL power required curve ---------- 35
11. Power required during transition flight ---------- 36
12. Equivalent lift-to-drag ratios for various configurations ---------- 38
13. Various types of control methods for hovering and transition ---------- 40
14. Hovering flow field features ---------- 43
15. Effect of aircraft attitude on fountain impingement ---------- 43
16. Recirculation flow fields ---------- 45
17. Boundary layer control by blowing prevents separation ---------- 47
18. Effect on lift coefficient of blowing ---------- 49
19. Jet flap analogy with mechanical flap ---------- 50
20. Practical jet flap concepts ---------- 52
21. Total lift coefficient as a function of incidence and jet deflection angle ---------- 53
22. Total lift coefficient as a function of incidence and jet deflection angle ---------- 54
23. Jet flap for a rotor ---------- 57
24. Jet-flap rotor capability ---------- 57
25. Gas generator performance ---------- 61
26. Ideal rotor drive system efficiency for mixed cycle ---------- 61
27. The DH2011 rotor blade ---------- 65

28. The DH2011 jet flap ---------- 65
29. Jet-flap rotor force capability ---------- 66
30. Typical aircraft lift/drag ratios ---------- 68
31. A jet-flap stowable-rotor aircraft ---------- 70
32. Jet-flap rotor cascades ---------- 72
33. Pressure ratio optimization ---------- 72
34. Advantages of the jet-flap rotor ---------- 74
35. Rotor momentum coefficient as a function of jet deflection angle ---------- 77
36. Thrust-to-weight trends in engine development ---- 81
37. Rolls-Royce lift engine trends ---------- 81
38. Lift engine and lift fan characteristics --------- 84
39. Simple ejector schematic ---------- 86
40. Lockheed XV-4A ejector system ---------- 86
41. Ejector design of the XFV-12A ---------- 88
42. Fuel consumption of aircraft with auxiliary lift devices ---------- 94
43. Total lift system weight as a function of hover time for aircraft with auxiliary lift devices ---------- 96
44. Relative component weights for aircraft using auxiliary lift devices ---------- 97
45. Fuel consumption for primary lift generators ----- 101
46. Total system weight as a function of hover time for aircraft with primary lift devices ---------- 103
47. Potential of lift systems ---------- 106
48. The blade element concept ---------- 110
49. Sign conventions for blade element (positive as shown) ---------- 111
50. Elementary ring of rotor disc ---------- 115
51. Jet-flap rotor hover analysis computer program flowchart ---------- 120

LIST OF SYMBOLS

A	area of rotor disc
A'	total internal flow area of all blades
$\overline{A_0}$	collective jet deflection
AR	aspect ratio
a	sectional lift curve slope
a_∞	speed of sound in ambient air
$\overline{B_1}$	cyclic jet deflection
BPR	bypass ratio
b	number of blades
b_w	wing span
C_D	aircraft drag coefficient
C_{D_i}	aircraft induced drag coefficient
C_{D_o}	aircraft profile drag coefficient
C_j	jet momentum coefficient
$\overline{C_j}$	mean jet-flap momentum coefficient
$C_{j_{CRIT}}$	critical jet momentum coefficient
$C^*_{j_f}$	total jet-flap momentum parameter
C_{j_R}	rotor jet momentum coefficient
C_L	aircraft lift coefficient
C_{M_G}	exhaust mass flow coefficient
C_Q	shaft torque coefficient
C^*_Q	rotor torque parameter

C_{Q_t}	net tip-jet torque coefficient
C_T	thrust coefficient
C_{x_R}	rotor propulsion force coefficient
c	blade chord
c_d	total section drag coefficient
c_{d_o}	drag coefficient due to section shape (no jet effects)
c_{j_f}	local jet-flap momentum coefficient
c_l	total section lift coefficient
c_{l_o}	lift coefficient due to section shape (no jet effects)
D	total aircraft drag
D_h	ducting hydraulic diameter
D_i	induced drag
D_p	profile drag
D.L.	disc loading
d	local section drag per unit span
E_G	ideal gas energy available at gas generator exhaust
e	wing efficiency factor
g	acceleration of gravity
H	gas generator work output parameter
K	design parameter
K_T	pressure loss parameter, difference between pressure at gas generator and rotor nozzle, divided by the dynamic pressure in the blade
L	total aircraft lift

l	total section lift per unit span
$(L/D)_e$	equivalent lift/drag ratio
M	figure of merit
M_G	exhaust mass flow rate
M_j	total mass flow rate through blades
$\dot{m}$	mass flow rate
P	total power required
P_h	power required for hovering
P_i	power required due to induced drag
P_{id}	ideal power required from momentum theory
P_p	power required due to profile drag
P_{o_3}/P_{o_4}	compressor pressure ratio
p	static pressure
Q	rotor shaft torque
Q_t	net tip-jet output torque
q	dynamic pressure
q_b	bypass mass flow generated by fan or rotor
q_l	local dynamic pressure
q_t	mass flow through turbine
R	rotor radius
r	radial distance along blade from hub
S	wing area
SFC	specific fuel consumption
S.P.	specific power

s_d	supercirculation thrust parameter
s_l	supercirculation lift parameter
T	thrust
T_t	thrust generated by turbine
T_{o_4}	turbine inlet temperature
u	resultant velocity of Ωr and v_r
V	free-stream velocity
V_j	jet exhaust velocity
V_N	velocity in ejector nozzle with shroud
V_N'	velocity in ejector nozzle without shroud
V_R	vertical velocity at rotor in hover
V_s	slipstream velocity
V_t	rotor tip speed
V_u	ultimate velocity downstream of hovering rotor
v	local induced velocity
W	aircraft weight
X	propulsive force of rotor
x	dimensionless radial station, r/R
x_i	inner limit of blade integration
x_o	outer limit of blade integration
α	blade angle of attack
ΔV	velocity change
Δx_j	spanwise extent of slot in terms of x
δ	jet deflection angle

η	overall propulsion efficiency
η_a	bypass aerodynamic efficiency
η_g	gearing efficiency
η_R	rotor drive system efficiency
η_{th}	gas generator thermal efficiency
η_t	power turbine efficiency
θ	local blade pitch angle
θ_o	collective blade pitch at 0.75R
θ_t	blade washout
ρ	free-stream air dersity
σ	solidity
Φ	augmentation ratic
ϕ	local velocity inflcw angle
Ψ	blade azimuth angle
Ω	rotor rotational speed
Ωr	velocity at blade station r, perpendicular tc tip path plane

SUBSCRIPTS

r	radial station r
x	dimensionless radial station r/R
o	airfoil alone (as applied to L, D, C_d, C_ℓ)
j	jet influence (as applied to L, D, C_d, C_ℓ)

I. INTRODUCTION

The present naval interest in VTOL (vertical takeoff and landing) aircraft is based on requirements for tactical aircraft able to conduct operations without the benefit of runways or conventional aircraft carriers. Various VTOL configurations are now in the design or development stages. These configurations incorporate various means of providing a vertical lift capability.

The jet-flap rotor, although it holds many advantages as a lift generator, has not recently been proposed for use in a VTOL tactical aircraft. The purpose of this study was to examine the feasibility of using a jet-flap rotor to provide VTOL capability for a tactical aircraft. Specifically, the jet-flap rotor was envisioned as being incorporated in a stowable rotor aircraft.

The objectives of this study were first to determine the effectiveness of the jet-flap rotor relative to other lift generators, and second to examine the potential effectiveness of the jet-flap rotor in a tactical VTOL aircraft.

Section II contains an overview of VTOL technology in order to acquaint the reader with the important concepts peculiar to VTOL aircraft.

Section III presents a description of the jet flap itself and its characteristics.

The jet flap is extended to rotor applications in Section IV. A description of the jet-flap rotor and its characteristics is presented. Rotor propulsion methods, efficiency, and requirements are described. Finally, jet-flap rotor experiments are summarized.

The application of the jet-flap rotor in a stowable rotor aircraft is described in Section V, including a detailed description of a proposed design.

Section VI describes the jet-flap rotor hover analysis and the computer program used to determine the air mass flow requirements.

Section VII examines the jet-flap rotor and other lift generators both as auxiliary and as primary lifting devices. A determination is made of the relative effectiveness of the jet-flap rotor on the basis of fuel consumption, weight, and other factors.

Finally, conclusions are made concerning the potential of the jet-flap rotor for use in a VTOL aircraft.

Included in appendixes are a detailed description of the jet-flap rotor theory and the computer program, as well as sample calculations used in the determination of mass flow requirements for the jet-flap rotor.

II. VTOL CONCEPTS AND AIRCRAFT

A. BASIC RELATIONS

Consider a rotor in a steady-state hover, so that the upward thrust produced by the rotor equals the weight. The surrounding air is influenced by the rotor as shown in Figure 1.

The momentum theory of lift stems from Newton's second law of motion, F=ma. The force, here the upward thrust, produced by the rotor is equal to the mass of air passing through the rotor per unit time, multiplied by the increase in velocity of the air caused by the rotor.

The momentum theory assumes the rotor is an actuator disc, infinitely thin and composed of an infinite number of blades. Across the actuator disc there is assumed to be an instantaneous change in pressure but no discontinuities in velocity. As shown in Figure 1, the airflow forms a streamtube, and no flow is assumed to pass through the boundary.

At an infinite distance upstream of the disc, the velocity of the air is zero and the static pressure is equal to the total pressure. At a distance downstream, the velocity converges to a value V_w and the static pressure once again converges to the total pressure.

Since a pressure discontinuity exists at the disc, Bernoulli's equation must be applied both above and below the disc.

Applying Bernoulli's equation from ⓪ to ①,

$$p_0 = p_1 + \tfrac{1}{2}\rho V_R^2 \qquad (1)$$

and from ② to ③,

$$p_2 + \tfrac{1}{2}\rho V_R^2 = p_0 + \tfrac{1}{2}\rho V_w^2 \qquad (2)$$

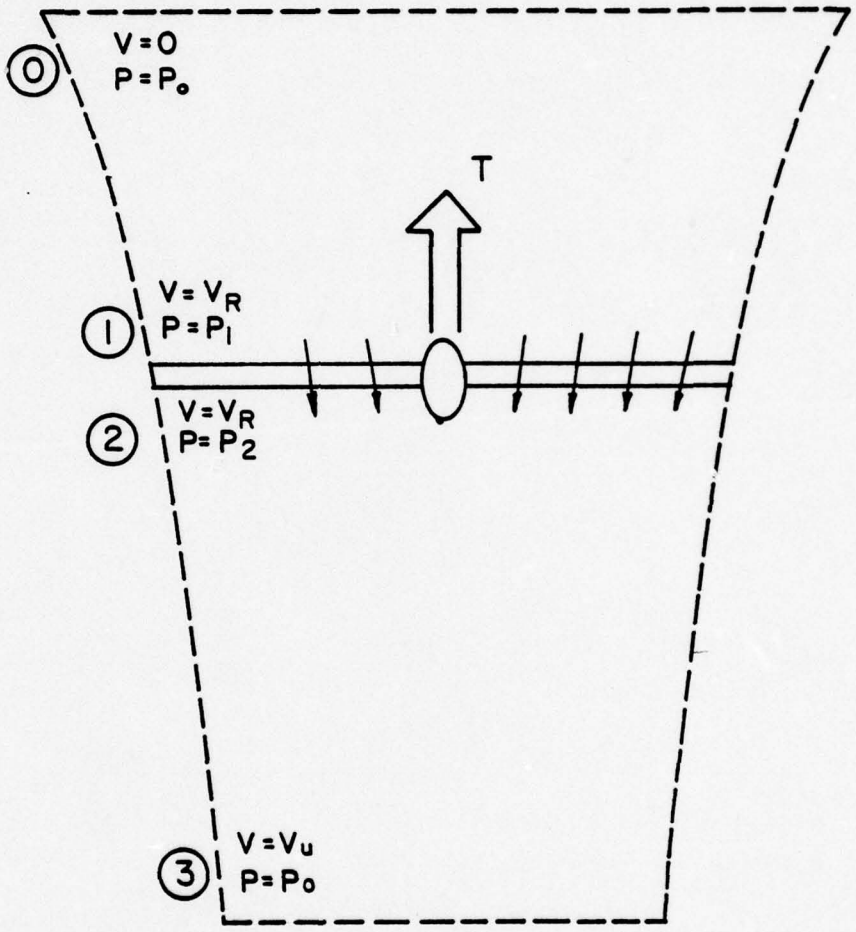

Figure 1.
The hovering rotor.

The pressure change across the disc, by combining equations (1) and (2), is

$$p_2 - p_1 = \tfrac{1}{2} \rho V_w^2 \tag{3}$$

From Newton's second law, the thrust produced by the disc can be expressed as

$$T = \dot{m} \Delta V \tag{4}$$

where $\dot{m}$ is the mass flow rate of air passing through the disc, and ΔV is the velocity change from the upper boundary ① to the lower boundary ③.

For a disc of radius R,

$$\dot{m} = \rho A V_R = \rho \pi R^2 V_R$$

so that from equation (4),

$$T = \rho \pi R^2 V_R V_w \tag{5}$$

The force developed by the rotor disc can also be expressed as the pressure difference across the disc multiplied by the disc area. Thus,

$$T = \pi R^2 (p_2 - p_1) \tag{6}$$

Substituting equation (3) yields,

$$T = \tfrac{1}{2} \pi R^2 \rho V_w^2 \tag{7}$$

Equating the right-hand sides of equations (5) and (7), it is seen that

$$V_R = \tfrac{1}{2} V_w \tag{8}$$

or,

$$V_w = 2 V_R \tag{9}$$

Thus the ultimate velocity downstream of the disc is twice the velocity at the disc.

From equation (7) the ultimate, or downwash, velocity is given by

$$V_u = \sqrt{\frac{2T}{\rho \pi R^2}} \tag{10}$$

Disc loading is defined as

$$D.L. = \frac{T}{\pi R^2}$$

and since in a hover, thrust equals weight, equation (10) becomes

$$V_u = \sqrt{\frac{2\,D.L.}{\rho}} \tag{11}$$

Thus the downwash velocity is a function of the disc loading. This relationship is shown in Figure 2.

The ideal power required by the rotor disc is defined as

$$P_{id} = T V_R \tag{12}$$

Since $V_R = \frac{1}{2} V_u$, then the ideal power is given by

$$P_{id} = \frac{T V_u}{2} \tag{13}$$

Rearranging, the specific thrust T/P_{id} is given by

$$\frac{T}{P_{id}} = \frac{2}{V_u} \tag{14}$$

Specific thrust is a measure of hover efficiency, since for a given power input a high specific thrust indicates a high thrust output. Thus, for hovering efficiency it is necessary to have a low V_u, that is to accelerate slowly a large mass of air. This relationship is shown in Figure 3.

The previous analysis used the assumptions of the momentum theory, which neglected such effects as:

(1) blade profile drag

(2) non-uniform inflow over the disc

(3) pressure losses at the blade tips

(4) interaction of the induced air and surrounding air.

Thus, the momentum theory represents the ideal case for hover.

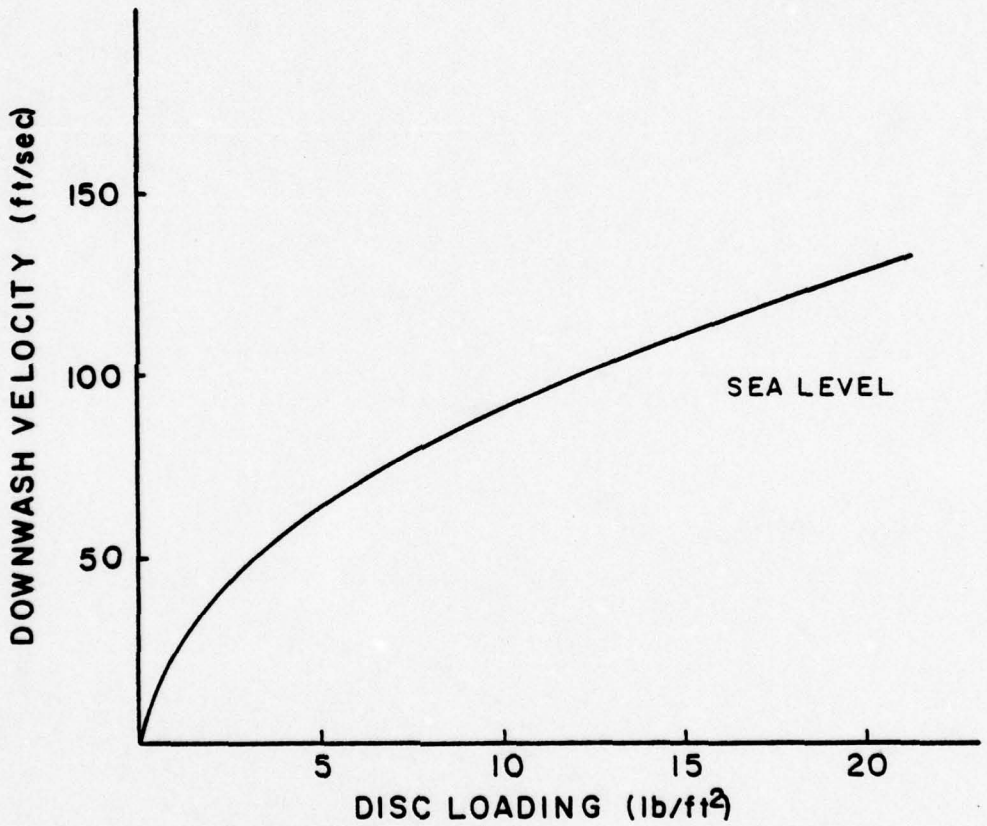

Figure 2.

Downwash velocity as a function of disc loading.

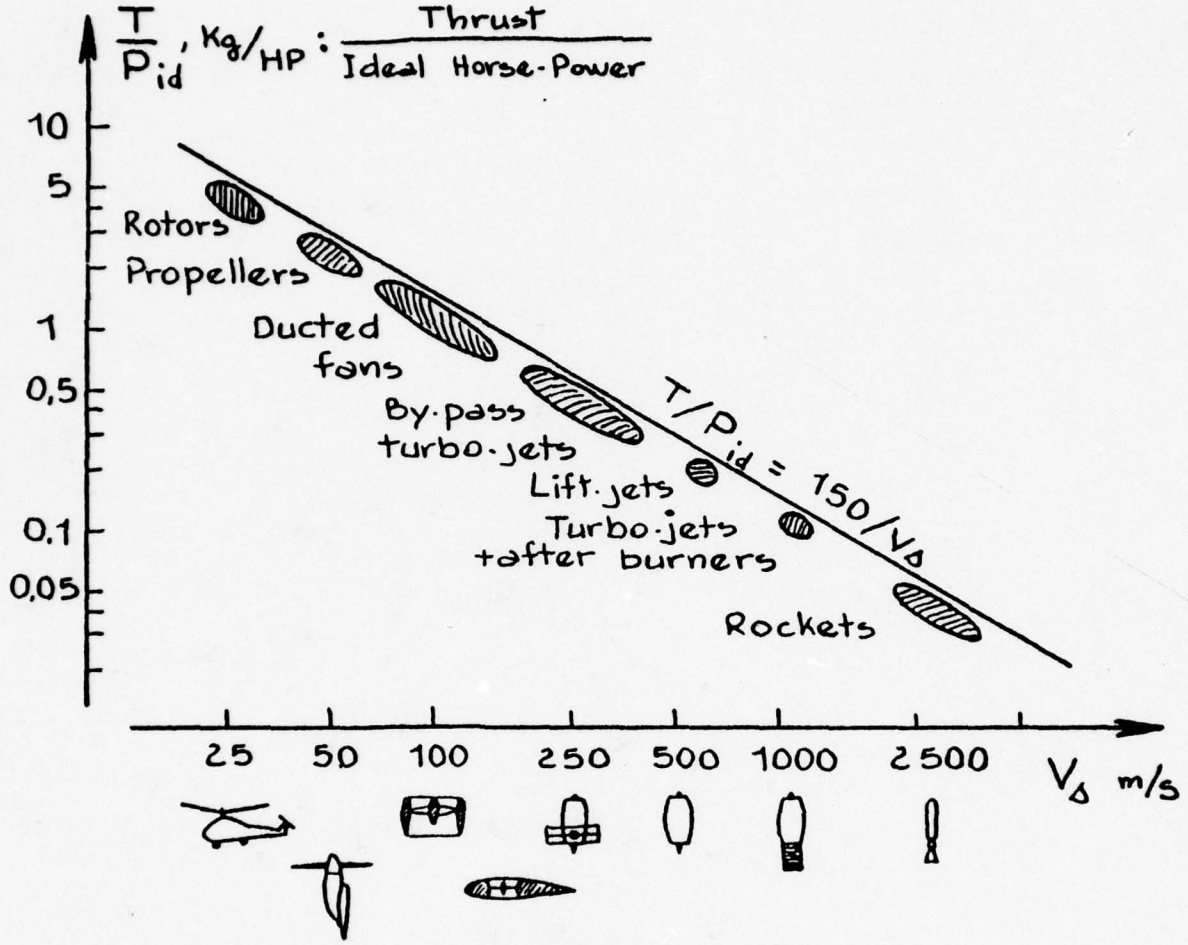

Figure 3.

Lift efficiency as a function of downwash velocity. (Ref. 1)

The classical measure of rotor hovering efficiency is the figure of merit, defined as the ratio of the ideal power required (using momentum theory) to the actual power required. Thus,

$$M = \frac{P_{id}}{P} = \frac{\text{IDEAL POWER}}{\text{ACTUAL POWER}}$$

Since the ideal power required from momentum theory ignores blade profile drag, whereas the actual power required necessarily includes it, then the figure of merit will always be less than one. The other assumptions of the momentum theory also account for the discrepancy between ideal and actual power required, so that a typical helicopter figure of merit is 0.75.

B. LIFT AMPLIFICATION

As mentioned in Ref. 1, there are three major methods for amplification of the thrust of a gas generator:

(1) Reheating the exhaust gases to increase the exit velocity (i.e. afterburner).

(2) Using the exhaust gases as the primary flux in an ejector.

(3) Using the gas generator to drive a fan or rotor.

The use of reheat is an inefficient process due to the high fuel consumption, and is impractical for a VTOL aircraft near the ground due to the high exhaust temperatures and velocities.

The ejector system, used on the Lockheed XV-4A and the Rockwell XFV-12A, appears to be an elegant process. However, with a thrust augmentation of 1.5 at best, the process is not very efficient, and it is relatively voluminous.

The third method, the use of a bypass system, is the most efficient and most widely used. In Figure 4 the same gas generator is used in three ways: as a lift engine itself; to drive a turbine connected to a ducted fan; and to drive a turbine connected to a rotor.

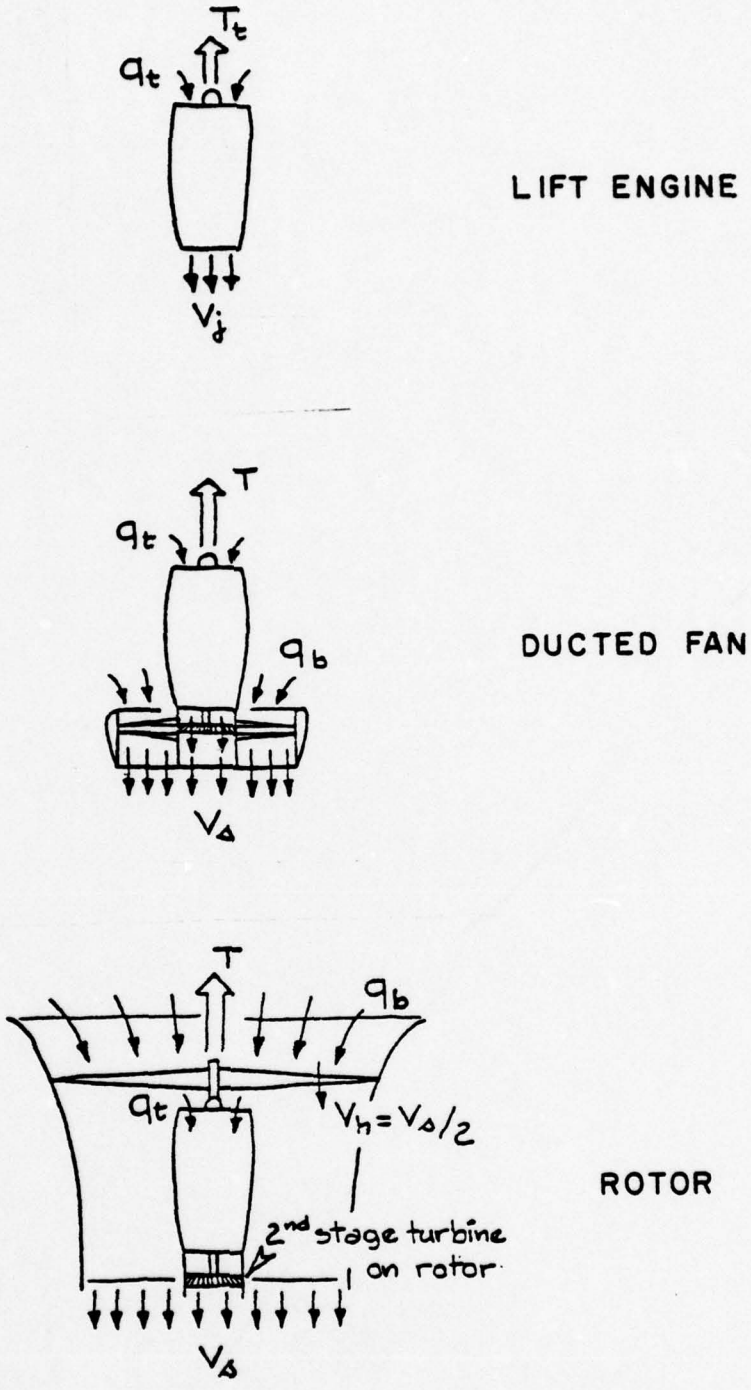

Figure 4.
Thrust generators for hovering.

The thrust generated by the basic turbine is given by

$$T_t = q_t V_j \tag{15}$$

where q_t is the mass flow through the turbine and V_j is the turbine exit velocity.

The thrust produced by the bypass system is given by

$$T = (q_b + q_t) V_s \tag{16}$$

where q_b is the bypass mass flow generated by the fan or rotor and V_s is the slipstream velocity. The simplifying assumption has been made that $V_s = V_j$.

The thrust augmentation is defined as the ratio of the total thrust to the basic turbine thrust. By combining equations (15) and (16), it can be expressed as

$$\frac{T}{T_t} = \left(1 + \frac{q_b}{q_t}\right) \frac{V_s}{V_j} \tag{17}$$

The bypass ratio is the ratio of mass flow rates of the bypass air to the turbine air. That is

$$BPR = \frac{q_b}{q_t}$$

From equation (17) it is seen that the thrust augmentation is a function of the bypass ratio and the slipstream velocity.

If the power turbine efficiency η_t and the bypass aerodynamic efficiency η_a are introduced, then from equation (17),

$$\frac{q_b}{q_t} = \eta_t \cdot \eta_a \left[\left(\frac{V_j}{V_s}\right)^2 - 1\right] \tag{18}$$

These relationships are plotted in Figure 5, using a jet exhaust velocity of 2000 fps from the turbine, and power turbine and bypass aerodynamic efficiencies of 0.85.

From these graphs it is evident that, in order to obtain a high thrust augmentation, it is necessary to have a high bypass ratio which therefore results in a low downwash velocity.

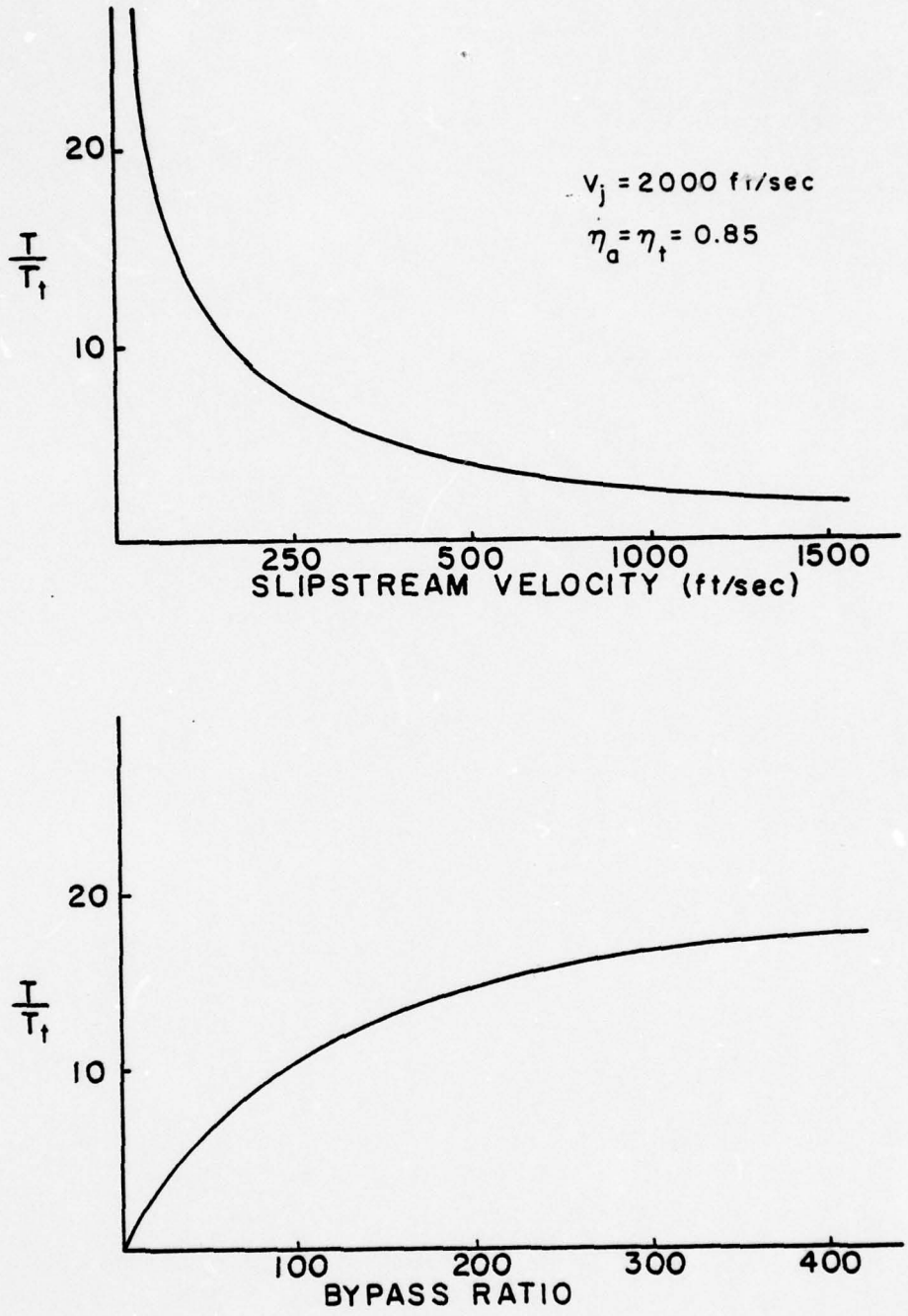

Figure 5.

Thrust augmentation as a function of slipstream velocity and bypass ratio.

Thus a rotor with V_s = 100 fps has a bypass ratio of 290 and a thrust augmentation of 15. A ducted fan with V_s = 500 fps has a bypass ratio of 12 and a thrust augmentation of 3.

It is thus evident that a high bypass ratio is necessary to achieve significant thrust augmentation. For example, a bypass ratio of 5 is necessary to produce a thrust augmentation of only 2.

A criterion of efficiency in VTOL aircraft is the fuel consumption during hover. Poisson-Quinton in Ref. 1 calculated the specific fuel consumption (SFC = fuel flow/thrust) as a function of slipstream velocity. The general trend in Figure 6 shows that specific fuel consumption increases as slipstream velocity increases. For example, a ducted fan with V_s = 500 fps has a SFC = 0.3, while a lift jet engine with V_s = 2000 fps has a SFC = 1.0.

However, fuel consumption itself is not an accurate measure of hovering efficiency. The weight and volume of the entire lifting system must be considered. Thus, the useful efficiency of a lifting system is measured by the ratio (thrust)/(engine weight + hover fuel) as a function of hover duration. Figure 6 shows the trend of thrust/engine weight as a function of slipstream velocity. It is seen that the lift engine has a higher thrust-to-weight ratio than a rotor, but it must be remembered that the lift engine has a much higher specific fuel consumption.

Thus the lift engine with its high thrust-to-weight ratio has a lower total weight (engine weight + fuel), if the hover time is short. However, the rotor with its low fuel consumption will have a lower total weight, if the hover time is large. This is shown in Figure 7 as general trends for various VTOL vehicles. Figure 7 also shows the trend of hovering time for a given percentage of fuel as a function of cruise speed.

Figure 8 graphically depicts the problem for a transport VTOL aircraft, whose mission requires 8 minutes of hover and 1.5 hours of cruise. In going from the helicopter to a lift

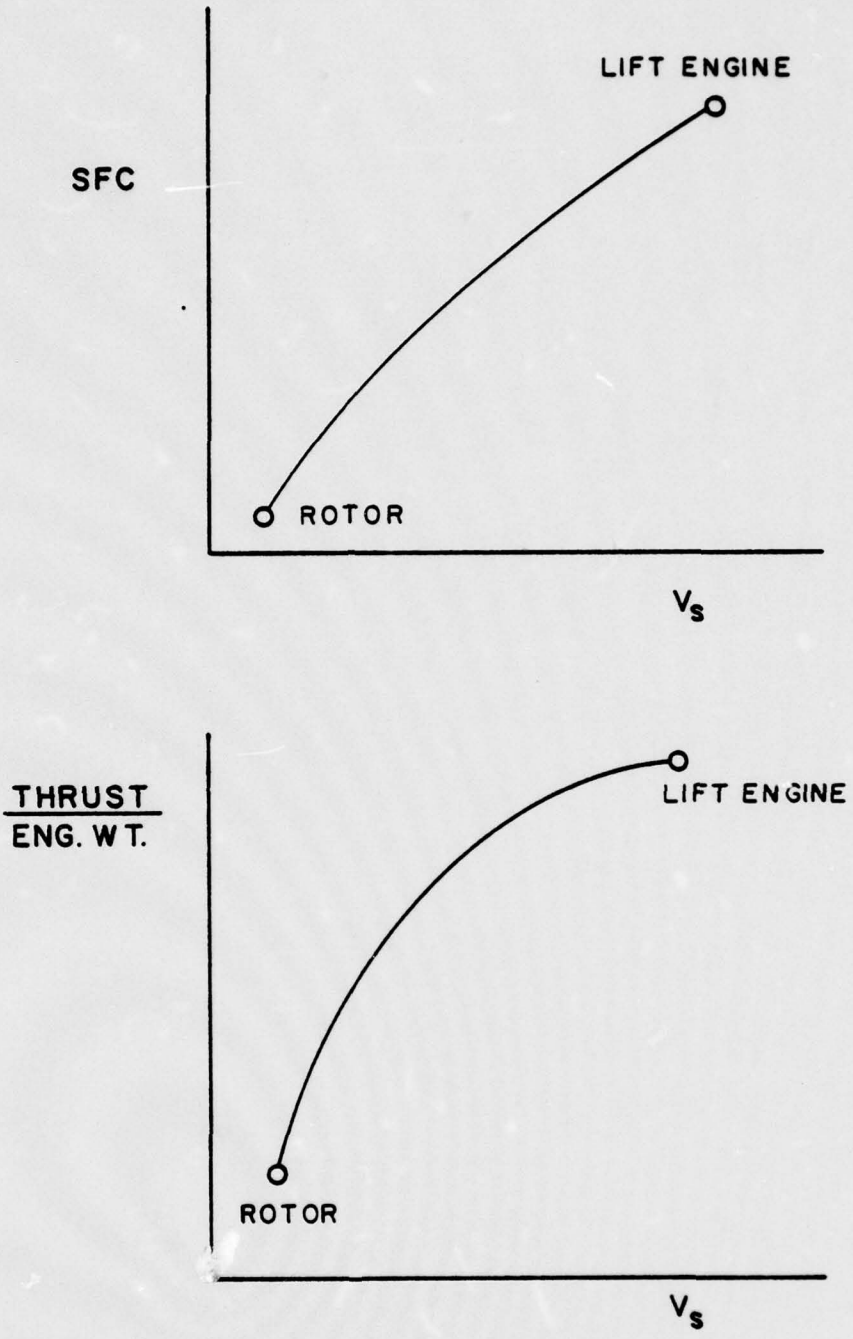

Figure 6.

Specific fuel consumption and engine thrust/weight ratios as a function of slipstream velocity.

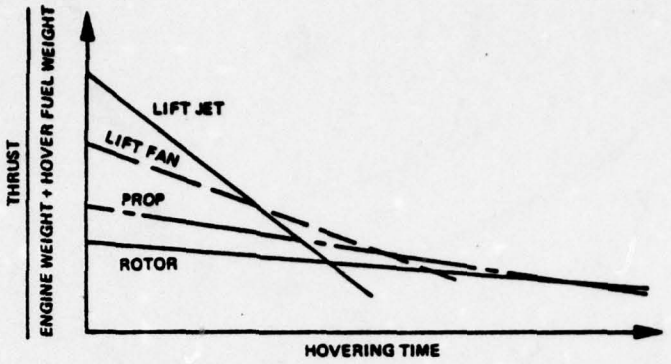

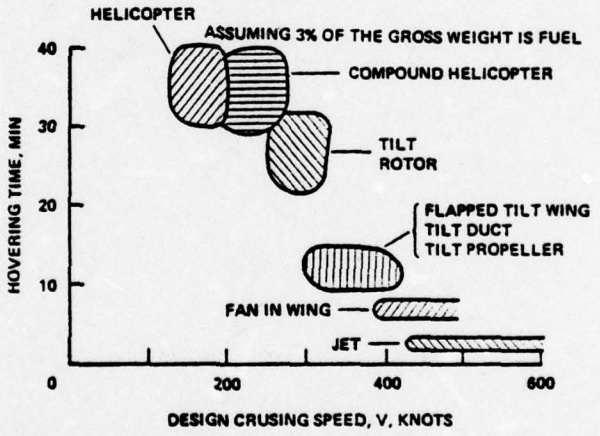

Figure 7.
Hovering and cruise performance of VTOL systems. (Ref. 17)

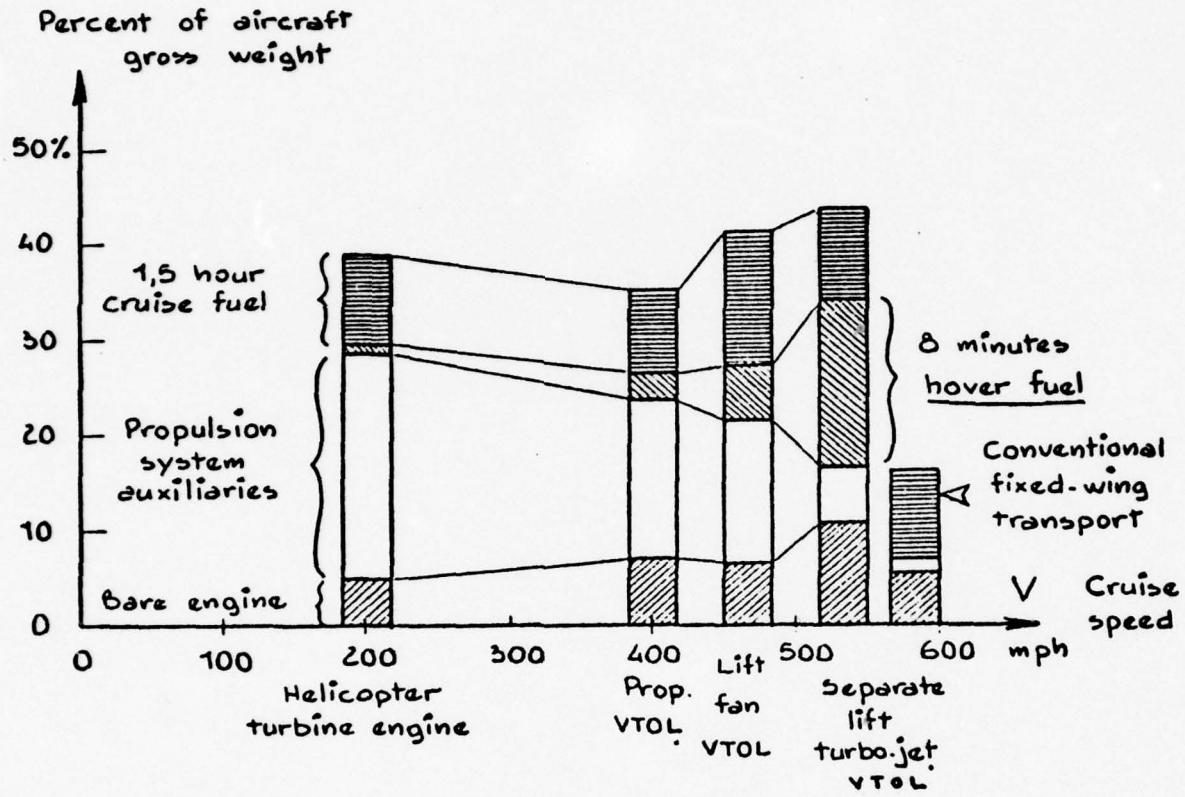

Figure 8.

Relative component weights of VTOL aircraft. (Ref. 1)

jet configuration, the hover fuel increases while the propulsion weight decreases. For a longer hover duration, the helicopter would show a distinct advantage due to its low fuel consumption. For a shorter hover duration, the lift jet would have the advantage due to its low propulsion weight.

Thus, it is evident that criteria for the interded mission are of fundamental importance in the evaluation of a VTOL aircraft, namely: cruise speed and hover duration.

C. VTOL AIRCRAFT CONFIGURATIONS

There is a wealth of possible VTOL configurations considering the various lifting means available. There are also a number of means available to perform the transition between hover and forward flight.

A typical classification of VTOL configurations is based on the method of hovering and the method of performing the transition to forward flight.

Four general methods are available for hover: rotors, free propellers, ducted fans, and jet engines.

There are also four methods available to perform the transition between hovering and forward flight: aircraft tilting, thrust tilting, thrust deflection, and separate propulsion for vertical and forward flight.

The chart in Figure 9 depicts the possible combinations of VTOL configurations using a grid system, as in Ref. 1, and gives representative examples.

D. TRANSITION FLIGHT

The transition flight phase is defined as the speed range from hovering flight to wing-borne flight. This flight regime is usually the most critical for VTOL aircraft.

METHODS TO PERFORM THE TRANSITION	TYPES OF LIFT GENERATORS			
	ROTORS	FREE PROPELLERS	DUCTED FANS	TURBO-JETS
AIRCRAFT TILTING	HELICOPTERS	CONVAIR XFY-1 LOCKHEED XFV-1	FLYING JEEPS	RYAN X-13
THRUST TILTING	BELL XV-3 BELL XV-15	VERTOL VZ-2 VOUGHT XC-142 CURTISS X-19	DOAK VZ-4 BELL X-22	BELL A.T.V. VJ-101
THRUST DEFLECTION		RYAN VZ-3 FAIRCHILD VZ-5		BELL X-14 LOCKHEED XV-4A H.S. HARRIER
SEPARATE PROPULSIONS	McDONNELL XV-1 FAIRGY ROTODYNE		RYAN XV-5A	VAK-191 MIRAGE 3V DORNIER DO-31

Figure 9.
VTOL configurations.

The most important variable during transition is the power required. The power required in a hover can be obtained by first recalling equation (14),

$$\frac{T}{P_{id}} = \frac{2}{V_u} \tag{19}$$

From equation (10),

$$V_u = \sqrt{\frac{2T}{\rho \pi R^2}} \tag{20}$$

Substituting equation (20) into (19), the following is obtained for the ideal power required in a hover:

$$P_{id} = \frac{T^{3/2}}{\sqrt{2\rho\pi R^2}}$$

Assuming thrust equals weight, and introducing the figure of merit, the power required for a hovering rotor is given by

$$P_h = \frac{W^{3/2}}{M\sqrt{2\rho\pi R^2}} \tag{21}$$

Recalling that induced drag can be expressed as

$$C_{D_i} = \frac{C_L^2}{\pi e AR}$$

and assuming lift equals weight so that

$$C_L = \frac{2W}{\rho V^2 S}$$

then

$$C_{D_i} = \frac{4W^2}{\rho^2 V^4 S^2 \pi AR e}$$

If $AR = b_w^2/S$, then

$$C_{D_i} = \frac{4W^2}{\rho^2 V^4 S \pi b_w^2 e}$$

Recalling that

$$D_i = C_{D_i} \tfrac{1}{2} \rho V^2 S$$

then

$$D_i = \frac{2\,(W/b_w)^2}{\rho V^2 \pi e}$$

Introducing the propulsion efficiency, η , and the fact that $P_i = DV$, then the induced power in forward flight is

$$P_i = \frac{2\,(W/b_w)^2}{\rho \pi e \eta V} \tag{22}$$

Recalling that profile drag can be expressed as

$$D_p = C_{D_o} \tfrac{1}{2} \rho V^2 S$$

then similarly, the profile power in forward flight is given by

$$P_p = \frac{C_{D_o} \rho V^3 S}{2\eta} \tag{23}$$

If equations (22) and (23) are plotted, as in Figure 10, the result is the classical helicopter/VTOL power required curve. It should be noted that induced power is a function of (1/V) and is therefore large at low airspeeds. Profile drag, on the other hand, is a function of V^3 , and therefore is dominant at high airspeeds.

The power required at low airspeeds (i.e. transition) could be reduced if the induced drag was lowered, since parasite drag has little effect at low airspeeds.

Recalling that the minimum induced drag will occur for a spanwise elliptical lift distribution, a goal for efficient transition should be to approach as close as possible an elliptical lift distribution.

Configurations which have high concentrations of lift, such as lift jets or ducted fans, have poor lift distributions, as shown in Figure 11. In contrast, good load distributions can be obtained with such configurations as tilt-wings or spanwise ejectors.

The power required curves thus are different during transition, depending on the shape of the lift distribution. For the case of one engine cut, for example, the minimum flight speed is lower for the configuration with a good load distribution. The control and safety aspects of this comparison are evident.

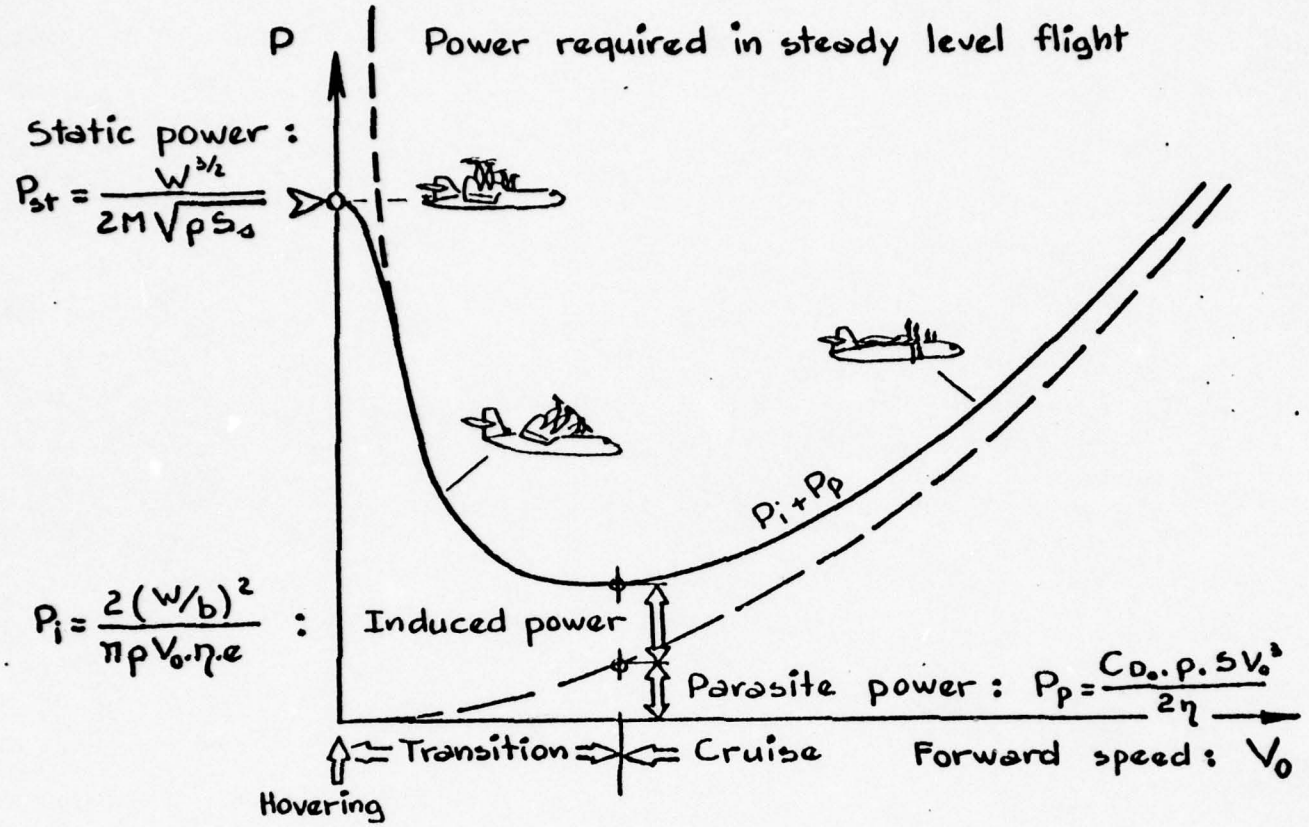

Figure 10. Typical VTOL power required curve. (Ref. 1)

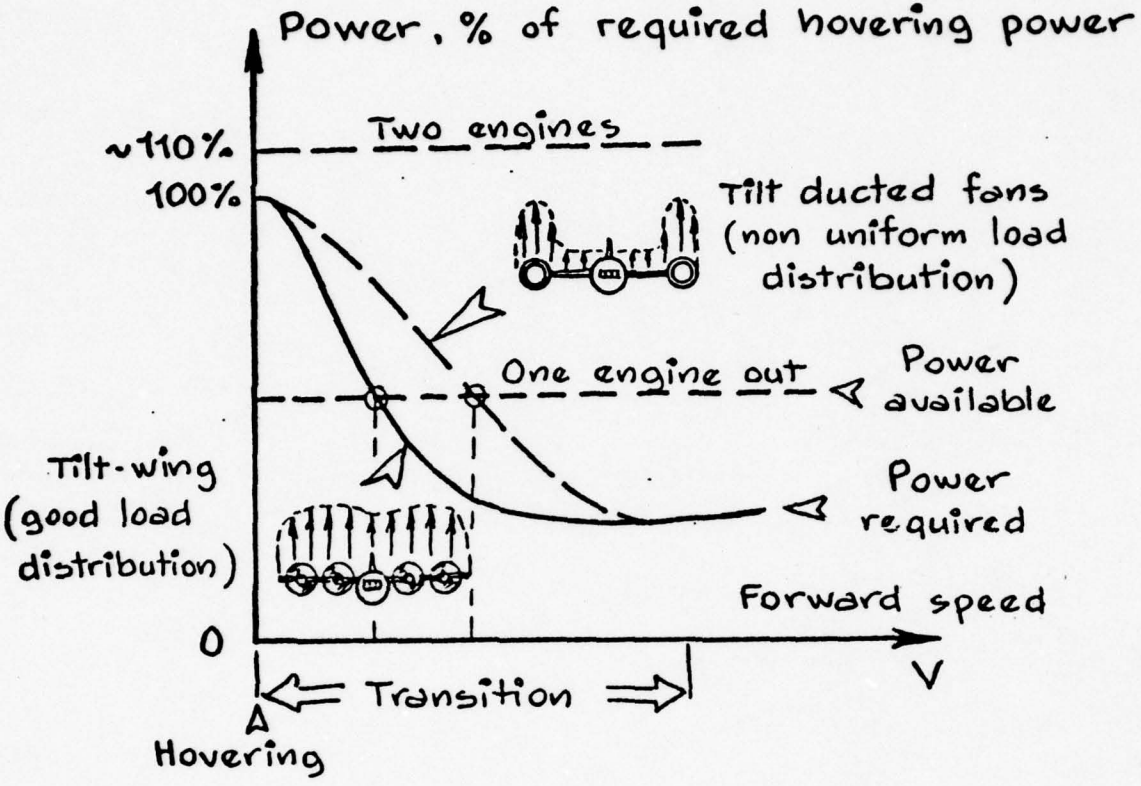

Figure 11.
Power required during transition flight. (Ref. 1)

E. CRUISE FLIGHT

The purpose of the present thrust of VTOL development is to provide fast, efficient cruise while allowing vertical takeoff and landing. If a prolonged hovering capability were required, a helicopter would be the most logical choice, yet in cruise the helicopter is limited in forward speed due to retreating blade stall and high Mach numbers on the advancing blades.

A measure of cruise efficiency is the specific power, defined as the power available in cruise divided by the gross weight times the cruise velocity. That is

$$\text{Specific Power} = P/WV$$

Helicopters, with S.P. $\approx$ 0.25, are much less efficient in cruise than conventional jet transports with S.P. $\approx$ 0.05. Other VTOL aircraft have values between these two extremes. For example, a tilt rotor has a S.P. $\approx$ 0.15. The high values of specific power for VTOL aircraft can be attributed both to the higher values of installed power necessary for vertical flight as well as to higher drag values resulting from the special configuration requirements of vertical flight devices.

Another measure of cruise efficiency is the equivalent lift/drag ratio $(L/D)_e$, which is related to the specific power as

$$\text{S.P.} = P/WV = D_e V/WV = 1/(L/D)_e$$

Thus, the low specific power of conventional jet transports corresponds to a lift/drag ratio $\approx$ 20, while the high specific power of helicopters corresponds to a low lift/drag ratio $\approx$ 4. Figure 12 illustrates the equivalent lift/drag ratio versus speed of flight for various VTOL configurations.

As seen from Figure 12, the advantage of unloading the rotor, as in a compound helicopter, is small, but the advantage from a tilt wing in cruise is evident. However,

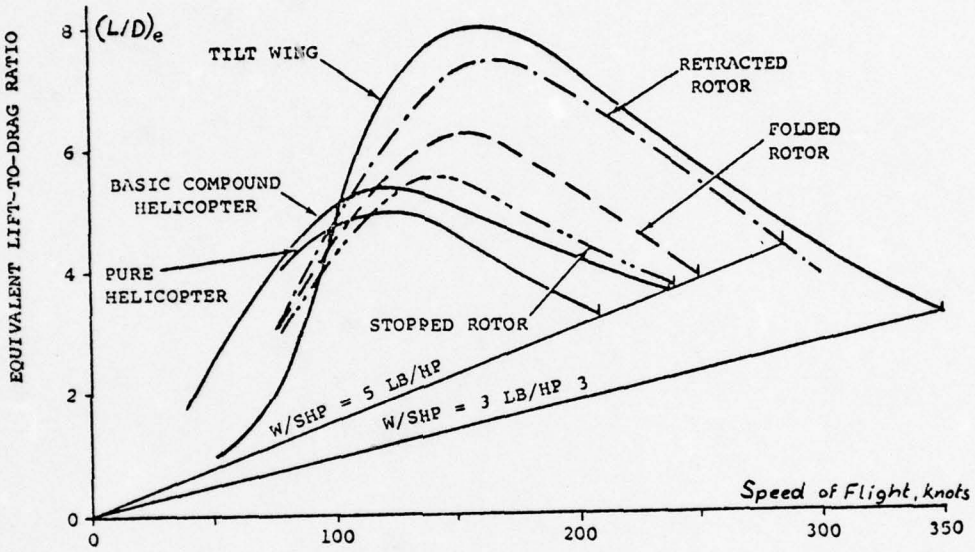

Figure 12.

Equivalent lift-to-drag ratios for various configurations. (Ref. 15)

tilt wing aircraft have a cruising speed of only 200-300 knots. High speed VTOL capability has been shown in configurations such as the vectored-thrust Harrier (M = 0.9) or the VJ-101 (M = 1.4), which uses separate lift engines. The presence of vertical flight capability in these and similar configurations has not detracted from a clean efficient cruise configuration. This is the key to efficient VTOL cruise: namely, a vertical capability integrated into an efficient cruise design.

F. CONTROL SYSTEMS

Most VTOL aircraft require special hovering controls because conventional control surfaces are ineffective in a hover unless they are immersed in the slipstream of the lift generators. During transition, a special mixing of control systems is required to transfer authority from hover controls to conventional controls as airspeed increases.

Depending on the configuration, various means are available to control the hovering aircraft in the roll, pitch, and yaw axes.

The helicopter uses a tilting of the rotor disc to control pitch and roll, while the tail rotor provides yaw control. For aircraft which have lift generators located a distance from the center of gravity, differential variations or tilting of the thrust vectors can be used to control the aircraft. If the lift generators are centrally located in the fuselage, reaction controls using engine bleed air can be placed on the aircraft extremities to provide the necessary control moments. If conventional controls, such as ailerons, are located in the hovering high-energy slipstream, such as below a tilt-wing propeller or a tilting engine pod, then these controls retain their effectiveness in a hover by virtue of the dynamic pressures exerted on them by the slipstream.

Control methods for four VTOL configurations are depicted in Figure 13.

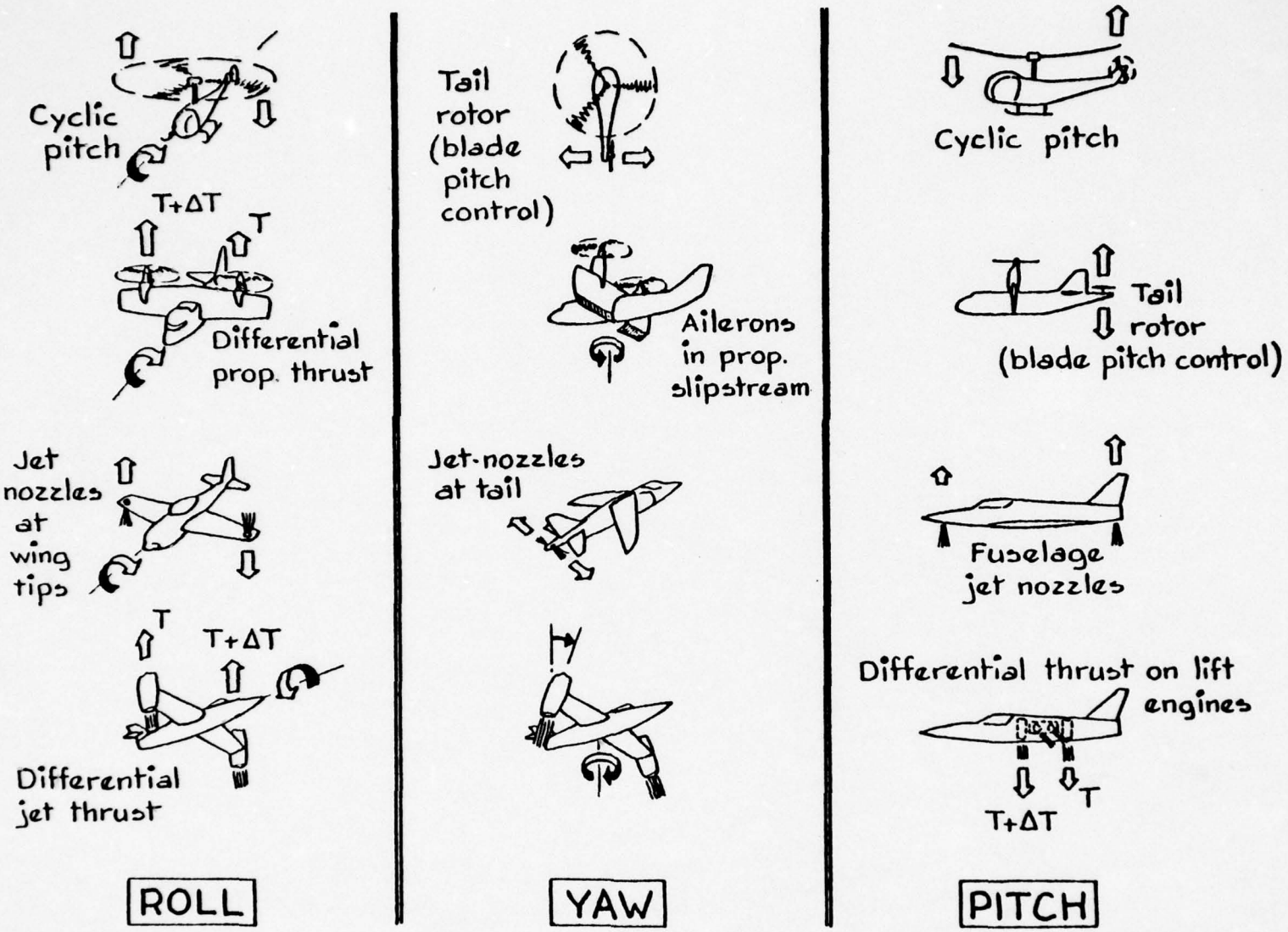

Figure 13. Various types of control methods for hovering and transition. (Ref. 1)

G. INTERACTION PROBLEMS

The large velocities and flow rates necessary for hovering and transition induce many aerodynamic and operational problems on VTOL aircraft, depending on the particular configuration. Those problems occurring out of ground effect are due primarily to aerodynamic interaction between the airframe and the lift generator slipstream, while those in ground effect are due to ground proximity.

1. Interactions Out of Ground Effect

The large velocities and mass flow rates in hover and transition necessarily entrain surrounding air, thus inducing velocities and suction forces on the underside of wings and fuselage. As transition takes place, this effect can increase, inducing a lift loss as forward speed increases, until the wing begins to generate lift. Besides the lift loss, pitching moments can occur due to the shifting center of lift caused by interactions.

Tilt wing aircraft are extremely susceptible to aerodynamic interactions during transition. At moderate forward speeds, the wing is necessarily at a high tilt angle, and thus the angle of attack on the wing can be very large, causing separation and resulting buffeting. Therefore, tilt wing aircraft have a narrow corridor of velocity, rate of descent, and wing tilt angle during transition in order to prevent wing flow separation and the resulting buffeting.

It must be emphasized that aerodynamic interactions are configuration-dependent to a high degree, and that slight changes in configuration, such as exhaust jet placement, can alter considerably any interaction effects.

2. Ground Interference Effects

The presence of high-velocity and high-temperature flows near the ground in combination with the airframe causes a complicated flow pattern to develop, as shown in Figure 14. The effects of the exhaust gas include such phenomena as recirculation, suckdown, reingestion, ground erosion, and the fountain effect.

a. Ground Effect

Unlike a helicopter, which experiences a favorable ground effect as it approaches the ground, the ground effect on a VTOL aircraft may be favorable or unfavorable, depending on the particular configuration.

The high-velocity exhaust flows induce secondary flows which generally produce a low pressure field on the underside of the aircraft. This lower pressure under the aircraft produces what is called the suckdown effect. However, this effect may be positive or negative depending on the particular configuration.

A configuration with a single exhaust jet will experience up to a 15% loss of thrust at ground level. However, a configuration with two exhaust jets can experience an upward force on the underside of the aircraft where the two flows meet on the ground and reflect upwards. This fountain effect can completely negate the effects of suckdown, so that a net positive ground effect occurs.

Of course, the relative ground effect is a function of the type of lift generator. A propeller will approach the favorable ground effect of the helicopter, while a lift jet will experience suckdown in ground effect.

b. Fountain Effect

The fountain effect, shown in Figure 15, may cause the problem of aircraft skin heating in the impingement area. The magnitude of the problem depends on the exhaust temperatures and the duration of impingement.

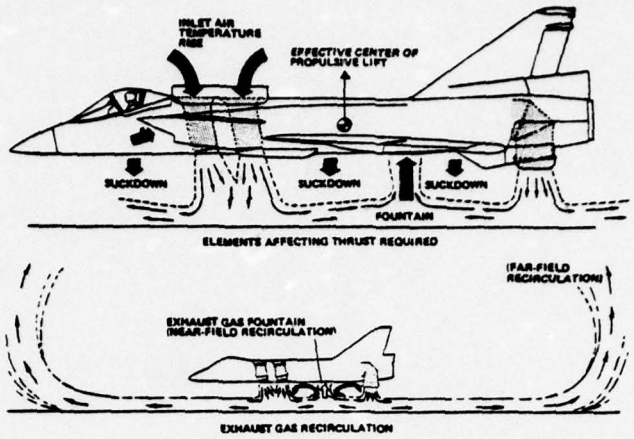

Figure 14.
Hovering flow field features. (Ref. 18)

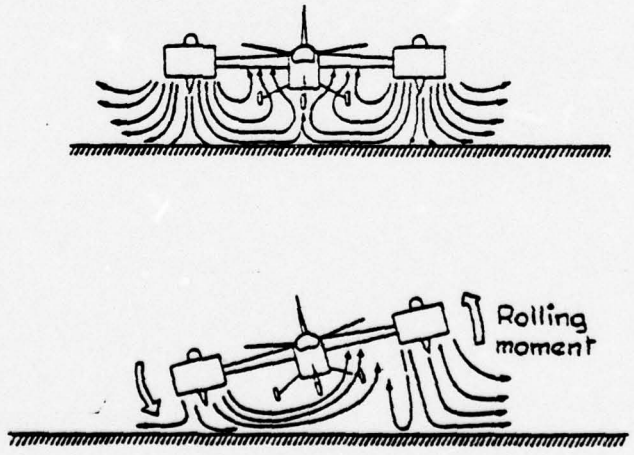

Figure 15.
Effect of aircraft attitude
on fountain impingement. (Ref. 1)

Another problem of the fountain effect is the loss of lift which occurs if that effect is changed because of hover altitude or surface winds. Since the fountain effect can cause appreciable lift forces and moments, a change in the point of impingement can cause control problems near the ground, as shown in Figure 15.

c. Recirculation

The flow pattern in a hover can be described as consisting of near-field or far-field recirculation, as shown in Figure 16. Near-field recirculation is caused by the direct impingement of the exhaust flow on the ground, and its reflection, or fountain effect. Far-field recirculation occurs as the exhaust gases fan out along the ground and rise eventually due to their heat, to be sucked back down into the flow field.

d. Ground Erosion

The proximity to the ground of high-velocity flows will necessarily cause ground erosion problems. The amount of erosion will depend on the velocity of the flow, the type of terrain, and the duration. From Equation (11) it is recalled that the slipstream velocity is a function of the disc loading. Thus a rotor will have less effect than a lift jet on ground erosion.

e. Reingestion

Hot-gas reingestion is a problem because the increase in inlet temperature due to exhaust ingestion will cause a decrease in engine thrust near the ground. For example, an inlet temperature rise of 40 degrees F. can cause a 15% loss of thrust. Here again, the particular configuration has an important effect on the susceptibility to hot-gas reingestion. The location of the exhaust jets, the intakes, and the airframe design are important design considerations. Aircraft attitude, hover height, and surface winds are operational variables which affect the reingestion problem.

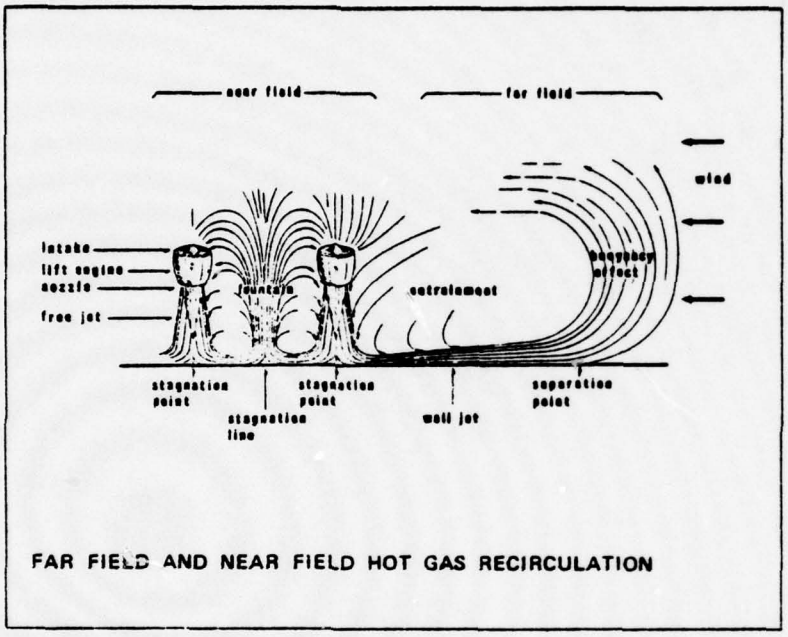

FAR FIELD AND NEAR FIELD HOT GAS RECIRCULATION

Figure 16.
Recirculation flow fields. (Ref. 14)

III. THE JET FLAP

A. BOUNDARY LAYER CONTROL

The maximum lift coefficient which can be obtained using a conventional flapped airfoil is limited by boundary layer separation. This separation of the boundary layer occurs when the boundary layer is experiencing an adverse pressure gradient and does not have sufficient energy to remain attached to the airfoil surface. If this flow separation can be eliminated by energizing the boundary layer, then higher lift coefficients can be obtained. This is the goal of boundary layer control - to raise the lift coefficient of an airfoil to its theoretical value (from potential flow theory).

A common form of boundary layer control is to expel a thin jet of air at the flap hinge, as shown in Figure 17. The energy imparted to the boundary layer from the jet allows the flow to remain attached over the flap and thus prevents separation of the flow.

B. SUPERCIRCULATION

If the jet momentum is increased beyond that necessary to obtain the theoretical lift, an interesting phenomenon called supercirculation occurs. As the jet momentum increases, the lift coefficient is increased beyond the theoretical maximum.

The characteristic parameter of the jet is the jet momentum coefficient c_j (or c_μ) defined as

$$c_j = \frac{\dot{m}_j V_j}{q S}$$

where $\dot{m}_j$ is the mass flow rate of the jet and V_j is its velocity.

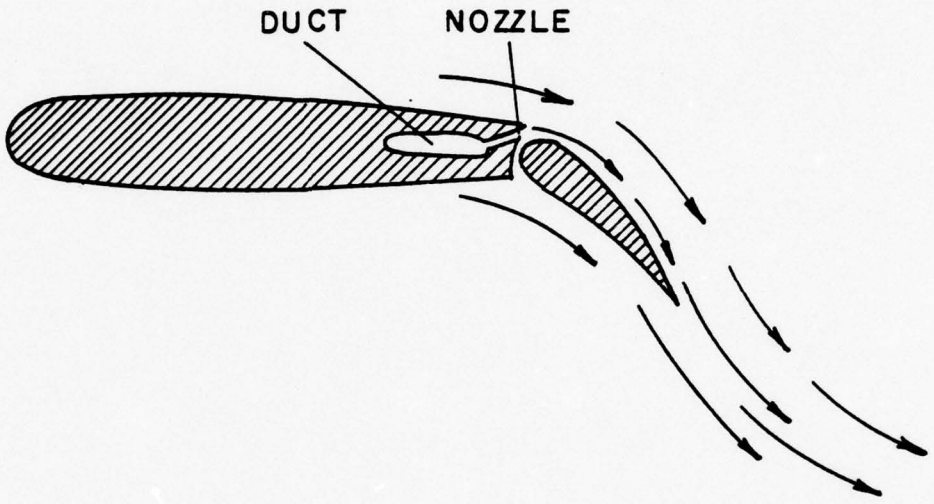

Figure 17.

Boundary layer control by blowing prevents separation.

For an airfoil which uses a blowing jet to augment its lift, the magnitude of the jet momentum coefficient determines whether this lift increase is due to boundary layer control or supercirculation.

The value of jet momentum coefficient required to obtain the theoretical lift coefficient on an airfoil is referred to as the critical jet momentum coefficient. Values of the jet momentum coefficient above or below this value indicate supercirculation or boundary layer control, respectively.

The effect of a jet on lift coefficient is shown in Figure 18, which plots the general trend of lift coefficient with jet momentum coefficient. With no jet momentum, the lift in viscous flow is less than the theoretical value. As c_j increases to $c_{j_{CRIT}}$, the value of lift coefficient obtainable increases to the theoretical maximum. This is the region of boundary layer control. As the jet momentum is increased beyond this value, the lift coefficient increases, although at a slower rate. This is the region of supercirculation.

C. JET FLAP BASICS

1. Description

Consider an airfoil equipped with a Zapp flap as shown in Figure 19, and a similar one equipped with a trailing edge jet sheet. These two configurations each have the same effect upon the airfoil characteristics. The term "jet flap" originated from this analogy between the jet sheet and the mechanical flap.

2. Principle of the Jet Flap

The principle of the jet flap is to create supercirculation by means of a high-momentum jet sheet.

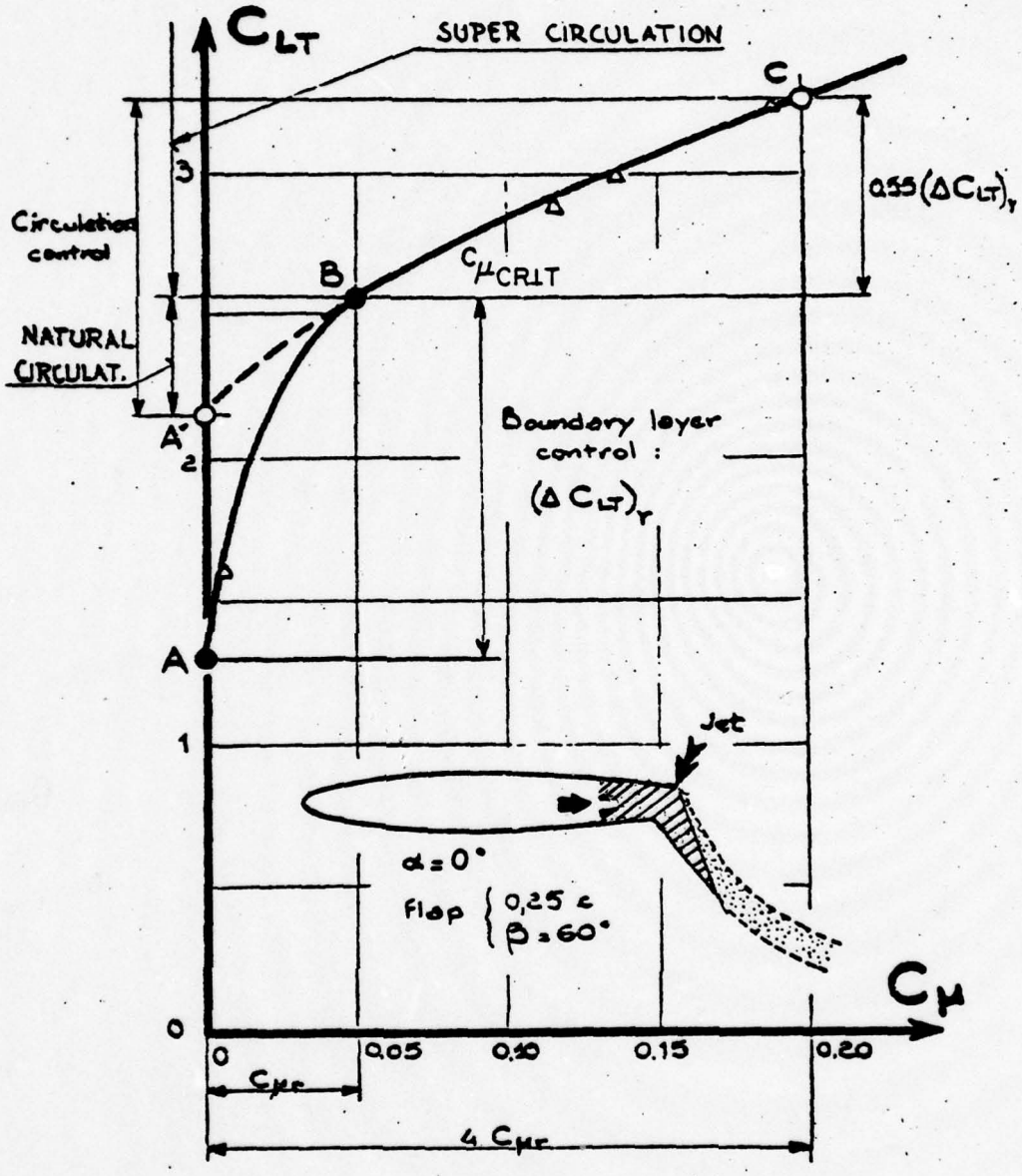

Figure 18.
Effect on lift coefficient of blowing. (Ref. 2)

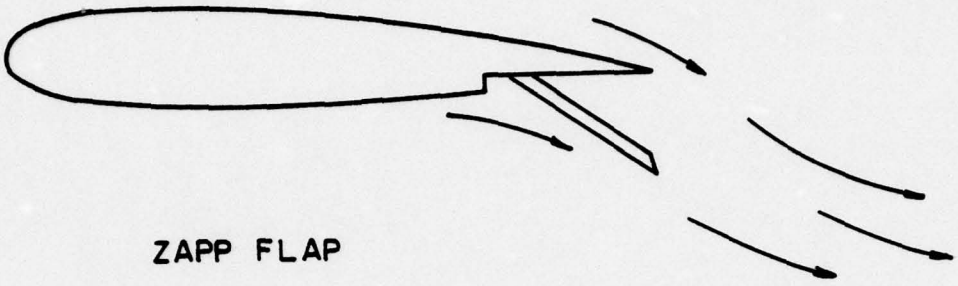

ZAPP FLAP

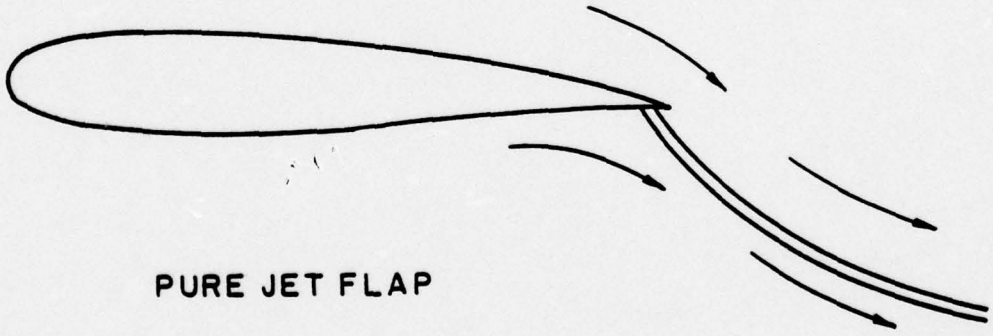

PURE JET FLAP

Figure 19.
Jet flap analogy with mechanical flap.

3. Configurations

Originally, the jet flap was envisioned as a full-span jet sheet which used the entire propulsion exhaust to supply the jet momentum. Thus, the jet flap provided for the complete integration of propulsive and lift systems.

However, the practical application of the pure jet flap is unlikely because the jet deflection angle must be controllable in flight and because of the consequences of failure of the blowing system.

Thus, several concepts have been proposed which utilize the jet-flap principle in a practical manner. These are illustrated in Figure 20. Each of these concepts has been successfully utilized to provide high lift coefficients during takeoff and landing, e.g.: externally blown flaps on the McDonnell Douglas YC-15, upper surface blowing on the Boeing YC-14, and the augmentor wing on the DeHavilland/NASA C-8A Buffalo.

4. Characteristics

Basic two-dimensional jet flap effects are summarized in Ref. 2. Figures 21 and 22 illustrate the effect on lift coefficient of the jet deflection angle and the jet momentum coefficient.

The important characteristics of the two-dimensional jet flap are summarized below:

(1) Blowing increases the slope of the lift curve.

(2) A jet-flap airfoil is essentially unstallable, since an increase in lift can be obtained merely by increasing blowing, and not solely by increasing the angle of attack.

(3) Blowing decreases the profile drag of the airfoil due to the propulsive effects of the jet.

UPPER SURFACE BLOWN

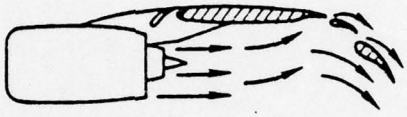

EXTERNALLY BLOWN

AUGMENTOR WING

Figure 20.
Practical jet flap concepts.

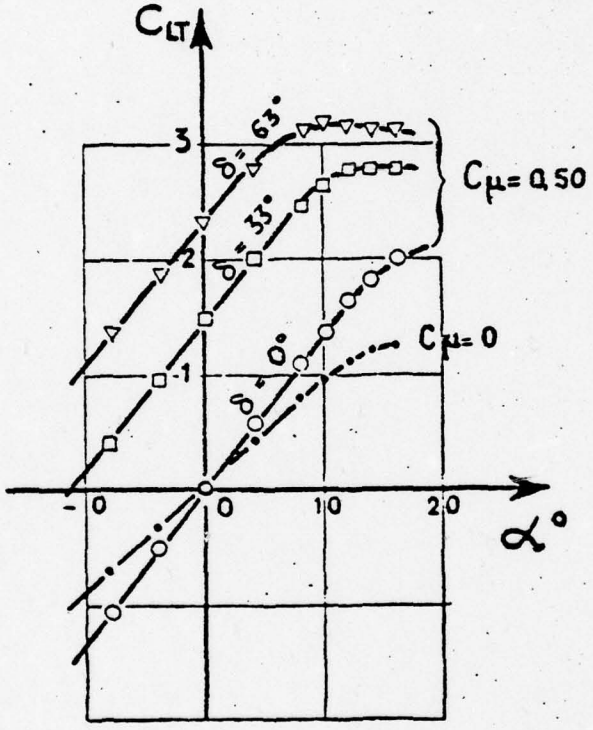

Figure 21.

Total lift coefficient as a function of incidence and jet deflection angle. (Ref. 2)

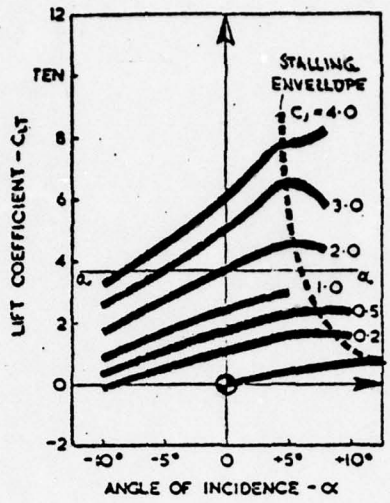

$\delta = 31.4°$

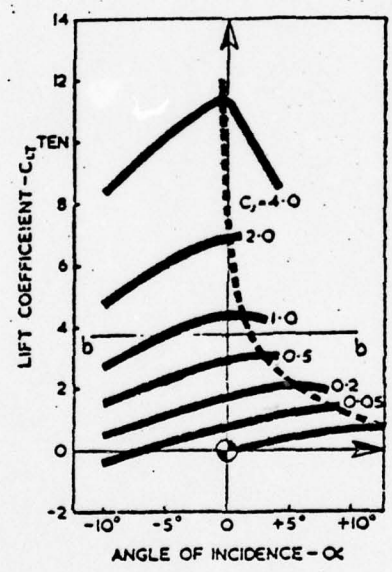

$\delta = 58.1°$

Figure 22.

Total lift coefficient as a function of incidence and jet deflection angle. (Ref. 2)

(4) The lifting effectiveness is independent of the type and thickness of the airfoil.

(5) Blowing increases the drag rise Mach number, thus delaying compressibility effects.

IV. THE JET-FLAP ROTOR

A. INTRODUCTION

The advantages of the jet flap would tend to lend it to applications in helicopters as well as conventional aircraft. The application of the jet-flap principle to helicopters has been discussed in References 3 through 5. Despite the advantages of the jet-flap rotor over conventional configurations, no jet-flap helicopters have been built. Several jet-flap rotors have been tested, however, and will be discussed later.

B. DESCRIPTION

The most common concept of a jet-flap rotor involves a rotor blade with a narrow slot at the trailing edge of a conventional airfoil. The slot runs along a major portion of the blade. Thus a large portion of the rotor disc is influenced by the jet flap.

Air is supplied by either a compressor or by the direct jet exhaust of a gas generator, and is ducted to the rotor hub and then through the hollow blade to the slot. Rotor propulsion is provided by the thrust of the jet flap itself or by tip jets, which are more efficient for rotor propulsion as will be shown later. The ducting within the blade necessitates a somewhat thicker blade than on conventional rotors, on the order of 15 to 20% thickness as compared to 12%.

The ability to control the jet deflection angle is a requirement in most jet-flap rotor designs. This is most commonly accomplished by exhausting the air over a short mechanical flap at the trailing edge, as shown in Figure 23. A deflection of the flap deflects the flow as the air follows the upper surface by the Coanda effect.

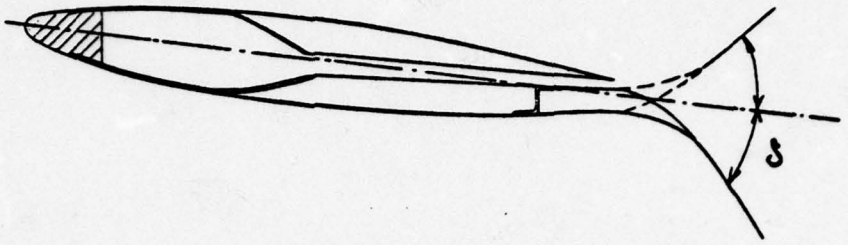

Figure 23.
Jet flap for a rotor. (Ref. 4)

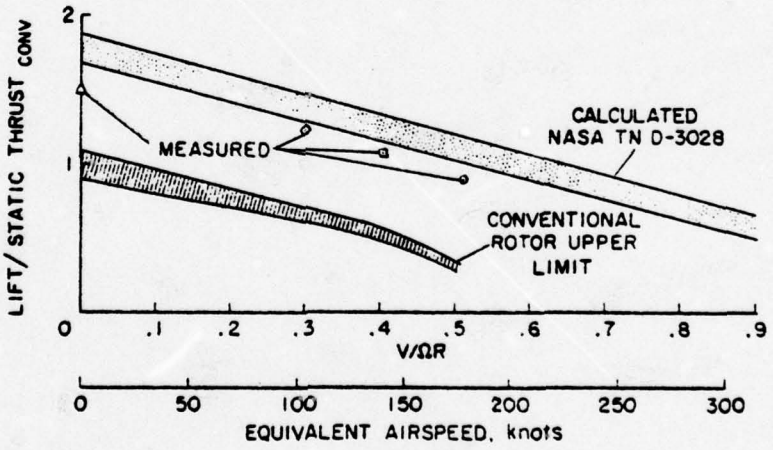

Figure 24.
Jet-flap rotor capability. (Ref. 8)

The rotor blades can be fixed or variable in pitch. A fixed-pitch rotor can be used since the jet deflection angle can be varied, which can provide necessary changes in collective or cyclic lift. The simplicity inherent in a fixed-pitch rotor is evident.

C. CHARACTERISTICS

Analytical studies of jet-flap rotors have been reported in References 6 and 7, and experiments in References 3 and 8.

The advantages of a jet-flap rotor are evident from Figure 24, which depicts test results full-scale. It is seen that both increased static lift capability and increased high-speed capability are realized with the jet flap. The increased static lift is due to the higher lift coefficients and the resulting higher disc loading possible with the jet flap. The increased speed capability is due to the elimination of retreating blade stall which is possible because of the high lift coefficients available with the jet flap.

Figure 24 also shows the close correlation between the calculated results from Ref. 6 and the measured test results from Ref. 8.

The reduction of vibration is another advantage of the jet-flap rotor. Since the local lift can be controlled by the jet deflection angle, any azimuthal variation of lift is possible. The introduction of higher harmonic control of the jet flap enables the level of vibration transmitted to the fuselage and blade stresses to be reduced considerably.

D. PROPULSION REQUIREMENTS

A jet-powered rotor can be powered using one of three propulsion cycles: the hot cycle, in which hot gases of up to 750° C are delivered directly from a gas generator and ducted through the rotor to the nozzle; the cold cycle, in which relatively cold air of up to 200°C is supplied by a

compressor; or the mixed cycle which combines the hot and cold cycles and uses air from 200° to 400° C.

The selection of one of these systems must be based not only on their relative efficiencies, but also on the technical problems involved with each. The primary technical problem concerns ducting design.

A number of tip-jet powered helicopters have been built which utilize the cold cycle. The hot cycle, however, presents the problem of extremely hot gases passing through the rotor blade. With a hot cycle, it is necessary to minimize the heat loss through the blade. Thus, utilizing the blade structure itself as the duct is not advisable. Separate ducting is required which can be insulated to minimize heat losses through the blade. Thus, ducting requirements, especially for the hot cycle, dictate the construction of relatively heavy rotor blades.

Despite the problems involved in developing a hot cycle system, the potential efficiency is promising. The Dornier firm of Germany successfully developed a rotor system which ducted 700° C hot gases through the blade to a tip nozzle. See Ref. 9.

E. PROPULSIVE EFFICIENCY

The primary disadvantage of a jet-driven rotor is its poor efficiency relative to a conventional shaft-driven rotor. The overall efficiency of a jet-driven rotor can be readily estimated. This has been done for the hot cycle in References 7 and 10, and for the cold cycle in Reference 11.

1. Hot Cycle

The overall efficiency of the complete system, η, can be decomposed into the thermal efficiency of the gas generator, η_{th}, and the efficiency of the rotor drive system, η_R. Thus

$$\eta = \eta_{th}\,\eta_R$$

The thermal efficiency is defined as the ratio of the total energy in the output gases to the fuel energy input. The rotor drive efficiency is the ratio of the rotor drive mechanical output to the gas generator mechanical energy output.

The highest overall efficiency depends upon compromises in η_{th} and η_R. The thermal efficiency varies with the compressor pressure ratio P_{o3}/P_{o1} and with the turbine inlet temperature T_{o4} of the gas generator. Figure 25 shows the variation of thermal efficiency with pressure ratio and turbine inlet temperature for the rotor of Ref. 7.

The losses associated with η_R are due to friction in the blade, but more significantly, to the unavailable jet kinetic energy. In other words, the rotor drive efficiency increases with increasing energy output from the gas generator or increasing tip speed. Figure 26 shows the ideal rotor system efficiency (friction losses neglected) for a mixed cycle. The parameter H here is defined in Ref. 7 as

$$H = \frac{2E_G}{V_t^2}$$

The practical range of H is from 7.5 to 15 as shown.

The efficiencies of various systems can thus be readily calculated. From Figure 25 a gas generator with a pressure ratio of 16 and a turbine inlet temperature of 2500° R (which are within the state of the art) has a thermal efficiency of 0.41. From Figure 26 a typical rotor drive efficiency (using tip jets) for a hot cycle will be about 0.45. Thus an overall rotor efficiency of 18% is obtained.

For comparison, Figure 26 illustrates the rotor drive efficiency of a typical shaft drive (with a turbine efficiency η_t of 0.87 and a gearing efficiency η_g of 0.83). Using the same gas generator so that $\eta_{th} = 0.41$, the overall efficiency of the shaft drive is 34%.

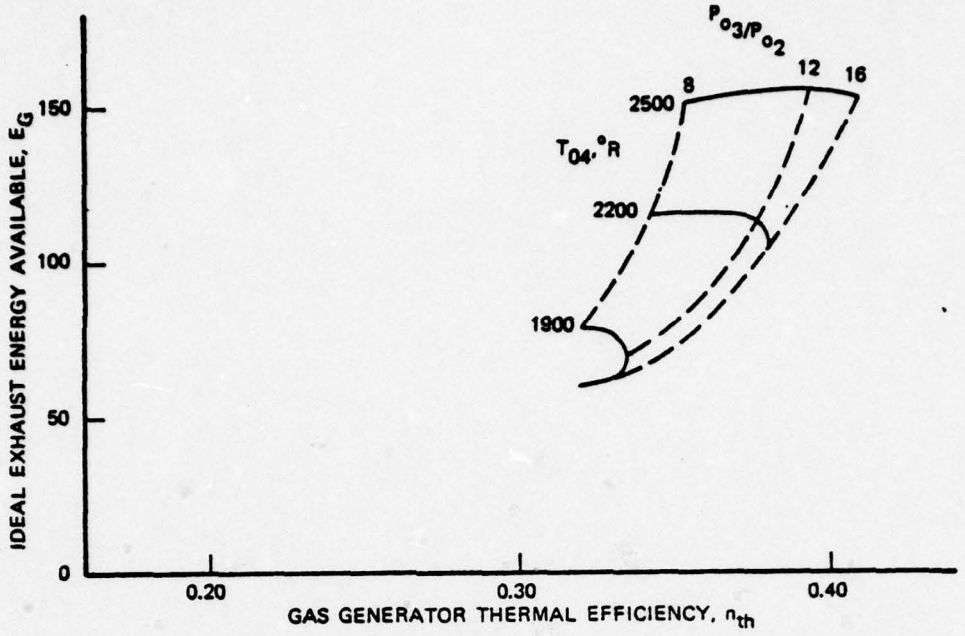

Figure 25.
Gas generator performance. (Ref. 7)

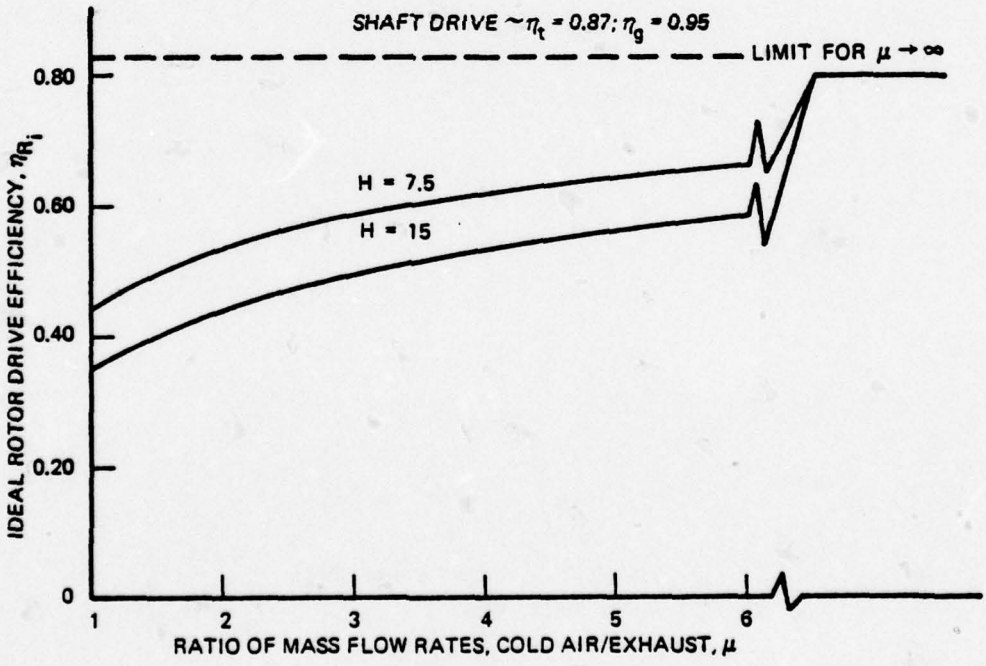

Figure 26.
Ideal rotor drive system efficiency
for mixed cycle. (Ref. 7)

The sensitivity of η_{th} to the pressure ratio and the turbine inlet temperature should be noted. The selection of a powerplant for a jet drive system is thus of overriding importance, for this and other reasons.

Figure 26 depicts the effect of a mixed cycle or cold cycle. For an increasing ratio of cold air to basic exhaust, the rotor drive efficiency rises. However the problem arises of accommodating the large mass flows necessary for a significant increase in efficiency.

2. Cold Cycle

Using the method of Ref. 11, a typical value of rotor drive efficiency is 0.42, which compares with a value of 0.83 for the shaft drive and 0.45 for the hot cycle.

3. Overall Comparison

Thus the overall efficiency for a jet drive system using tip jets is about 50 percent lower than that of a shaft-driven system.

F. TIP-JET PROPULSION

The potential of using tip jets was recognized early in the development of helicopters. Various forms of tip reaction drive were developed in the decade after World War II and included such devices as ram jets, pulse jets, tip burning, tip turbojets, and various forms of the pressure jet as described in Ref. 12. However, for various technical reasons only one jet rotor was used extensively, the French Djinn, built in 1953 and of which over 200 were constructed. This helicopter was simple, using compressed air ejected at the blade tips for rotor propulsion.

The tip-jet propulsion system offers a number of advantages over shaft-driven rotors. No extensive transmission systems are needed. Since virtually no rotor torque is transmitted to the fuselage, an anti-torque system is unnecessary. The high rotor inertia and wide rpm range

available reduce the critical area in the height-velocity diagram.

However, several disadvantages appear in the discussion of jet-driven rotors. The ducting requirements necessitate heavy, relatively thick blades. As discussed earlier, jet-driven rotors have a much lower propulsive efficiency than shaft-driven rotors, necessitating a high value of installed power.

Recent work on jet-driven rotors centers on the simple pressure jet system as discussed in Ref.9.

The use of a tip jet is a logical means of propulsion for a rotor also utilizing a jet flap as a means of lift control. In fact, a tip jet is more efficient as a means of rotor propulsion than a jet flap alone. After an analytical investigation, Gray and Hubbartt concluded that, for a jet-flap drive with the local jet momentum coefficient constant along the blade radius, the overall efficiency and torque output are about 35% lower than those for a tip-jet drive. As the distribution of the momentum coefficient is increased toward the tip, the performance of the jet-flap drive approaches that of the tip jet.

Thus a rotor which utilizes a large-span jet flap can be more efficiently propelled by a tip jet than by the jet flap itself. The incorporation of a tip jet with a jet flap merely involves ducting a portion of the air to the blade tip to be used for the rotor propulsion.

G. JET-FLAP ROTOR EXPERIMENTS

The most extensive research on jet-flap rotors has been conducted by the French firm of Giravions Dorand. After encouraging results on small jet-flap rotors, a 12-meter rotor designated the DH2011 was projected in 1959. This rotor was tested in the Ames 40x80-foot wind tunnel and the results reported in Ref. 8. The same rotor was also investigated analytically and reported in Ref. 6.

The DH2011 was a two-bladed rotor, driven and controlled by a jet flap located in the outer 30 percent radius of each blade, as shown in Fig. 27. The blades were fixed in pitch and the rotor force output was controlled by varying the jet deflection angle, both cyclically and noncyclically.

The jet flap is shown in Figure 28. The compressed air was ducted through the blade spar and then, by a series of cascades, was exhausted out a slot over a short mechanical flap. The flow was deflected by deflecting the flap, which directed the flow by the Coanda effect.

The basic results of the wind tunnel test are shown in Figure 29. These plots show the lift and propulsive force coefficients at advance ratios of 0.30 and 0.51. The limits shown for a standard rotor with 8 degrees of twist are due to retreating blade stall. Here $\overline{A}_0$ is the collective jet deflection, and $\overline{B}_1$ the cyclic jet deflection. The increased lift of the jet-flap rotor is evident. As discussed earlier, Figure 24 shows the tremendous capability of the jet-flap rotor, both in lift and in forward speed capability. The calculated data, which compare favorably with the measured data, indicate that flight is possible up to a speed of 300 knots with a jet-flap rotor, as compared with a speed of 200 knots for a conventional rotor due to retreating blade stall effects.

The wind tunnel tests of the DH2011 rotor demonstrated the potential of the jet-flap rotor. Examination of the test results has led to the following conclusions:

1. High advance ratios can be attained without encountering retreating blade stall.
2. The large forces produced per unit blade area exceed conventional rotor capabilities by factors of 2 or more.
3. By varying the jet deflection angle, both cyclically and noncyclically, it is possible to control and direct the rotor's force.

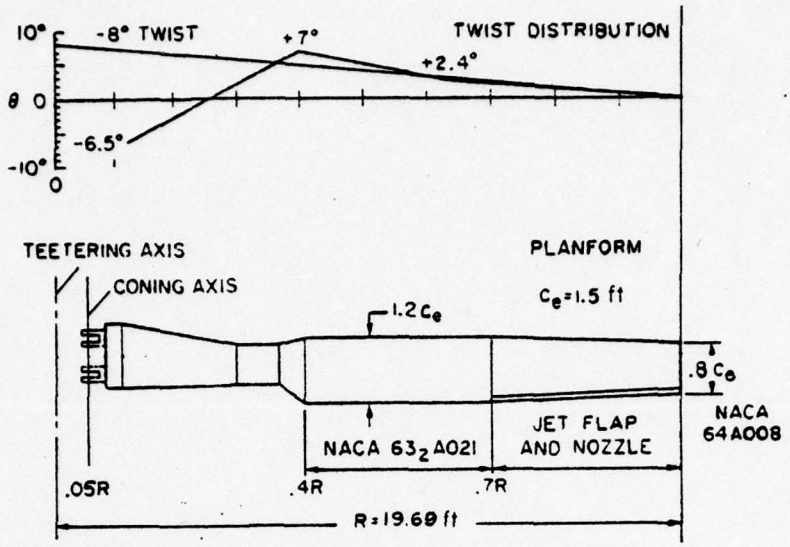

Figure 27.
The DH2011 rotor blade. (Ref. 8)

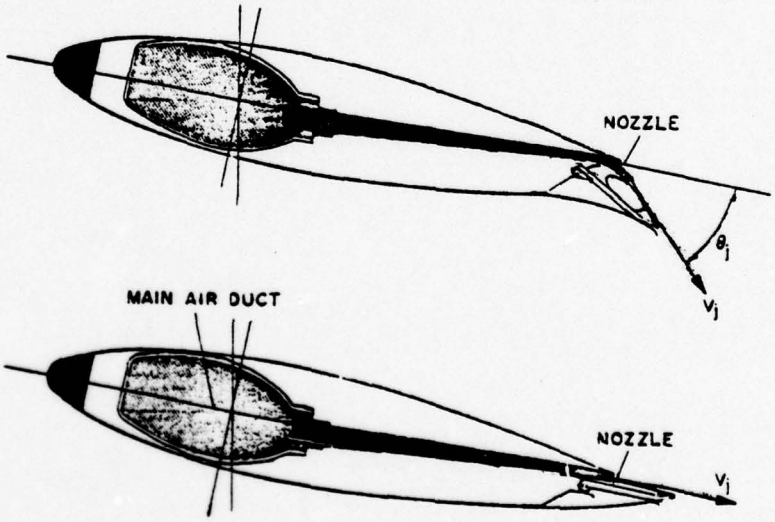

Figure 28.
The DH2011 jet flap. (Ref. 8)

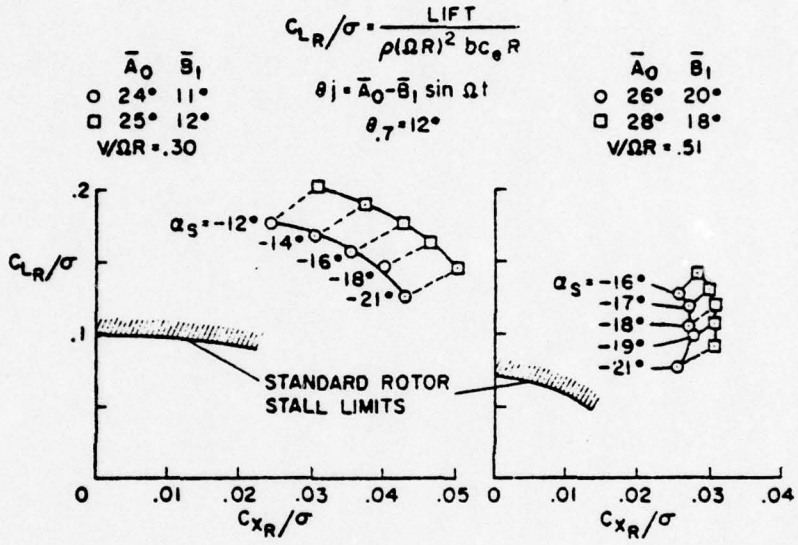

Figure 29.
Jet-flap rotor force capability. (Ref. 8)

V. STOWABLE ROTOR AIRCRAFT

A. GENERAL

The speed limitations of the pure helicopter are well-known, as is its low lift/drag ratio compared to fixed-wing aircraft.

In order to increase the speed, range, and endurance of an aircraft and yet maintain the efficient hovering capability of the helicopter, it is necessary to increase the lift/drag ratio in forward flight while retaining the rotor system for hovering flight. There are three general configurations which extend the performance of rotorcraft beyond that of the pure helicopter:

(1) The compound helicopter, in which a wing unloads the rotor system at high speeds

(2) The tilt-rotor, in which the rotor is tilted to a propeller mode for high speeds

(3) The stowable rotor aircraft, in which the rotor is retracted for high speeds

As shown in Figure 30, the stowable rotor aircraft has a lift/drag ratio much greater than the pure helicopter, and has the highest speed capability of any aircraft retaining a rotor for hovering capability. Thus the stowable rotor aircraft combines the speed and efficiency of a fixed-wing with the efficient hovering capability of the helicopter.

The potential of the stowable rotor concept was recognized in the 1950's, and various studies and experiments were performed in this area. See References 13 and 14.

In the stowable rotor concept, the major technical problem is the rotor start-stop process. The major problems associated with the start-stop process are:

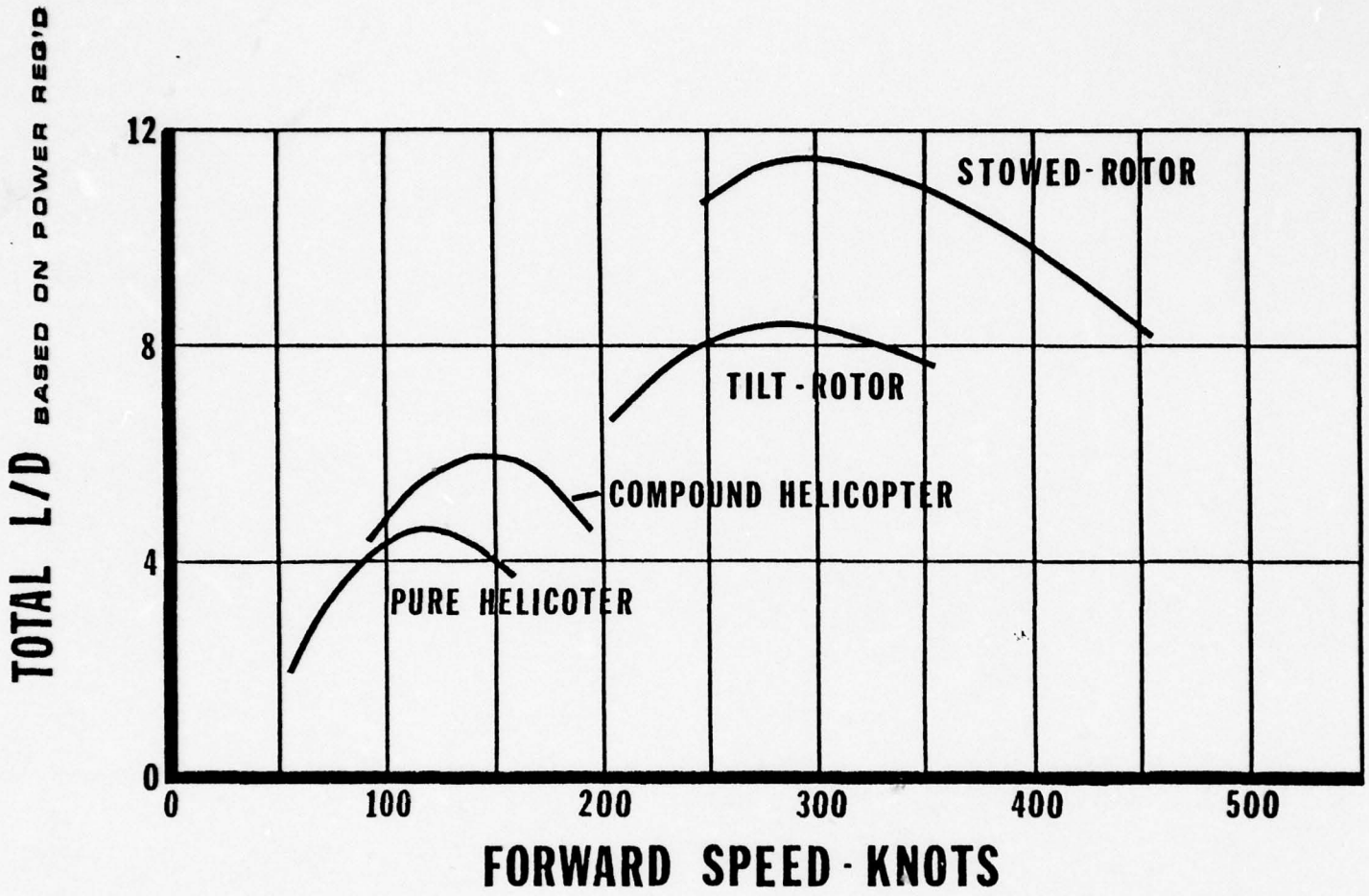

Figure 30.
Typical aircraft lift/drag ratios. (Ref. 20)

(1) Rotor control

(2) Rotor and aircraft gust response

(3) Rotor vibratory loads

(4) Aeroelastic characteristics of the blades

Several successful wind tunnel tests have been conducted in which rotors have been started and stopped. But the problems involved are very sensitive to airspeed, rotor attitude, and gusts. Tests have concluded that a responsive cyclic pitch control must be used to prevent excessive blade stresses and flapping during the start-stop process.

Along with the problem of the start-stop process has been the problem of folding the rotors once stopped. The size of typical rotors requires that they be folded in order to fit inside the aircraft structure. Here is encountered the problem of aeroelastic divergence of the blades, some of which may move 180 degrees during the folding cycle.

B. A JET-FLAP STOWABLE ROTOR AIRCRAFT

The use of a jet-flap rotor as a stowable rotor can eliminate many of the problems associated with using a conventional rotor in such a design. Such a configuration was proposed by Kretz in Ref. 4.

The aircraft, which is typical of the stowable rotor type, is shown in Figure 31. Designed for a VTOL tactical mission, the rotor is used for only a short period during takeoff and landing. Maximum speed at sea level is Mach 0.85.

Since the rotor is placed close to the fuselage, the rotor provides only roll control, while reaction control jets provide pitch and yaw control in hovering flight. The rotor is servo-controlled so as to remain in a fixed plane. Stopping of the rotor, which occurs at an airspeed of 135 knots, takes only 7 seconds and is accomplished by reversal of the tip jet. Flapping angle, for gusts up to 20 knots, does not exceed one degree during the stopping evolution.

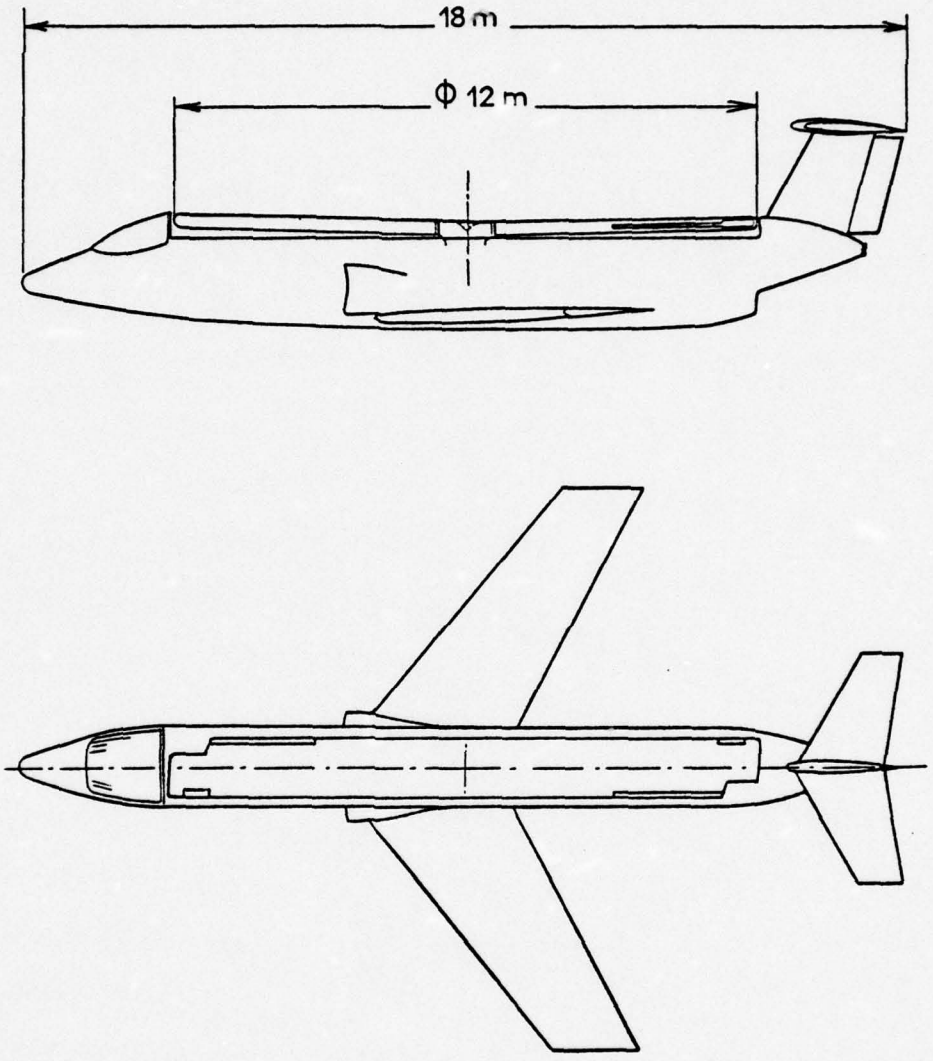

Figure 31.
A jet-flap stowable-rotor aircraft. (Ref. 4)

The jet flap extends along the outer 50% radius, while a tip jet provides rotor propulsion. The air flow is ducted through the hollow blade and turned by a series of cascades to exhaust out the slot, as shown in Figure 32. The cascades have very carefully defined shapes, derived from a series of tests, in order to minimize pressure losses.

Propulsion in both vertical and forward flight is provided by a gas turbine, with the air being ducted to the rotor for hovering or to the nozzle for forward flight by means of a diverter valve.

The relatively poor rotor drive efficiency necessitates careful design to minimize power losses between the power at the gas generator outlet and the power at the rotor. This loss is essentially due to the pressure loss and can be defined by a parameter K_T , defined as the difference between the total pressure at the gas generator and the rotor nozzle, divided by the dynamic pressure in the blade. The parameter K_T depends essentially on the duct geometry, and thus requires exhaustive testing to obtain the best design. Figure 33 illustrates the tremendous influence on K_T (and therefore efficiency) of the pressure ratio. A slight change in pressure from the optimum severely affects power transmission efficiency.

The use of the jet-flap rotor allows operation of the rotor at disc loadings far above conventional rotor limits. These high disc loadings allow a reduction in solidity for a given weight. Thus, in this configuration a two-bladed rotor, with a diameter of 12 meters, is able to lift a weight of 26455 lbs. The obvious advantage of the relatively short, two-bladed rotor is that blade folding becomes unnecessary in order to stow the rotor.

The capability for arbitrary cyclic variation of the jet deflection angle allows for precise control of forces on the blade during the start-stop cycle. Thus, blade flapping can be controlled at any rpm.

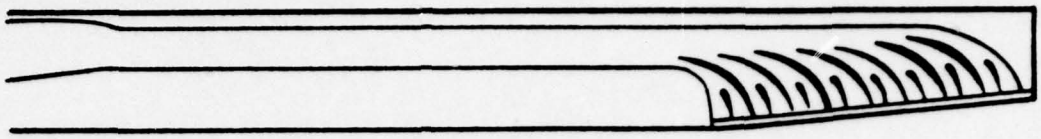

Figure 32.
Jet-flap rotor cascades. (Ref. 4)

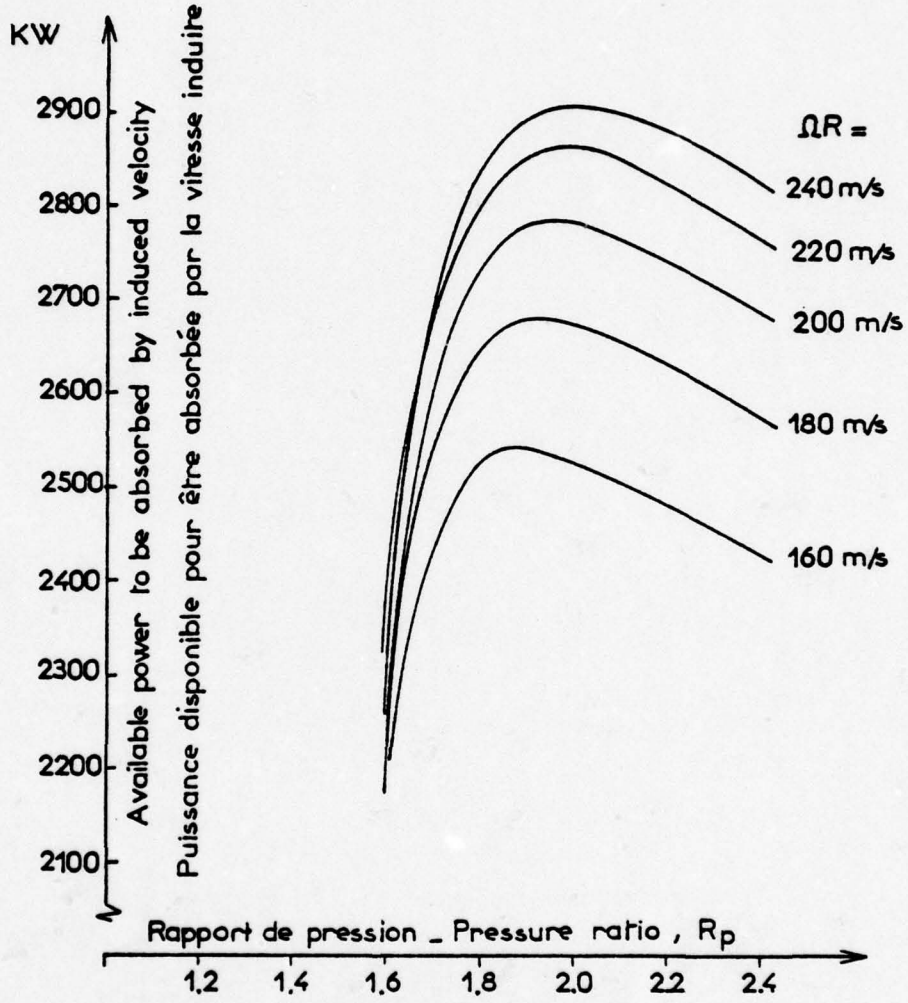

Figure 33.
Pressure ratio optimization. (Ref. 4)

Although the jet-flap rotor is relatively heavy, its torsional rigidity eliminates the aeroelastic problems associated with the start-stop process.

The stowable rotor design exhibits a number of other advantages. Because of the jet flap, the rotor is fixed in pitch, making the rotor a very clean design. Since the rotor is jet-driven, no anti-torque device is necessary.

The major advantages of using the jet-flap rotor rather than a conventional rotor in a stowable rotor design are listed in Figure 34. It is evident that the use of the jet-flap rotor allows the simplicity in the aircraft design described.

- FIXED PITCH ROTOR.
- TWO BLADED HIGH SPEED ROTOR.
- ALLEVIATION OF FATIGUE AND VIBRATION PROBLEMS BY MULTI-CYCLIC CONTROL.
- STOPPED ROTOR CAPABILITY BY CONTINUOUS CONTROL OF FORCES ON THE BLADE.
- ELIMINATION OF AEROELASTIC PROBLEMS BY HIGH RIGIDITY IN TORSION.
- LOW CHORD BLADE.
- ALLEVIATION OF WEIGHT BALANCE PROBLEMS OF THE BLADE.
- LOW CONTROL FORCES.
- VARIABLE R.P.M.
- NO ANTITORQUE DEVICE.

Figure 34.
Advantages of the jet-flap rotor. (Ref. 4)

VI. JET-FLAP ROTOR HOVER ANALYSIS

A. BACKGROUND

In order to make intelligent performance calculations of an aircraft, it is necessary to calculate its fuel consumption, which is based on the installed powerplant and its power setting. For the case of jet-powered rotors, the determination of the required powerplant requires a knowledge of the air mass flow necessary to supply the rotor jets.

A glance at the power required curve of Figure 10 shows that the greatest power is required in a hover. The power required at high airspeeds is disregarded here, since a stowable rotor aircraft is designed to operate the rotor only in the low-speed flight regime. Thus, for a jet-flap rotor on a stowable rotor aircraft, the critical power requirements occur in hover. For this reason, this study is limited to the analysis of the jet-flap rotor in the hovering flight condition.

B. GENERAL DESCRIPTION

As stated earlier, it was necessary to first calculate the air mass flow requirements for the rotor in order to determine a suitable powerplant. This was done using a computer program which used the classical blade element and momentum theories, modified for the inclusion of jet-flap characteristics, to obtain required momentum coefficients for a specified rotor.

The theory and equations used in the computer program are described in Appendix A, and a detailed description of the computer program is contained in Appendix B. A listing of the program and a sample output are contained following Appendix C.

A brief description of the method of obtaining the performance of the jet-flap rotor follows:

(1) The basic rotor geometry and operating conditions were input to the program.

(2) The program used two major iteration loops to obtain the required jet-flap momentum coefficient and torque coefficient, as described in Appendix B.

(3) These two coefficients were used to obtain the required air mass flow (in pounds of air per second) by the method described in Appendix C.

(4) Using the air mass flow requirement, a suitable powerplant was selected, which in turn determined the fuel consumption.

C. ASSUMPTIONS

The blades were assumed to have a constant chord with a constant NACA 0012 airfoil along the span. A linear washout of 8 degrees from hub to tip was used.

The distribution of jet-flap momentum was specified as constant along the blade. Thus, the jet-flap momentum coefficient varied as the square of the radius. As concluded in Ref. 7, this distribution achieves the minimum total jet-flap momentum required.

Gray and Hubbartt concluded that the collective pitch angle for minimum jet-flap momentum is close to that associated with a zero angle of attack at the blade tips. Therefore, the pitch angle used in the program was chosen to achieve approximately a zero angle of attack at the tip section.

The jet-flap rotor computer program was used to analyze the rotor jet momentum coefficient as a function of the jet deflection angle. The results are shown in Figure 35 for the stowable rotor aircraft described in the preceding section. Since most of the reduction in C_{J_R} is obtained at a jet deflection angle of 50 degrees, this value was used in the subsequent analyses.

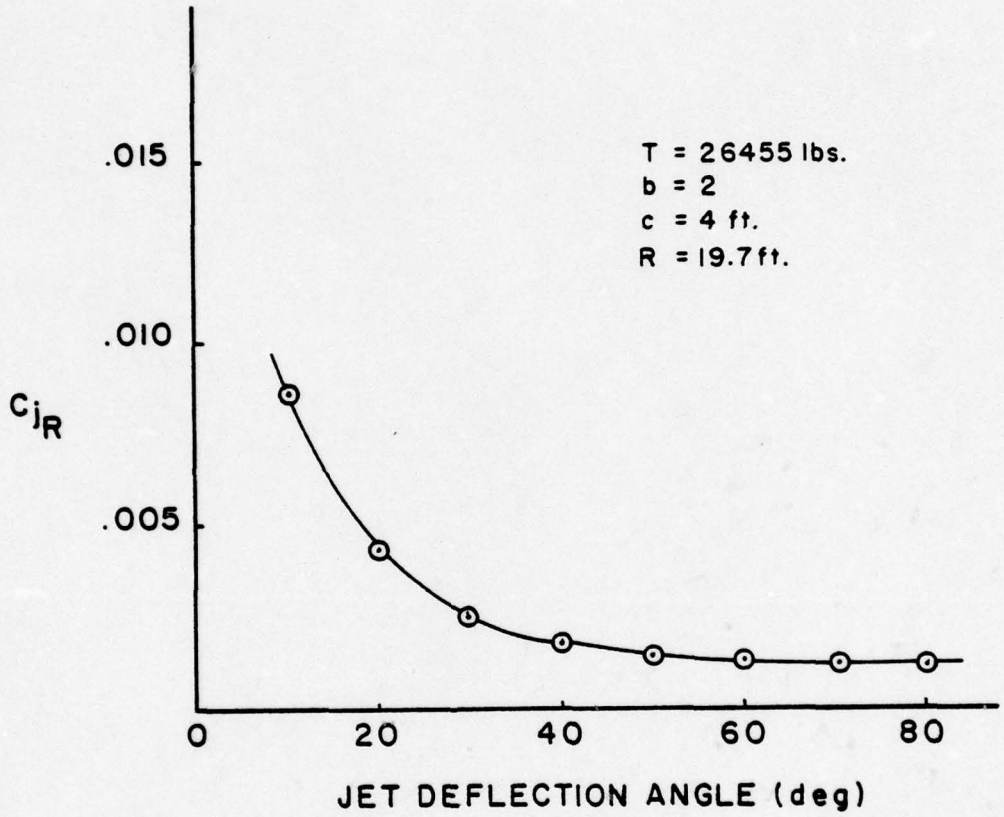

Figure 35.

Rotor momentum coefficient as a function of jet deflection angle.

D. PROGRAM VALIDATION

Various runs were made using data points from the charts of Ref.7. The program results agreed with those of Ref. 7 within 5%. This is a good agreement, since the equations used in Ref. 7 were not identical to those developed by the author in Appendix A.

VII. LIFT GENERATOR COMPARISONS

A. LIFT GENERATOR TYPES

There are four major methods of providing the thrust necessary for vertical flight: lift engines, lift fans, rotors, and ejectors. Each of these methods is described in detail below.

1. Lift Engines

a. Description

A lift engine is a relatively small, self-contained jet engine which is mounted vertically and provides lift by direct jet reaction. A typical lift engine has a thrust/weight ratio of 16 as compared with a cruise engine which typically has a thrust/weight ratio of less than 10. Specific fuel consumption is higher than for most cruise engines.

The relatively small size of lift engines allows them to be conveniently placed within the aircraft fuselage and thus can provide a vertical lift capability with minimum impact on an aircraft design.

b. Examples

Few successful lift engines have been developed. The dominant lift engines have been the Rolls-Royce RB.108 and RB.162 series, which have been used on such VTOL aircraft as the VFW-Fokker VAK-191B, the Dornier DO.31E, and the Dassault Mirage 3V.

The RB.162 has a 6-stage axial compressor and a single-stage turbine drive. It operates at a pressure ratio of 4.5 with an air mass flow of 85 lbm/sec. It weighs only 375 pounds yet develops 6000 pounds of static thrust at sea

level. Specific fuel ccnsumption is 0.96 lb/lbt/hr. With a diameter of 29 inches and a length of 58 inches, it cccupies a volume of only 22 cubic feet.

c. Development

The trend of engine develcpment is shcwn in Figure 36. Lift engines have a significantly higher thrust/weight ratio than cruise engines.

In Figure 37 the development of the Rclls-Rcyce lift engines is shown. The significant improvement in thrust/weight ratio and engine volume is evident. The third engine shown is a proposed lift engine fcr future VTOL aircraft. There is little doubt that significant improvements in lift engine performance are pcssible given sufficient incentive.

The problem in lift engine develcpment is the tremendous ccst in time and money necessary to achieve a reliable new design with significant improvements over past designs. The present state of VTCL development has not provided sufficient stimulus to develcp the next generaticn of lift engines to succeed the RB.162 series.

d. Advantages and Disadvantages

A lift engine can intrcduce a vertical lift capability into an aircraft with a minimum of design effcrt. However, the lift engine has a high fuel consumptien and the weight of the fuel required becomes prohibitive for operation in excess of a few minutes.

Another serious disadvantage of the lift engine is its external characteristics. The RB.162 has an exhaust velocity of 2000 feet per second with a temperature cf at least 1500° F. It is evident that the fcctprint characteristics of a lift engine aircraft would certainly limit its operational envircnment.

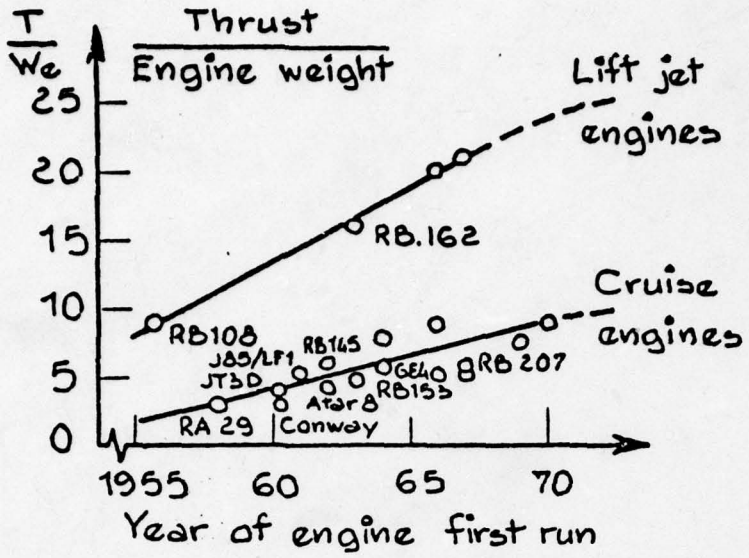

Figure 36.

Thrust-to-weight trends in engine development. (Ref. 1)

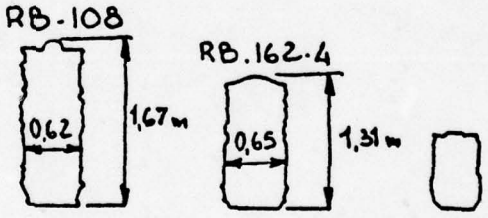

Thrust/weight	8.7/1	16/1	21/1
Installed Thrust/weight	5/1	10/1	16/1
Volume	100%	85%	27%
	1st generation	2nd g.	3rd generation

Figure 37.

Rolls-Royce lift engine trends. (Ref. 1)

2. Lift Fans

a. Description

A lift fan is mounted horizontally in the wing or fuselage so as to provide vertical thrust. A lift fan can be tip-driven by ducted turbine exhaust, as in the Ryan XV-5A, or can be mounted axially and driven by the turbine itself, such as the proposed RB.202 turbofan.

The use of a ducted fan provides for the amplification of the basic jet exhaust. Typical values of thrust amplification (fan thrust/engine thrust) range from 1.8 to 2.8. The fan thrust/weight ratio typically ranges from 15 to 20.

b. Examples

The lift fans used in the XV-5A are tip-driven by ducted exhaust from the two cruise engines. These fans provide a thrust augmentation of 2.5.

The Rolls-Royce RB.202 is a proposed self-contained lift fan which uses a compressor core to drive a front fan. With a thrust of 13000 pounds and a weight of 865 pounds, a thrust/weight ratio of 15 is achieved. This engine has a low specific fuel consumption of 0.45, making it a much more efficient hovering device than the lift engine.

c. Development

Advanced lift fans such as the RB.202 are certainly possible if, as in the case of the lift engine, sufficient incentive exists. A major technical problem in the development of lift fans is their performance at forward airspeed during transition. With the complicated crossflow existing across the fan and the aircraft structure, a tremendous testing effort is involved to achieve a good design.

d. Advantages and Disadvantages

The major advantage of the lift fan is its thrust augmentation of the basic jet thrust, and the resulting efficiency over the lift engine. Another important advantage is its footprint characteristics, as shown in Figure 38. The use of a fan instead of a lift jet decreases the exhaust velocity and temperature significantly.

However, a lift fan is relatively voluminous and must be placed either within the wing, as in the XV-5A, or in the fuselage where it occupies a relatively large volume.

3. Rotors

a. Description

The rotor is certainly the most widely used VTOL device, because of its hovering efficiency and its low downwash. A rotor produces a typical thrust augmentation of 15 as compared with 3 for a good lift fan.

Conventional rotors are gear-driven from a reciprocating or turbine powerplant. As discussed earlier, another means of rotor propulsion is the jet-driven rotor.

Conventional rotors use collective and cyclic blade pitch control to control the magnitude and direction of the rotor thrust. A fixed-pitch rotor is possible if rotor forces are controlled by actuation of a jet flap or by the use of circulation control.

b. Examples

Conventional rotor systems are quite familiar and will not be discussed here. A summary of conventional and advanced rotor designs can be found in Ref. 15.

c. Development

Conventional rotor systems have been under constant improvement for more than four decades. Advanced concepts such as the advancing blade concept, the circulation control rotor, and the jet-flap rotor have been or are being examined as well.

LIFT-ENGINE DEVELOPMENT TRENDS	RB162	ADVANCED LIFT FAN
By-pass ratio	0	12
Fuel C_s, $K_F/hr/K_T$	1.12	0.41
Thrust/Weight, T/W	16	17
Thrust/(Volume)$^{2/3}$, Kg/m^2	3 400	2 500
Nozzle velocity V_j, m/s { Hot	610	260
Nozzle velocity V_j, m/s { Cold	—	180
Exhaust temp., T°C	800	110
Noise at 500 ft, PNdb (2 pods = 12 lift-engs.)	135	98

Figure 38.
Lift engine and lift fan characteristics. (Ref. 1)

The development of an advanced rotor concept such as those mentioned would certainly require a major undertaking at a considerable cost in time and money.

d. Advantages and Disadvantages

The conventional rotor has the obvious advantage of being a highly-refined system, with an inherent hovering efficiency.

The footprint characteristics of a rotor are far less severe than even those of the lift fan. With a low downwash velocity and no temperature increase, the rotorcraft is capable of operating in virtually any environment, while lift fans and lift jets are limited in their operating terrain.

The conventional rotor does not lend itself to application to aircraft as an easy means of providing VTOL capability. The bulk and weight of the rotor and its associated controls and transmission systems require a dedicated design process for its incorporation into an aircraft. In vertical flight, the aircraft is burdened with the additional area of the rotor disc; and in forward flight, with the speed restrictions inherent in a rotor design, unless a compound, stopped, or stowed rotor configuration is used.

4. Ejectors

a. Description

An ejector uses a central jet to entrain ambient air whose momentum provides a thrust augmentation of the primary jet. A simple ejector is shown in Figure 39. A core flow is ejected, which entrains a secondary flow through the diffuser. The increased momentum due to the secondary flow provides the thrust augmentation. Therefore, the greater the entrainment the greater the augmentation.

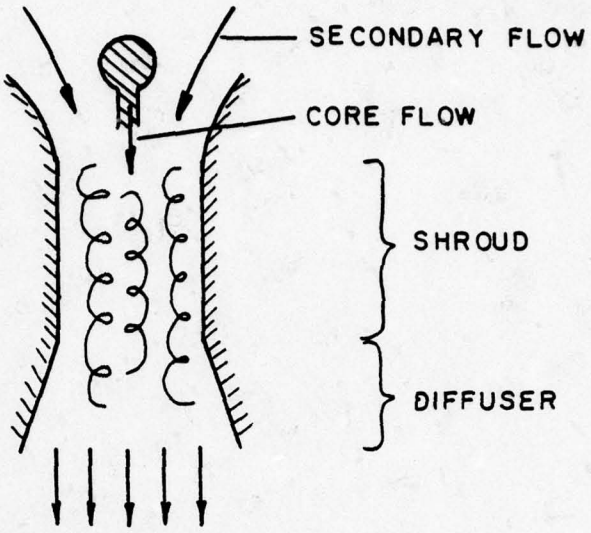

Figure 39.
Simple ejector schematic.

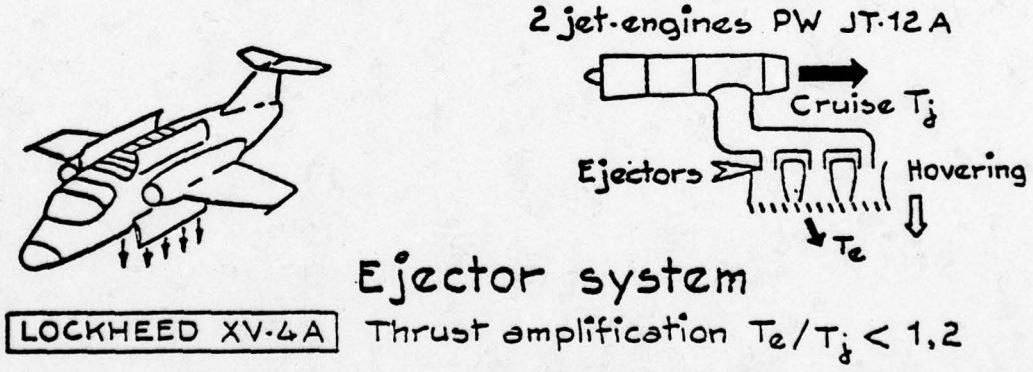

Figure 40.
Lockheed XV-4A ejector system. (Ref. 1)

The degree of entrainment is directly proportional to the amount of mixing of the primary and secondary flows, and to the length of the diffuser. A design goal of the ejector is therefore to have fully mixed flow at the diffuser exit.

The characteristic parameter of the ejector is the thrust augmentation ratio, Φ , which is defined as the thrust produced by the ejector divided by the thrust which would be produced by an isentropic expansion of the same mass flow to ambient conditions. Analytically, the augmentation ratio is given by

$$\Phi = \frac{T}{(\rho V_N) V_N'}$$

where T is the thrust produced by the ejector, ρ is the density, V_N is the velocity of the nozzle with the shroud, and V_N' is the velocity of the nozzle without the shroud. The difference between V_N and V_N' is due to the different outlet pressures with and without the shroud.

Tests of ejectors suitable for installation in VTOL aircraft have been shown to be capable of augmentation ratios of 1.2 to 1.6.

b. Examples

An ejector system was used in the Lockheed XV-4A shown in Figure 40 which achieved an augmentation ratio of 1.2. The intakes and ejectors occupied a major portion of the fuselage.

A different type of system is used in the Rockwell XFV-12A, which incorporates the ejectors into the canard and wing structures as shown in Figure 41. Jet exhaust is ducted to the central panel where it is ejected through a nozzle and used as the primary flow. The diffuser is formed by two panels which, by their movement, can modulate the thrust produced for control purposes. All three panels move in a coordinated manner during transition, so that in forward flight the panels are flush with the wing surfaces.

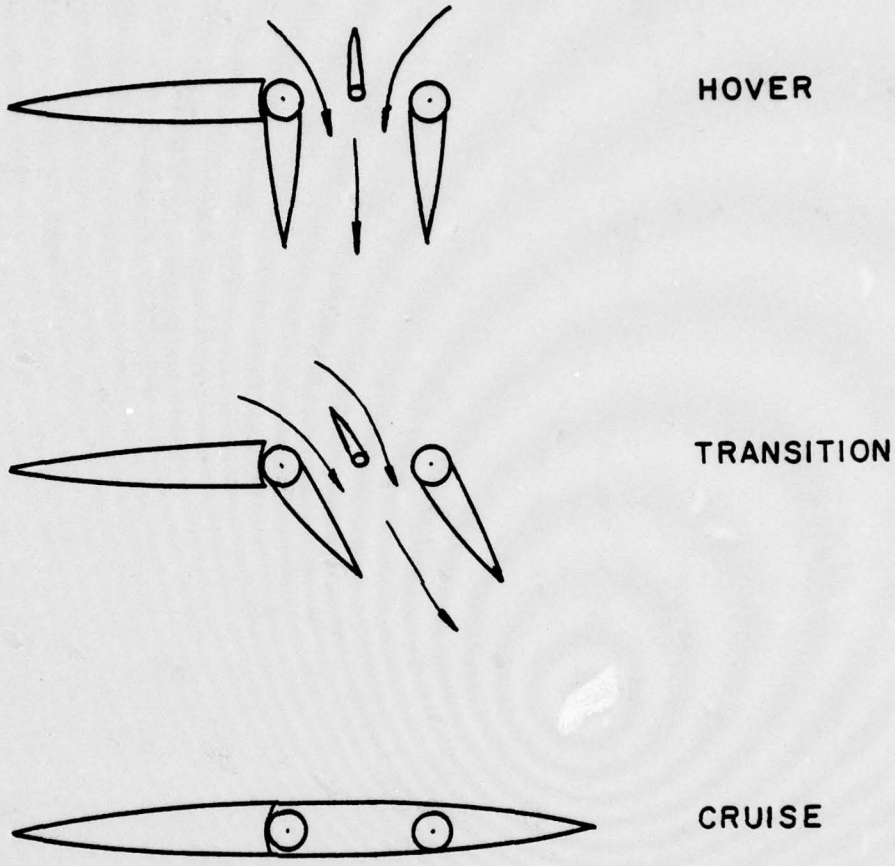

Figure 41.
Ejector design of the XFV-12A.

c. Development

Very little practical experience has been obtained in the use of ejectors in aircraft. Ejector design is essentially an empirical process, since theoretical modeling methods are not available for all but the simplest examples. During transition flight, the flow field of an ejector is a complicated three-dimensional flow which is impossible to model as of yet.

Aircraft ejectors are necessarily limited in the length of the diffuser, and therefore must emphasize mixing to enhance entrainment of a maximum of secondary flow. Various techniques have been proposed to increase mixing, such as hypermixing nozzles, swirling, acoustic stimulation, and forced oscillation. A major area of ejector development is the investigation of these techniques to increase entrainment. Thus, the design of ejectors is not well-developed and is a very time-consuming process.

d. Advantages and Disadvantages

The principal advantage of the ejector system is its relative simplicity. In an ejector system there are few moving parts and little weight involved. It appears to be a rather elegant means of providing thrust augmentation. However, the incorporation of an ejector system into an aircraft requires extensive design work. Ducting is required for the primary flow from the turbine, and inlets are required for the secondary flow. If the ejector system is located in the fuselage, as in the XV-4A, it will occupy a significant volume. If incorporated in the wing, as in the XFV-12A, extensive ducting is required, with its attendant losses.

The ejector system has footprint characteristics similar to those of the lift fan, since the hot exhaust core flow is mixed with ambient secondary air. In this regard the ejector is preferable to the lift jet.

It should be remembered that the ejector can produce a thrust augmentation of 1.6 at best, compared with 3 for a lift fan and 15 for a rotor. In this regard, the ejector may not seem efficient. However, the ejector does not require a separate powerplant, as do many other systems, since it uses the powerplant exhaust as the core flow. Although the powerplant would thus be operating at near maximum conditions in a hover, it would probably be doing so in any other configuration also. Many of these configurations would use the thrust of the primary powerplant in a hover, plus an auxiliary system to provide additional lift.

The use of ducted exhaust from a main powerplant is also used in the XV-5A, in which the gases are used to power tip-driven lift fans, providing a thrust augmentation of 2.5.

Despite the relatively low augmentation ratio available with an ejector, its simplicity makes it a promising lift system for the future.

B. LIFT GENERATORS AS AUXILIARY LIFT DEVICES

1. Introduction

For this section, it was desired to investigate the use of a lift generator as an auxiliary lifting device for hover. It was desired to modify an existing conventional aircraft to a VTOL aircraft. The cruise engine was modified by a movable nozzle to allow operation as a lift/cruise engine, providing direct jet thrust for hover. The remaining thrust necessary for hover was to be provided by either a lift jet, lift fan, or a jet-flap rotor.

2. Assumptions

Assume a high-subsonic tactical aircraft with a thrust/weight ratio of 0.6. The aircraft has a gross weight of 25000 pounds and is powered by a turbofan engine with a military rating of 15000 pounds thrust. The engine has a specific fuel consumption of 0.63 lb/lbt/hr.

Assuming a VTOL version of such an aircraft, a 10% margin of thrust available is required for control and acceleration in a hover. Therefore the thrust required is 1.1 times the weight, or 27500 pounds.

If the same cruise engine is modified with a movable nozzle so that its thrust can be deflected downward in a hover, then assuming a 2% turning loss, the downward thrust will be 14700 pounds. The weight of the deflector is assumed here to be contained in the weight of the basic aircraft.

In order to hover, then, an additional thrust of (27500 - 14700) = 12800 pounds must be generated. In addition, the extra weight of the lift generator system, plus 10%, must be added to this. Therefore, the auxiliary lift generator must supply thrust to lift 12800 pounds plus its own weight times 1.1.

3. Computations

a. Lift Engines

Assume that the additional 12800 pounds of thrust comes from RB.162-81 lift jets, which produce a maximum of 6000 pounds thrust and weigh 375 pounds each. The RB.162 has a specific fuel consumption of 0.96 lb/lbt/hr.

It is assumed that three lift jets will be required, to be operated at less than maximum thrust. Therefore, the additional weight is (3 x 375) = 1125 pounds, and the additional thrust required is (1125 x 1.1) = 1238 pounds. The total thrust required is therefore (12800 + 1238) = 14038 pounds.

Assuming the cruise engine is operated at maximum thrust, its fuel flow is (15000 x 0.63) = 9450 lb/hr. The fuel flow of the lift engines is (14038 x 0.96) = 13476 lb/hr. The total fuel flow is therefore 22926 lb/hr.

b. Lift Fans

Assume the additional thrust is supplied by RB.202 lift fans, which produce 13000 pounds thrust and weigh 865 pounds each. The RB.202 has a specific fuel consumption of 0.45 lb/lbt/hr.

Therefore two fans will be required, for a total additional weight of 1730 pounds. The additional thrust required is (1730 x 1.1) = 1903 pounds. The total thrust required is therefore (12800 + 1903) = 14703 pounds.

The fuel flow of the lift fans is (14703 x 0.45) = 6616 lb/hr. Adding this to the cruise engine fuel flow of 9450 lb/hr, the total fuel flow is 16066 lb/hr.

c. Jet-Flap Rotor

Assume a jet-flap rotor is used to supply the additional thrust required. It will use a separate powerplant to supply the air flow necessary for the jet flap and for rotor propulsion. Envisioned is a configuration similar to that proposed by Kretz and described previously. However, to maintain continuity in this study, the cruise engine exhaust will be used as the primary lifting device.

For this lift generator, there are two main components, the rotor and the gas generator. The jet-flap rotor described by Kretz had a radius of 19.7 feet, a chord of 4 feet, and weighed 2425 pounds. By scaling down this rotor to a radius of 18 feet and a chord of 3 feet, a weight of 1773 pounds was obtained. It was desired to make the rotor as small as possible, yet remain practical. Using the jet-flap rotor computer program, it was found that rotor dimensions smaller than this required very high disc loadings and high air mass flow rates.

The selection of the gas generator was determined by the mass flow requirements of the rotor. For the range of mass flow rates considered, the GE1 turbojet was selected as the gas generator for the rotor alone. The GE1 operates at a pressure ratio of 11:1 and can supply an air mass flow of 77 lbm/sec and a thrust of 5000 pounds. It weighs 700 pounds and has a specific fuel consumption of 0.70 lb/lbt/hr.

The rotor and engine thus weigh a total of (1773 + 700) = 2473 pounds. The additional thrust required is (2473 x 1.1) = 2720 pounds. The total thrust required is therefore (12800 + 2720) = 15520 pounds.

The computer program was used to determine the mass flow requirements. For the specified rotor and the desired thrust, a mass flow rate of 43 lbm/sec is required. The computer program results are located in the program output section, and the mass flow calculations are shown in Appendix C.

Since a mass flow of 43 lbm/sec is required, the gas generator can be used in a derated condition. At 80% operation, the gas generator will produce about 4000 pounds of thrust, so that its fuel flow will be (4000 x 0.70) = 2800 lb/hr. Adding this to the cruise engine fuel flow of 9450 lb/hr, the total fuel flow is 12250 lb/hr.

4. Fuel Consumption Analysis

By knowing the fuel consumption of each of the three configurations, a comparison among them can be made. The fuel flows of each configuration are summarized in Figure 42, which is a graph of fuel used as a function of hover time. The slopes of the curves are indicative of the relative fuel flows of each configuration. As can be expected, the lift engine has the highest fuel flow while the rotor has the lowest. In fact, the fuel flow of the lift engines is greater than that of the lift/cruise engine, while the lift engines are delivering less thrust.

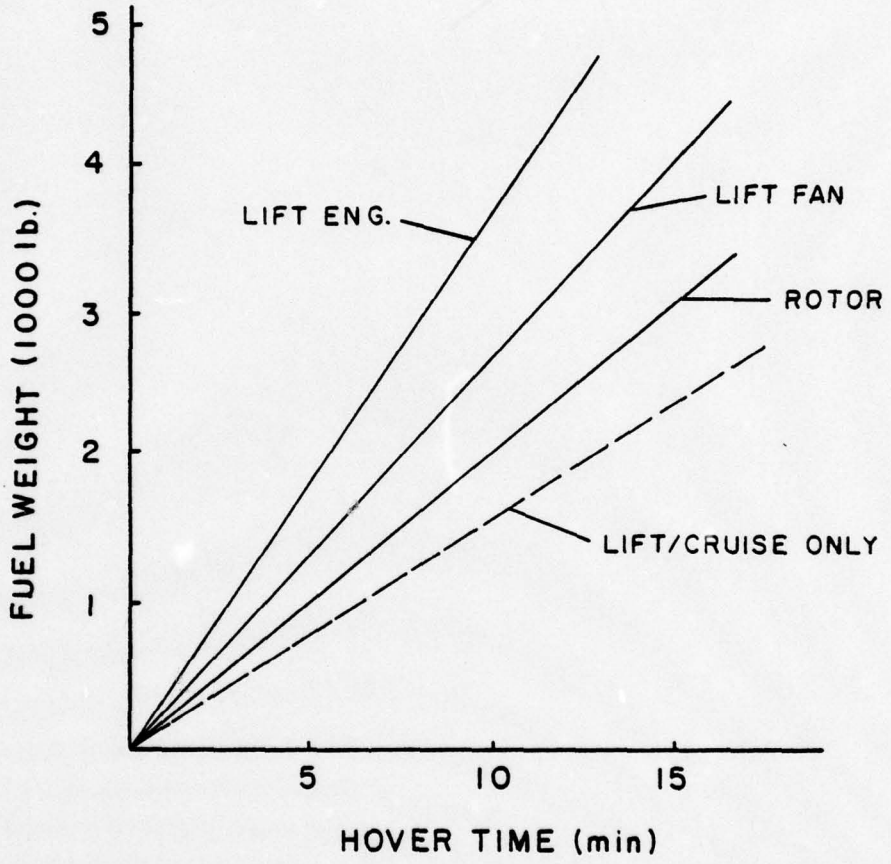

Figure 42.

Fuel consumption of aircraft with auxiliary lift devices.

5. Weight Analysis

More revealing than simply fuel consumption would be the study of total lift system weight, that is, the weight of the lift system components plus the weight of the required fuel. In Figure 43 is shown the relation of the auxiliary lift generator weight plus its required fuel as a function of hover time.

Figure 43 reveals the tremendous influence of hovering time on required fuel weight. The proposed mission hovering time is of great importance in determining the most efficient lift generator. For short hover times (less than 5 minutes), the lift engine is most efficient as a lifting system. The lift engine's low component weight makes it the best choice until at longer times its high fuel consumption degrades this advantage. The rotor, on the other hand, is most efficient for long hovering times (greater than 12 minutes), since its low fuel consumption is advantageous here despite its high component weight. The lift fan is most advantageous in the range of hover duration of from 5 to 12 minutes.

For a typical VTOL mission requirement of 1.5 hours of cruise and 8 minutes of hover, the engine and fuel weights are shown in Figure 44 as a percentage of gross weight. It is interesting to note the percentage of fuel required for an 8 minute hover. For the lift engine configuration, a greater percentage of fuel is required to hover for 8 minutes than is required to cruise for 1.5 hours. It should be noted that if specified hovering time were increased or decreased, the relative percentage of lift component plus hover fuel weight would change as shown in Figure 43.

For a specified 8 minutes of hovering time, which is typical of VTOL requirements, Figure 43 reveals that the difference between lift systems is small, based on weight considerations.

AD-A050 214 NAVAL POSTGRADUATE SCHOOL MONTEREY CALIF F/G 1/3
THE FEASIBILITY OF THE JET-FLAP ROTOR AS A LIFT GENERATOR FOR V--ETC(U)
DEC 77 J C BALL

UNCLASSIFIED NL

2 OF 2
AD
A050 214

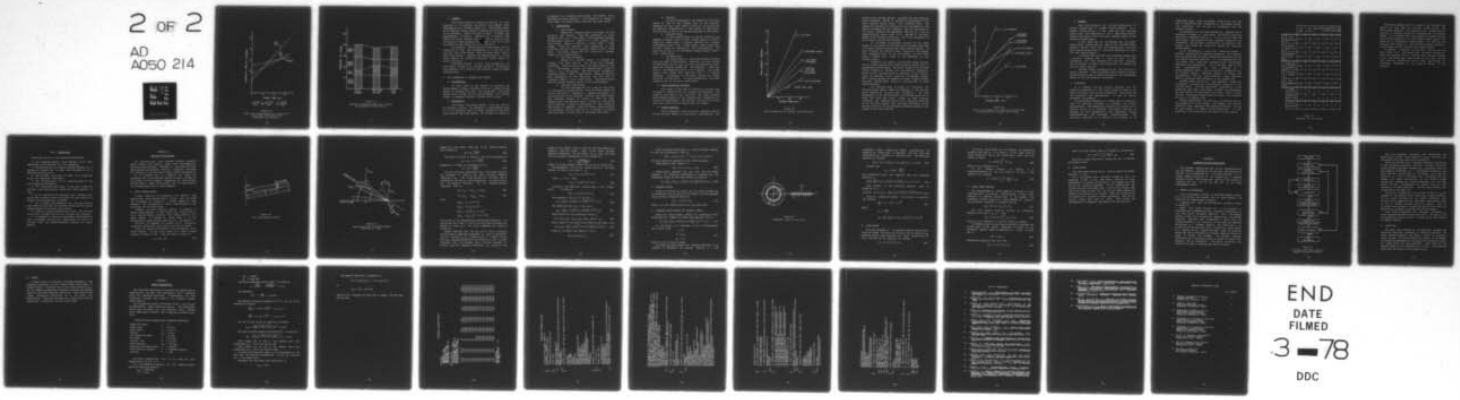

END
DATE
FILMED
3-78
DDC

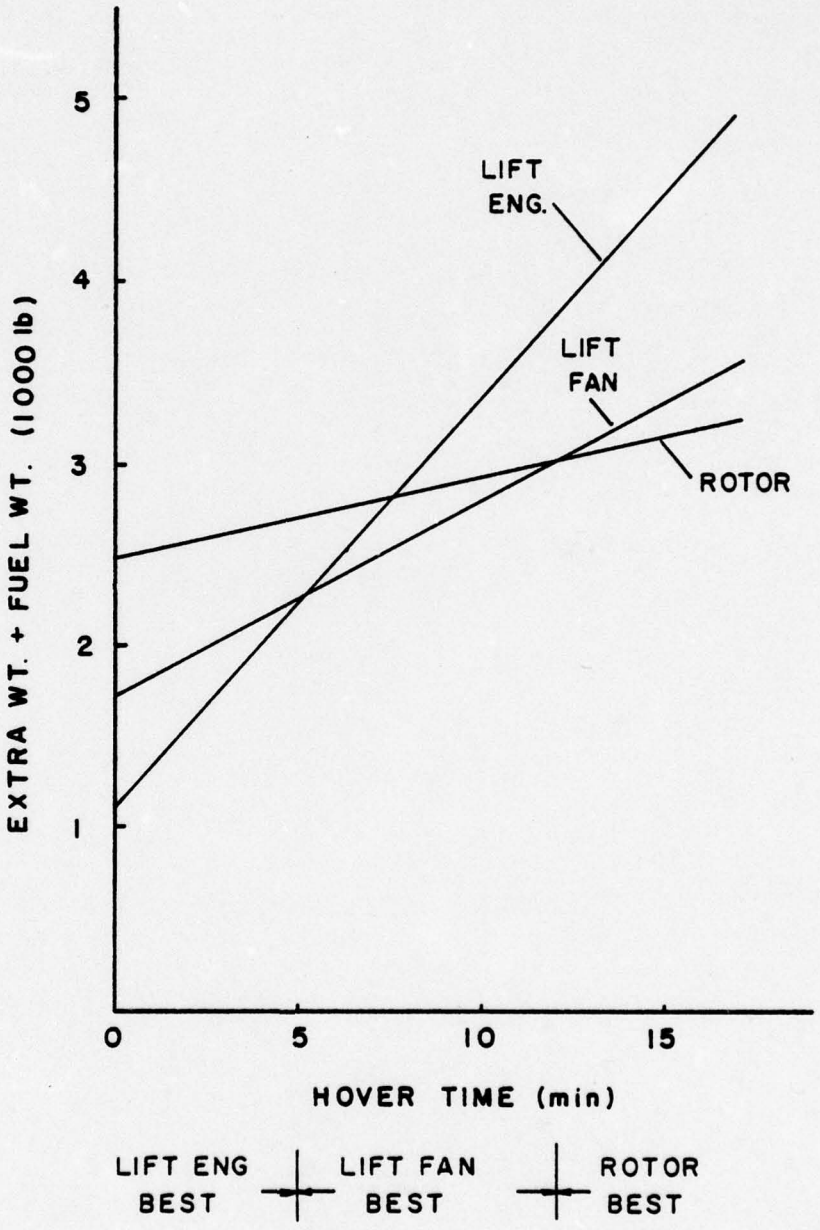

Figure 43.

Total lift system weight as a function of hover time for aircraft with auxiliary lift devices.

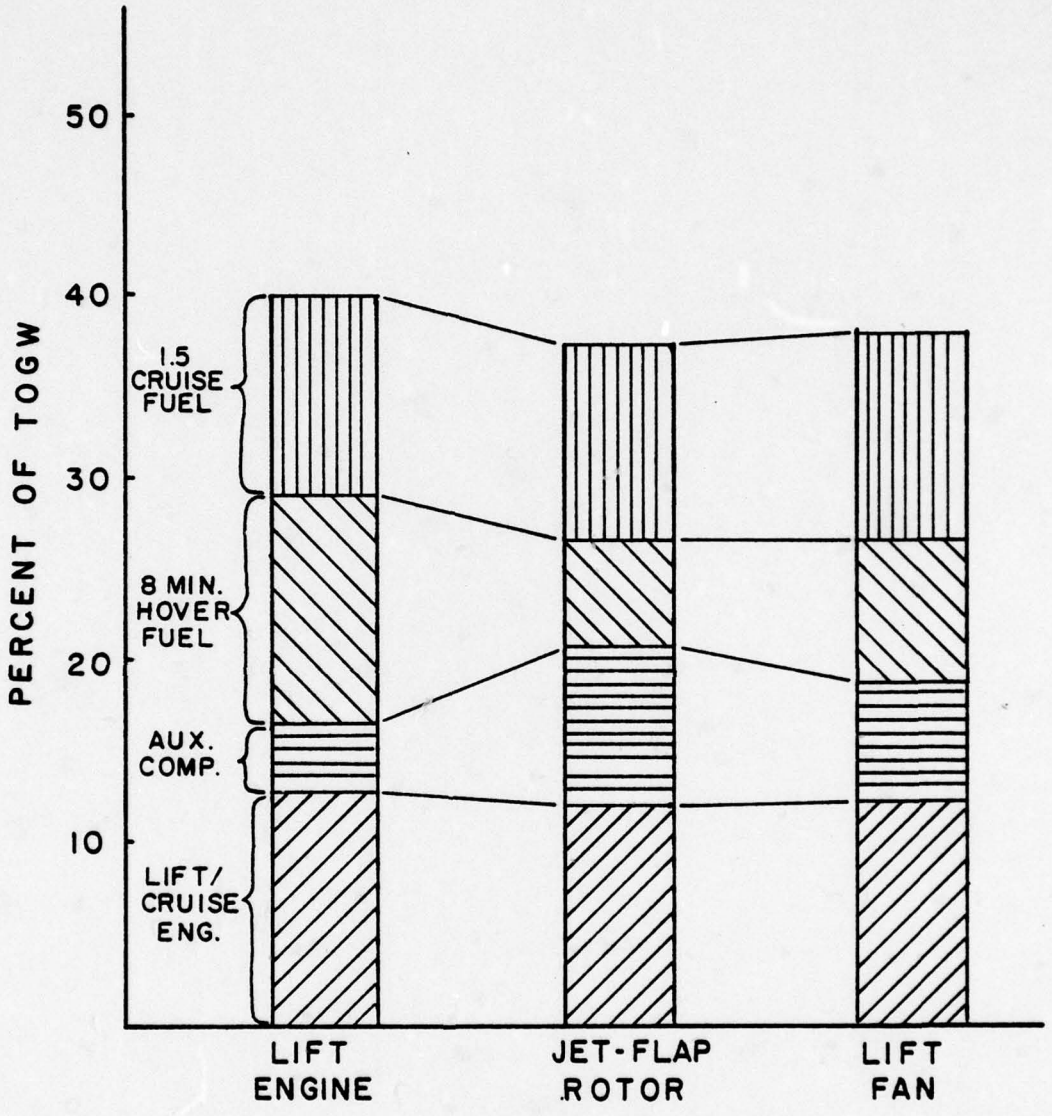

Figure 44.

Relative component weights for aircraft using auxiliary lift devices.

6. Summary

This study concerned itself with the use of a lift generator as an auxiliary lift device for hovering only, supplementing the vectored thrust of a lift/cruise engine. As an auxiliary lifting device it appears the jet-flap rotor is not advisable, unless the hover duration is longer than approximately 12 minutes. Moreover, for a tactical VTOL vehicle the hover duration will certainly be kept as short as possible to save required fuel. Thus a lift jet or lift fan seems the best choice for a lift generator.

The physical characteristics of the system must be considered as well. The incorporation of a lift jet or a lift fan into a VTOL design would not drastically alter a good cruise design. However, the incorporation of a rotor would require an extensive dedicated design effort to include the rotor.

Therefore, despite its high fuel consumption, the lift engine is seen to be the best choice as an auxiliary lift generator for a tactical VTOL aircraft, based on weight considerations.

C. LIFT GENERATORS AS PRIMARY LIFT DEVICES

1. Introduction

In this study it was desired to evaluate the effectiveness of using a jet-flap rotor as a primary lifting device, as compared with other lift generators. The cruise engine could be used as the main powerplant for hovering flight, or separate propulsion systems could be used.

2. Assumptions

An aircraft was chosen similar to the one used in the previous section. For hovering, a thrust/weight ratio of 1.1 was necessary, thus the thrust required for the 25000 pound aircraft was 27500 pounds. The aircraft is assumed to

be powered by a turbofan which weighs 3313 pounds. For a configuration which requires a lift generator in excess of this weight, the excess weight increases the gross weight.

3. Computations

a. Lift Engines

Assume the required thrust is provided by five RB.162-81 lift engines. This then prescribes an extra weight of (375 x 5) = 1875 pounds, which therefore requires an additional thrust of (1875 x 1.1) = 2063 pounds. The total thrust required is therefore (27500 + 2063) = 29563 pounds. Using the specific fuel consumption of 0.96 lb/lbt/hr, the fuel flow is therefore (29563 x 0.96) = 28380 lb/hr. The cruise engine does not provide any vertical thrust in this configuration.

b. Lift Fans (Integral)

Assume the required thrust is provided by integral lift fans such as the RB.202 fan described previously. Using two RB.202 fans, the extra weight is (865 x 2) = 1730 pounds, so that the required extra thrust is (1730 x 1.1) = 1903 pounds. The total thrust required is therefore (27500 + 1903) = 29403 pounds. Using the specific fuel consumption of 0.45 lb/lbt/hr, the fuel flow is therefore (29403 x 0.45) = 13231 lb/hr. The cruise engine does not provide vertical thrust in this configuration.

c. Lift Fans (Tip-Driven)

In this configuration, lift fans are used which are tip-driven by ducted exhaust from the cruise engine, as in the Ryan XV-5A. Therefore, a separate powerplant for vertical flight is not required. However, the cruise engine must therefore operate in a hover to drive the fans. Assuming that two lift fans total a weight of 1800 pounds and the ducting a weight of 500 pounds, an extra weight of 2300 pounds is required. Since the cruise engine provides the propulsion for the fans and it is assumed to operate near full power, the fuel flow is therefore 9900 lb/hr.

d. Ejectors

In this configuration, the exhaust of the cruise engine is used as the primary flow in the ejectors. Therefore the only extra weight is that of the ducting and the ejectors themselves for a total weight of 500 pounds. The fuel flow is due to the cruise engine and is 9900 lb/hr.

e. Vectored Thrust

In this configuration, an uprated version of the Pegasus 15 engine, rated at 24000 pounds thrust, is used to supply the 27500 pounds of thrust required, for a weight approximately that of the cruise engine. Thus, essentially no extra weight is required for this configuration. The fuel flow is that of the lift/cruise Pegasus engine (27500 x 0.60) = 16500 lb/hr.

f. Jet-Flap Rotor

The gross weight of the Kretz-proposed stowable rotor aircraft is 26455 pounds. Therefore, the rotor weight of 2425 pounds will be used for this configuration as well. Using the computer program for this aircraft, a mass flow rate of 100 lbm/sec was found to be required. The cruise engine could supply this mass flow even in a derated condition. If operated at two-thirds thrust, the engine fuel flow is 6600 lb/hr. In this configuration the extra weight is that of the rotor, 2425 pounds.

4. Fuel Consumption Analysis

The weight of fuel used in relation to hovering time is shown in Figure 45 for the various configurations. The slope of each curve is its fuel flow. The graph confirms the discussion earlier on the relative fuel consumptions of various lift generators. The jet-flap rotor has the lowest fuel flow, while the lift engines have the highest.

5. Weight Analysis

Fuel consumption alone is not an effective measure of the relative merits of a particular configuration. The

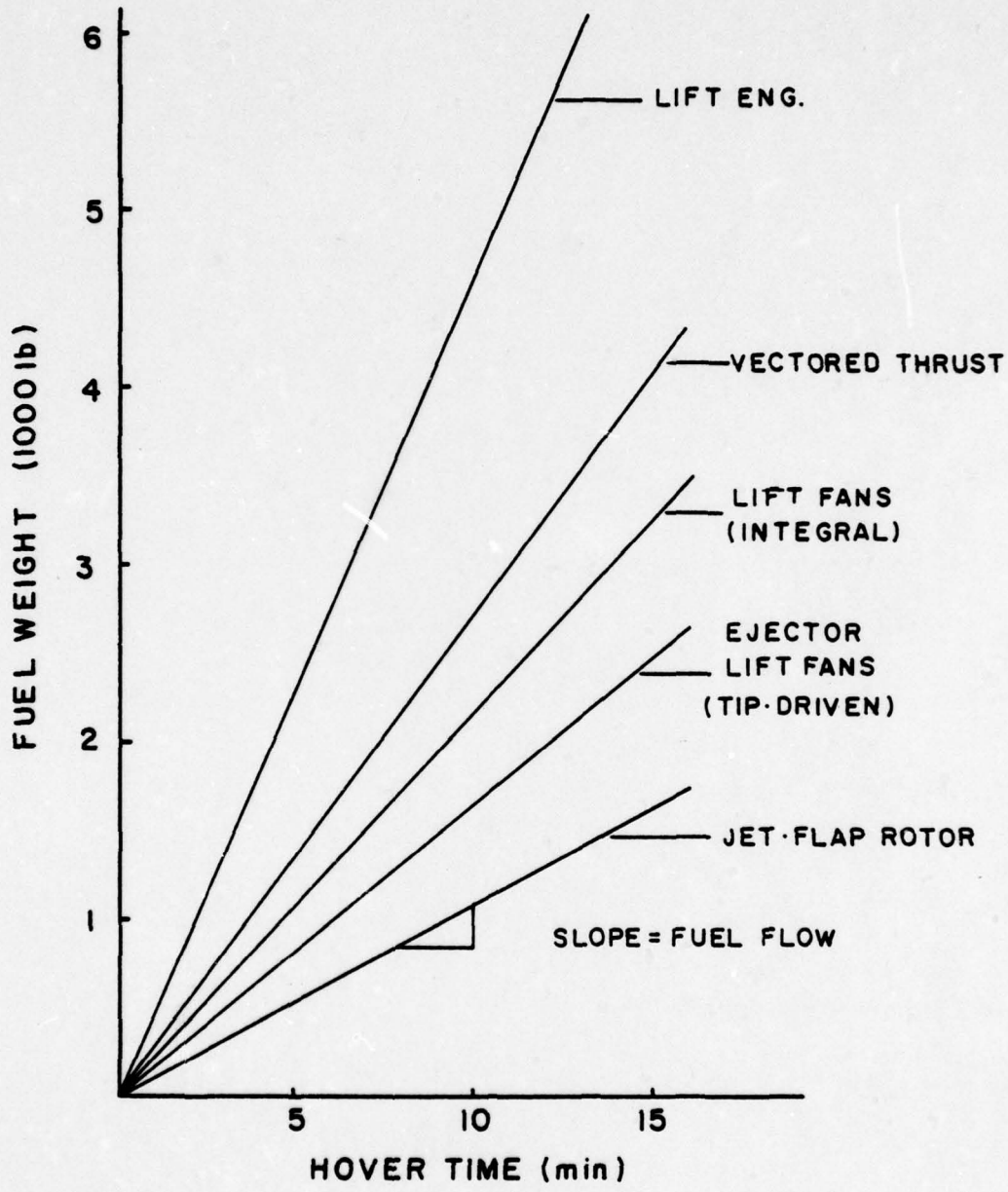

Figure 45.
Fuel consumption for primary lift generators.

weight of the lifting systems, including the fuel required, must be examined. Figure 46 graphs the relationship of the total lifting system weight with hovering time. The components necessary for hovering only are considered in the weight, including the fuel required. That is, the weight of the cruise engine is not considered even if it is used to supply hovering power, since it is included in the basic weight as the aircraft powerplant, and is not considered as extra weight required for hovering.

It is evident from Figure 46 that the low extra weight of the ejector and vectored thrust systems gives them the overall weight advantage over other lifting systems. In fact, although the vectored thrust system has the highest fuel consumption next to the lift engine, its low extra weight, besides fuel, gives it the advantage for low hovering times.

Except for the ejector and vectored thrust systems, all the lifting systems have extra weights, besides fuel, of approximately 2000 pounds. The extra weight of the ejector system consists of ducting and the ejectors themselves, while for the vectored thrust it consists of only nozzles, which are included in the weight of the Pegasus engine. Both of these systems can operate for about 8 minutes before the total system weight begins to approach that of other lifting systems.

For hovering times in excess of 15 minutes, the vectored thrust system loses its advantage to the jet-flap rotor because of its high fuel consumption. The fuel consumption of the ejector system and jet-flap rotor are so close that this has little effect on their relative standings. The dominant factor in the ejector's advantage is its low basic weight. The high fuel efficiency of the jet-flap rotor is not an overriding advantage because of the weight of the rotor required.

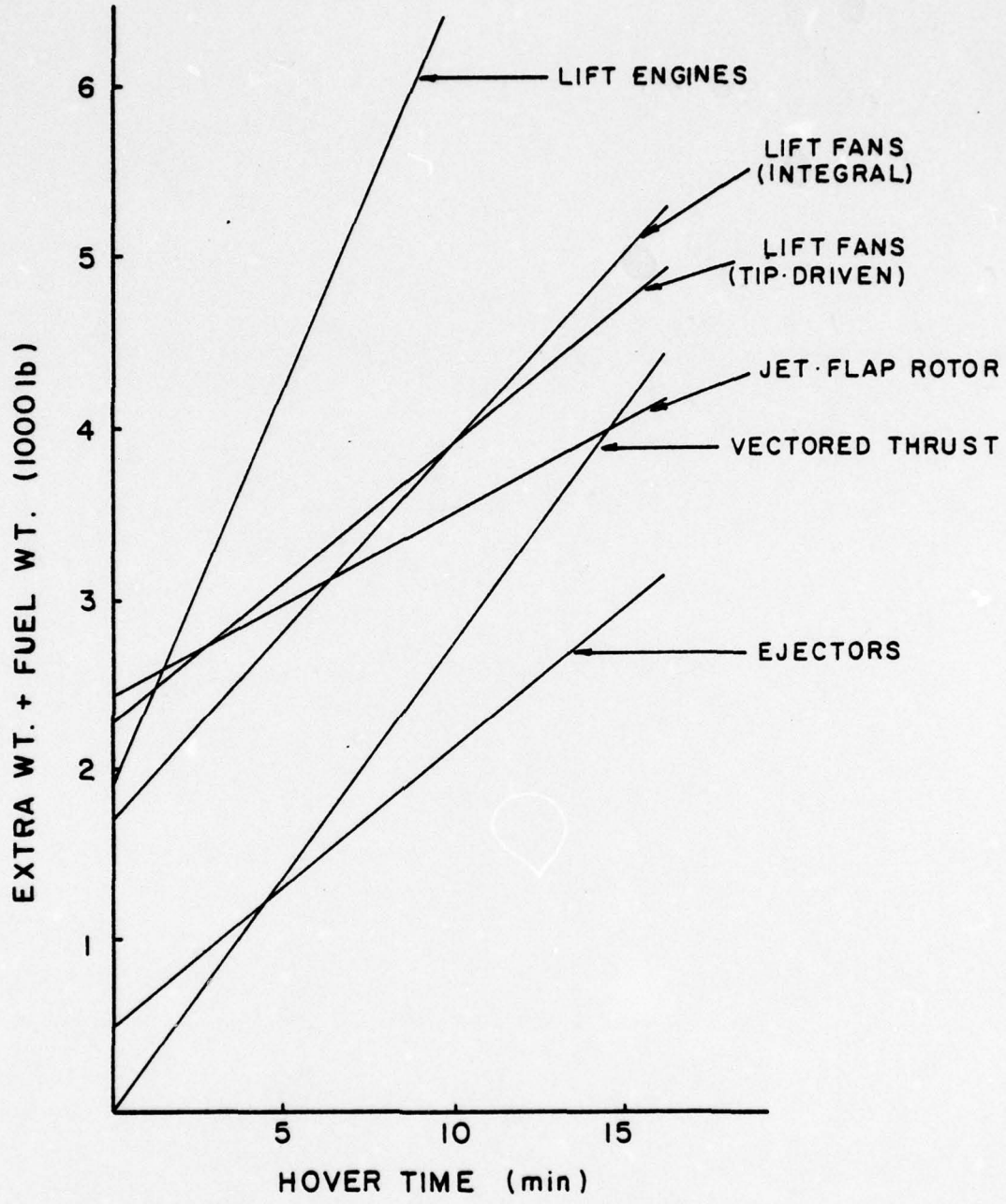

Figure 46.

Total system weight as a function of hover time for aircraft with primary lift devices.

6. Summary

This study examined the relative efficiencies of lifting systems used as primary lifting devices. As a primary lifting device, it was found that the jet-flap rotor's high fuel efficiency is not a significant factor, because the weight of the rotor has a negative impact on the system's overall weight.

It was found that the two systems with the lowest total system weights were the ejector and vectored thrust systems. Despite their high fuel consumptions, their low basic system weights were of overriding importance in their low total system weights.

A tactical VTOL aircraft will certainly require only a minimum hovering time in order to save on fuel consumption. For hover durations of less than 8 minutes, the two systems of lowest total weight are the ejector and vectored thrust systems.

However, weight considerations are only one area of design tradeoffs. Other sigrificant areas include footprint characteristics, ease of system integration, and development status of the lift generator technology.

D. DISCUSSION

It is evident from the previous sections that the potential usefulness of a lift system cannot be based on any single criterion, such as fuel consumption. Each system has its advantages and disadvantages, so that an overall assessment is necessary.

The theoretical potential of a system must be considered with its practical potential to determine its overall effectiveness. The theoretical potential of a system is its ability to act as an efficient lift system, and can be measured by such parameters as fuel efficiency, weight characteristics, and footprint characteristics. The practical potential of a system is its ability to be

effectively used, given the present state of the art, and can be measured by such parameters as development status, test experience, and its ease of integration into the aircraft system.

The potential of five lift systems was examined and is presented in Figure 47. Each system was rated in each area and given a numerical score of 1, 2, or 3, with 3 being the best rating. Each system was then assigned a score for its theoretical and practical potential as an effective lift system. The higher the score, the greater its potential effectiveness.

It is interesting to notice the difference between a system's theoretical and practical potential. For instance, the lift engine had the lowest theoretical potential yet had the highest practical potential. It is recognized that the lift engine has a high fuel consumption and high exhaust velocities and temperatures. Yet it has been used in many VTOL configurations, has been developed to a second-generation level, and can easily be integrated into an aircraft design. Therefore, taking all things into consideration, the lift engine presents a very practical means of providing VTOL capability at the present time.

Another system which has a high disparity between its theoretical potential and its practical potential is the jet-flap rotor. Its high theoretical potential as a lift system has been shown previously. However, its development has been limited to wind-tunnel rotor tests. Thus, a system of great theoretical effectiveness is simply not practical for use at the present time.

Mission requirements can also play an important part in the selection of a lift system. For example, if a mission called for VTOL operation from unimproved terrain, the use of lift engines is almost surely impractical. In this situation, the jet-flap rotor may become the best choice.

		LIFT ENG.	LIFT FANS	EJECTORS	VECTORED THRUST	JET-FLAP ROTORS
THEORETICAL POTENTIAL	FUEL EFFICIENCY	LOW 1	MED. 2	HIGH 3	MED. 2	HIGH 3
	WEIGHT EFFICIENCY	LOW 1	MED. 2	HIGH 3	HIGH 3	MED. 2
	FOOTPRINT CHAR.	POOR 1	MED. 2	MED. 2	POOR 1	GOOD 3
PRACTICAL POTENTIAL	EASE OF SYSTEM INTEGRATION	GOOD 3	MED. 2	MED. 2	GOOD 3	POOR 1
	DEVELOP. STATUS	GOOD 3	MED. 2	POOR 1	GOOD 3	POOR 1
	TEST EXPERIENCE	GOOD 3	GOOD 3	POOR 1	GOOD 3	POOR 1
	THEOR. POTENTIAL	3	6	8	6	8
	PRACTICAL POTENTIAL	9	7	4	9	3
	TOTAL POTENTIAL	12	13	12	15	11

Figure 47.
Potential of lift systems.

This study assumed that the weight of the vertical lift system was that used for vertical thrust alone. The lift/cruise engine was not included in the weight since it was used in forward flight and therefore was not "extra" weight. If a jet-flap rotor were stopped in flight and used as a lifting surface, as in the X-wing concept, then it too would not be included as "extra" weight. In this case the jet-flap rotor would be a very efficient system, serving as a lift system in both vertical and forward flight.

In summary, it appears the jet-flap rotor is not the best choice for a lift system when the hover duration is only a few minutes, as for a tactical VTOL aircraft, because of the relatively high basic weight of the rotor and the fact that the integration of the rotor would assume an overriding importance in the physical design of the aircraft.

VIII. CONCLUSIONS

This study has led to the following conclusions:

1. The specified mission hover duration is of great importance in the selection of a lift generator.

2. Through the use of a simple computer analysis, it is possible to predict the air mass flow requirements for a specified jet-flap rotor.

3. The jet-flap rotor has the lowest fuel consumption of all lift generators considered.

4. The jet-flap rotor is the least-developed of the lift generators considered.

5. The relatively high weight of the rotor makes the jet-flap rotor unattractive unless the hover duration is long.

6. As an auxiliary lift generator, the jet-flap rotor is the most efficient device only when the hover duration is greater than approximately 12 minutes.

7. As a primary lift generator, the jet-flap rotor is less effective than both the vectored thrust and the ejector systems because of its high rotor weight.

8. Based on weight considerations alone, the jet-flap rotor is not advisable for use in a tactical VTOL aircraft.

9. If emphasis is placed on operational characteristics such as downwash velocity and temperature, the use of a jet-flap rotor may become desirable despite its weight penalty.

APPENDIX A

JET-FLAP ROTOR THEORY

The jet-flap rotor hover analysis combines classical blade element and momentum theory with two-dimensional jet-flap characteristics. Reference 16 describes the basic blade element and momentum theories. Reference 7 describes the influence of the jet-flap on blade element aerodynamics.

It is intended here to summarize the theory and equations used in the analysis computer program. Included in the program are the standard assumptions of rigid blades, uniform inflow, small coning angles, and the applicability of two-dimensional data to blade elements.

A. BLADE ELEMENT THEORY

A rotor blade can be considered to be merely a high aspect ratio wing rotating about one end. Thus the blade can be assumed to consist of a finite number of blade elements, the integration of whose characteristics will yield that of the entire blade.

Consider the rotor blade of radius R is composed of narrow blade elements of width dr=Rdx, and having chord c, and a defined airfoil section. The radial position of a blade element is defined by r=Rx, where x is the dimensionless radial station given by r/R. See Figure 48.

The rotor is composed of b blades and is rotating at rotational velocity $\Omega = V_t/R$, where V_t is the tip speed.

Figure 49 depicts the positive sign conventions for a blade element. If the pitch angle of a blade element located at radius r is θ_r, then its angle of attack is

$$\alpha_r = \theta_r - \phi_r \qquad (24)$$

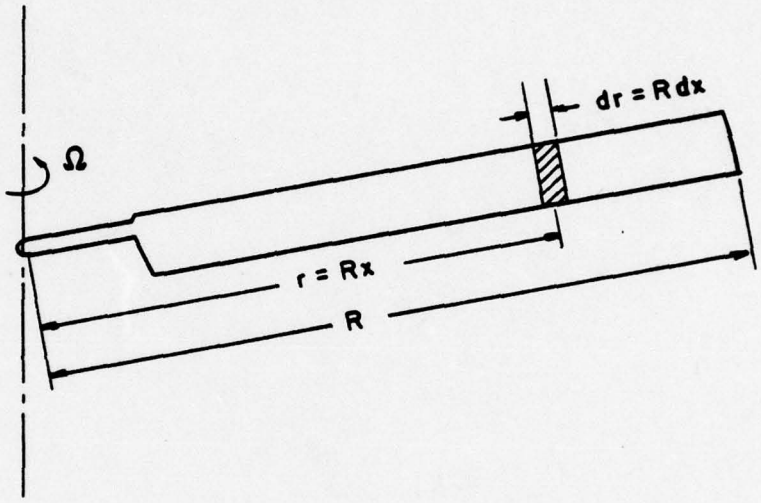

Figure 48.
The blade element concept.

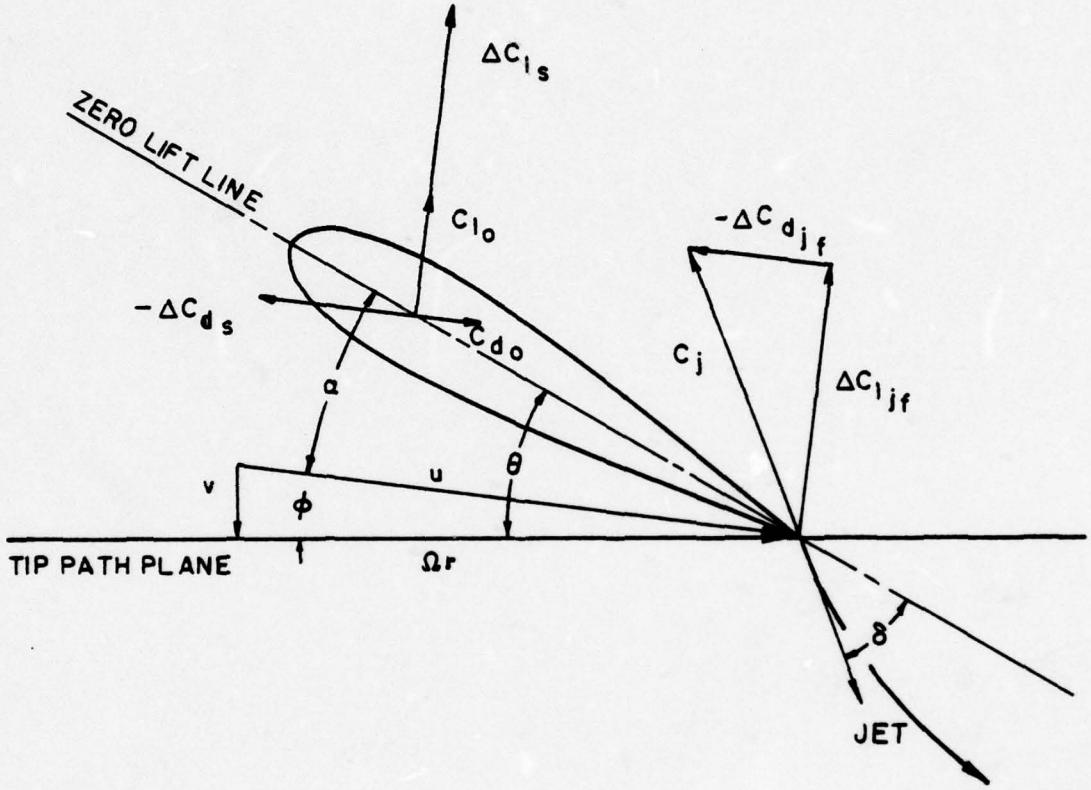

Figure 49.

Sign conventions for blade element (positive as shown).

where ϕ_r is the inflow angle due to the induced velocity and is given by

$$\phi_r = \tan^{-1}\left(\frac{v_r}{\Omega r}\right) \tag{25}$$

The angle of attack at station r can now be expressed as

$$\alpha_r = \theta_r - \tan^{-1}\left(\frac{v_r}{\Omega r}\right) \tag{26}$$

Assuming v_r is small in comparison to Ωr,

$$\alpha_r = \theta_r - \left(\frac{v_r}{\Omega r}\right) \tag{27}$$

The lift and drag coefficients for a jet-flapped airfoil are expressed in terms of the local jet-flap momentum coefficient c_{j_f}. The total section lift and drag can be expressed as the sum of three components: the basic force, the jet-reaction component, and the supercirculation component. That is,

$$c_\ell = c_{\ell_o} + \Delta c_{\ell_{j_f}} + \Delta c_{\ell_s} \tag{28}$$

$$c_d = c_{d_o} + \Delta c_{d_{j_f}} + \Delta c_{d_s} \tag{29}$$

where

$$\Delta c_{\ell_{j_f}} = c_{j_f} \sin(\alpha + \delta)$$

$$\Delta c_{d_{j_f}} = -c_{j_f} \cos(\alpha + \delta)$$

$$\Delta c_{\ell_s} = s_\ell \sqrt{c_{j_f}} \sin(\alpha + \delta)$$

$$\Delta c_{d_s} = -s_d c_{j_f} [1 - \cos(\alpha + \delta)]$$

and s_ℓ and s_d are experimentally-determined constants. For this study, as in Ref. 6, s_ℓ=3.0 and full thrust recovery is assumed so that s_d =1. The force components are shown in Figure 49.

Before equations (28) and (29) can be used, a spanwise distribution of momentum coefficient c_{j_f} must be specified. That is, specify c_{j_f} as a function of r. A study of the jet-flap momentum distribution was reported in Ref. 7, which concluded that the minimum total jet-flap momentum is reached when the momentum coefficient c_{j_f} varies as the

square of the radius, that is, when the jet-flap momentum is constant along the blade. Thus, if the total jet-flap momentum coefficient for all blades is C_{j_R} then the local jet-flap momentum coefficient at any station x is

$$C_{j_s} = \frac{2 C_{j_R}}{\Delta x_j \sigma_r \left(\frac{u_r}{V_t}\right)^2} \tag{30}$$

where Δx_j is the spanwise extent of the slot in terms of x.

The elementary lift of the airfoil alone on the blade element of width dr and chord c is

$$dL_{r_o} = C_{l_r} \tfrac{1}{2} \rho (u_r)^2 c_r \, dr \tag{31}$$

Since $u_r \approx \Omega r$, then

$$dL_{r_o} = C_{l_r} \tfrac{1}{2} \rho (\Omega r)^2 c_r \, dr \tag{32}$$

Similarly the elementary profile drag of the airfoil alone is given by

$$dD_{r_o} = C_d \tfrac{1}{2} \rho (\Omega r)^2 c_r \, dr \tag{33}$$

The elementary lift due to the jet is

$$dL_{r_j} = \left[\left(C_{j_s} + S_l \sqrt{C_{j_s}}\right) \sin(\alpha + \delta)\right] \tfrac{1}{2} \rho (\Omega r)^2 c_r \, dr \tag{34}$$

The elementary drag due to the jet is

$$dD_{r_j} = \left[\left(C_{j_s} + S_l \sqrt{C_{j_s}}\right) \cos(\alpha + \delta)\right] \tfrac{1}{2} \rho (\Omega r)^2 c_r \, dr \tag{35}$$

Using Figure 49, the elementary thrust is

$$dT_r = dL_{r_o} \cos\phi_r + dL_{r_j} \cos\phi_r + (dD_{r_j} - dD_{r_o}) \sin\phi_r \tag{36}$$

Using Figure 49 the second term above can be shown to be

$$dL_{r_j} \cos\phi_r = \left[\left(C_{j_s} + S_l \sqrt{C_{j_s}}\right) \sin(\theta + \delta)\right] \tfrac{1}{2} \rho (\Omega r)^2 c_r \, dr \tag{37}$$

Since ϕ_r is small, and $\cos\phi_r \approx 1$, then

$$dL_{r_o} \cos\phi_r \approx dL_{r_o} \tag{38}$$

Since the drag contribution to thrust is small compared to the lift contribution, that is,

$$(dD_{rj} - dD_{ro})\sin\Phi_r \ll (dL_{ro} + dL_{rj})\cos\Phi_r ,$$

the drag terms are neglected in the thrust analysis.

Thus equation (36) reduces to

$$dT_r = dL_{ro} + dL_{rj}\cos\Phi_r \tag{39}$$

Substituting equations (32) and (37) intc the above equation, the following expression is obtained fcr the elementary thrust on the blade element of width dr:

$$dT_r = \left\{c_{\ell_r} + \left[\left(c_{j_f} + s_\ell\sqrt{c_{j_f}}\right)\sin(\theta+\delta)\right]\right\}\tfrac{1}{2}\rho(\Omega r)^2 c_r\,dr \tag{40}$$

B. MOMENTUM THEORY

Using the notation in Figure 50, the thrust prcduced by an elementary ring of width dr and radius r can be expressed using classical momentum thecry as

$$dT_r = 4\pi\rho v_r^2\, r\,dr \tag{41}$$

where v_r is the induced velccity at the rotor disc.

C. COMBINED BLADE ELEMENT AND MOMENTUM THEORY

Using the blade element theory, the elementary thrust experienced by b number of blades from equation (40) is

$$dT_r = \left\{c_{\ell_r} + \left[\left(c_{j_f} + s_\ell\sqrt{c_{j_f}}\right)\sin(\theta+\delta)\right]\right\}\tfrac{1}{2}\rho(\Omega r)^2\, b\, c_r\,dr \tag{42}$$

If the radius r is expressed as the ncn-dimensicnal ratio x=r/R, then

$$\begin{aligned} r &= Rx \\ dr &= R\,dx \\ \Omega r &= V_t x \end{aligned} \tag{43}$$

where $V_t = \Omega R$ is the tip speed.

By combining blade elemert and momentum theories, it is possible to determine the induced velocity v_x , and

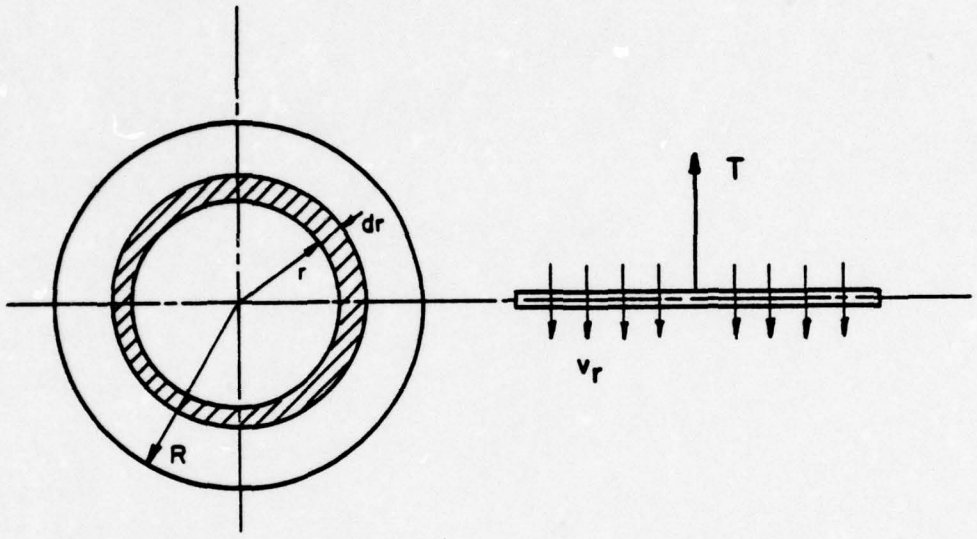

Figure 50.
Elementary ring of rotor disc.

ultimately thrust, torque, and power. Specifically, by equating the right sides of equations (41) and (42), and introducing the notation of equations (43), the following equation is obtained:

$$\left[c\ell_x + \left(c_{j\zeta} + s_\ell\sqrt{c_{j\zeta}}\right)\sin(\theta+\zeta)\right] V_t^2 \times bc_x = 8\pi v_x^2 R \qquad (44)$$

Knowing that

$$c\ell_x = a\left[\theta_x - \frac{v_x}{V_t x}\right]$$

and substituting this into equation (44), the resulting equation is

$$\left[a\left(\theta_x - \frac{v_x}{V_t x}\right) + \left(c_{j\zeta} + s_\ell\sqrt{c_{j\zeta}}\right)\sin(\theta+\zeta)\right] V_t^2 \times bc_x = 8\pi v_x^2 R \qquad (45)$$

This reduces to the following equation which is quadratic in v_x ,

$$(8\pi R)v_x^2 + (aV_t\, bc_x)v_x - \left[a\theta_x + \left(c_{j\zeta} + s_\ell\sqrt{c_{j\zeta}}\right)\sin(\theta+\zeta)\right] V_t^2 \times bc_x = 0 \qquad (46)$$

Using the quadratic formula, the solution to equation (46) becomes

$$\frac{v_x}{V_t} = N_1 - \left(N_1^2 + N_2\right)^{1/2} \qquad (47)$$

where

$$N_1 = \frac{a\sigma}{16}$$

$$N_2 = \frac{1}{8} \times \sigma\left[a\theta_x + \left(c_{j\zeta} + s_\ell\sqrt{c_{j\zeta}}\right)\sin(\theta+\zeta)\right]$$

D. ROTOR THRUST

With the knowledge of the induced velocity distribution along the blade, the thrust of the rotor can be found by the momentum theory using equation (41). After substituting Rx for r, and Rdx for dr, equation (41) becomes

$$dT = 4\pi\rho R^2 v_x^2 \times dx \qquad (48)$$

The total rotor thrust can be obtained by integrating equation (48) from x_i to x_o where x_i is the inner limit of blade integration and x_o the outer limit. Thus the total thrust is given

$$T = 4\pi\rho R^2 \int_{x_i}^{x_o} v_x^2 x\, dx \tag{49}$$

where v_x is a function of x.

If the induced velocity at station x is nondimensionalized by the tip speed as (v_x / V_t), then equation (49) becomes

$$T = 4\pi\rho R^2 V_t^2 \int_{x_i}^{x_o} \left(\frac{v_x}{V_t}\right)^2 x\, dx \tag{50}$$

E. ROTOR POWER REQUIRED

The determination of power required is similar to that described above for thrust. Profile power is that power required to overcome profile drag of the blades. The elementary profile power of b blade elements at station x can be derived similarly to equation (48) as

$$dP_\rho = \tfrac{1}{2}\rho b c R c_{d_o} V_t^3 x^3\, dx \tag{51}$$

The total profile power is obtained by integrating equation (51) from x_i to x_o. Thus

$$P_\rho = \tfrac{1}{2} b c R \rho V_t^3 \int_{x_i}^{x_o} c_{d_o} x^3\, dx \tag{52}$$

where c_{d_o} is a function of x and the chord is constant.

The induced power is that power required to overcome the induced drag of the blades. Referring to Figure 50, the elementary induced power corresponding to a ring of width Rdx is

$$dP_i = dT\, v_x \tag{53}$$

Substituting equation (48) into (53),

$$dP_i = 4\pi R^2 \rho v_x^3 x\, dx \tag{54}$$

Thus the total induced power is obtained by integrating:

$$P_i = 4\pi R^2 \rho V_t^3 \int_{\lambda_i}^{\lambda_0} \left(\frac{\bar{v}_R}{V_t}\right)^3 x\, dx \qquad (55)$$

The total power required is merely the sum of induced and profile power.

F. ROTOR TORQUE

The rotor shaft torque can be found by using the simple relation $Q = P/\Omega$.

For a jet-driven rotor the shaft torque is zero. As described in Ref. 7, the shaft torque consists of three components: the airfoil contribution, the pumping work, and the tip-jet reaction component. If the pumping work and tip-jet reaction are lumped into a net tip-jet torque, then since the torque is zero, the net tip-jet torque equals the airfoil contribution to the torque. Since the torque due to the airfoil can be found as shown previously, then the net tip-jet torque will also be known. This allows the determination of momentum requirements for the tip-jets.

APPENDIX B

COMPUTER PROGRAM DESCRIPTION

The computer program was used in the determination of the jet momentum required by the jet flap and tip-jets for various rotor configurations. Following Appendix C is a sample computer printout of the results and a complete program listing. The program was written in the Fortran IV language and was run on the IBM 360 at the Naval Postgraduate School.

A. METHOD OF COMPUTATION

Since the program is based on the blade element theory, the rotor radius was divided into 18 blade elements (19 stations) for computational purposes.

A general flow chart for the computer program is shown in Figure 51.

First, each blade station had to be analyzed to determine the corresponding blade element's contribution to the total thrust and power required. For a jet-flapped airfoil, there is no closed-form solution for the induced velocity. Equation (46) in Appendix A shows that the induced velocity v_x is a function of the local jet momentum coefficient c_{j_f}. However, Equation (30) shows that c_{j_f} is a function of the resultant local velocity u_x, which itself is a function of the induced velocity. Thus an iterative method was used to determine the induced velocity wherein an angle of attack was assumed, the induced velocity calculated, and a calculated angle of attack was found using Equation (26) in Appendix A. The method of halving the interval was used to converge the angle of attack.

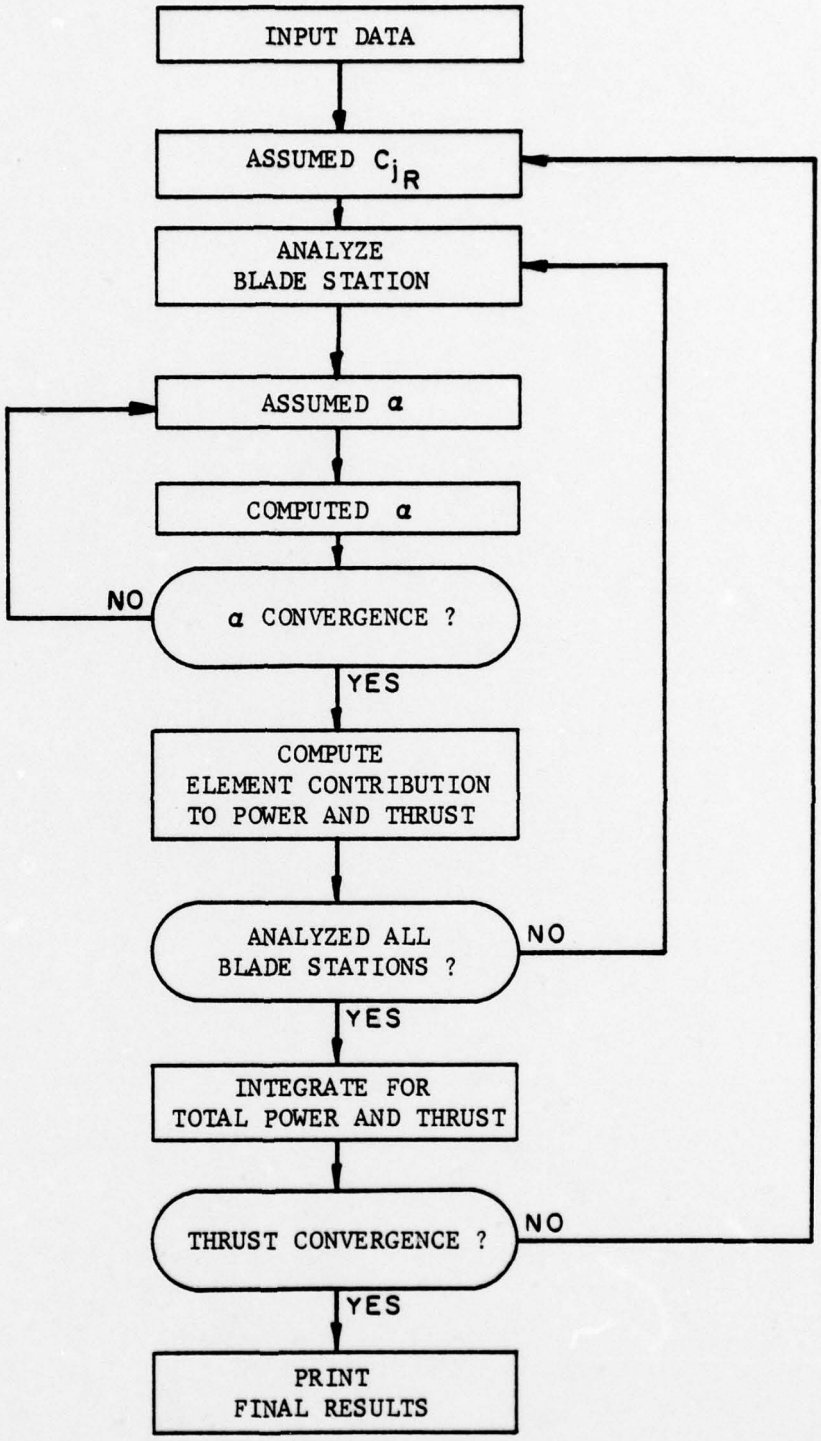

Figure 51.

Jet-flap rotor hover analysis computer program flowchart.

Once the sectional properties were calculated, the contribution of each blade element to thrust and power was calculated using the equations in Appendix A.

After all stations were analyzed, numerical integration of the sectional properties was used to obtain the total thrust produced and power required for a particular value of jet momentum coefficient C_{j_R} . Trapezoidal integration was used over the working span of the blade; i.e. from the cutout at x = .10R to the blade tip. To account for tip losses, the thrust contribution of the outboard blade element was reduced 40%, which corresponds to a tip loss factor of 0.98. Consequently the induced drag was also reduced in the same proportion. Profile drag, however, was integrated to the blade tip.

The thrust produced for the current value of C_{j_R} was compared to the desired thrust, which was an input constant. If the thrust produced was not within tolerance, then another entire computation was performed using another value of C_{j_R} to produce another value of thrust. Thus an iteration loop was used to obtain the value of the total jet momentum C_{j_R} required to produce the desired thrust.

Once thrust convergence was obtained, the values of power required and shaft torque were found. In order to use the performance charts of Ref. 7 a value of C_Q^* was obtained as defined therein.

B. INPUT DATA

The input data consists of the essential geometry and operating conditions necessary to define the problem. The blade geometry includes the radius, chord, and geometric twist, as well as the jet-flap slot location on the blade. The operating parameters of tip speed, jet deflection angle, and blade pitch are also specified. Also input is the desired thrust to be produced by the rotor. The essential input data is listed on the program output.

C. OUTPUT

A sample output is contained following Appendix C. The essential properties at each blade station are listed in tabular format. Following this is the final value of C_{JR}, the jet momentum coefficient required to produce the desired thrust at the given operating conditions. Also given is the torque coefficient calculated as if the rotor was shaft-driven. This then specifies the torque which must be produced by tip-jets for the jet-driven rotor.

APPENDIX C

SAMPLE CALCULATIONS

The following calculations illustrate the method used in computing the air mass flow requirements for a specified rotor and operating conditions. Specifically, the case illustrated follows that shown in the computer program output section.

The calculations follow the method of Ref. 7 and utilize the performance charts contained therein. The performance charts used are based on a gas generator with a turbine inlet temperature of 2500°R and a compressor pressure ratio of 16.

SPECIFIED BLADE GEOMETRY AND OPERATING CONDITIONS

Number of blades	b	= 2
Blade chord	c	= 3.0 ft
Rotor radius	R	= 18.0 ft
Washout	θ_t	= 8 deg
Jet deflection angle	δ	= 50 deg
Tip speed	V	= 750 fps
Pitch at .75R	θ_o	= 7.5 deg
Sonic velocity	a_∞	= 1116 fps
Sectional lift curve slope	a	= 5.73/rad
Free stream air density	ρ	= .0023769 slugs/ft
Solidity	σ	= .106

The blade extends from r =0.1 to 1.0 while the slot extends from r =0.5 to 1.0.

At a jet deflection angle of 50°, the computer output gives the following results:

C_{j_R} = .C0070763

C_T = .0114

$C_Q^* = .091537$

$T = 15520$ lbs

The design parameter used in Ref. 7 is found as

$$K = \sqrt{\frac{2\sigma}{C_T}} = \sqrt{\frac{2(.106)}{.0114}} = 4.312$$

The parameter

$$C_{j_f}^* = \frac{C_{j_f}}{C_T} = 0.06207$$

The geometric ducting parameters $A'/\pi R^2$ and D_h/R are computed as follows:

$$\frac{A'}{\pi R^2} = 0.0946 \left(\frac{\sigma^2}{b}\right) = 5.315 \times 10^{-4}$$

$$\frac{D_h}{R} = 0.300 \left(\frac{\sigma}{b}\right) = 1.590 \times 10^{-2}$$

The net tip-jet torque is computed as follows:

$$C_{Q_t} = 2\left(\frac{v_t}{a_\infty}\right)^2 \left(\frac{\pi R^2}{A'}\right)\left(\frac{\sigma}{K^2}\right) C_Q^* = 0.8869$$

The mean jet-flap momentum coefficient $\overline{C_j}$ is given as

$$\overline{C_j} = \frac{4}{(B - x_i)} \left(\frac{\pi R^2}{4}\right)\left(\frac{\sigma}{K^2}\right)\left(\frac{v_t}{a_\infty}\right)^2 C_{j_f}^* = 2.406$$

From Figure 37b of Ref. 7, the exhaust mass flow coefficient $C_{M_G} = 0.47$ for the tip jet.

From Figure 51b of Ref. 7, the exhaust mass flow coefficient $C_{M_G} = 0.47$ for the jet flap.

It should be noted that there is no significance to the fact that the mass flow coefficients for the jet flap and tip jet are equal here.

Therefore the total mass flow coefficient is

$$C_{M_G} = 0.94$$

The exhaust mass flow is computed as

$$M_G = C_{M_G} \rho a_\infty A' = 1.349 \text{ slugs/sec.}$$

or

$$M_G = 43.4 \text{ lbm/sec}$$

which is the required air mass flow tc supply the jet flap and tip jet.

COMPUTER PROGRAM OUTPUT

BLADE GEOMETRY

NO. BLADES = 2
CHORD (FT) = 3.000
RADIUS (FT) = 18.000
WASHOUT (DEG) = 0.000
INNER SLOT LIMIT = 0.500
OUTER SLOT LIMIT = 1.000
SPANWISE EXTENT OF SLOT = 0.500
BLADE INNER LIMIT = 0.100

OPERATING CONDITIONS

DESIRED THRUST (LBS) = 15520.00
TIP VELOCITY (FPS) = 750.000
JET DEFLECTION ANGLE (DEG) = 90.000
PITCH AT .75R (DEG) = 7.500
SONIC VELOCITY (FPS) = 1116.000
LIFT CURVE SLOPE (1/RAD) = 5.730
AIR DENSITY (SLUGS/FT3) = 0.23769E-02

STATION	MACH NO.	CJX	VX/VT	ALPHA	CL	CD	TH(I)
0.100	0.068	0.0	0.01793	11.67257	1.16913	0.020712	0.16079E-05
0.150	0.102	0.0	0.02438	10.90337	1.09528	0.019157	0.44574E-05
0.200	0.136	0.0	0.02983	10.15134	1.02756	0.017827	0.88972E-05
0.250	0.170	0.0	0.03451	9.52355	0.96570	0.016673	0.14884E-04
0.300	0.203	0.0	0.03856	8.85188	0.90755	0.015660	0.22257E-04
0.350	0.237	0.0	0.04207	8.25084	0.85283	0.014764	0.30972E-04
0.400	0.271	0.0	0.04512	7.71653	0.80105	0.013968	0.40711E-04
0.450	0.304	0.0	0.04775	7.16608	0.75180	0.013256	0.51298E-04
0.500	0.340	0.10406	0.07976	4.93530	1.40209	-0.093493	0.15905E-03
0.550	0.374	0.08632	0.08091	4.47402	1.26952	-0.076157	0.18002E-03
0.600	0.407	0.07275	0.08185	4.02049	1.15351	-0.062948	0.20058E-03
0.650	0.440	0.06214	0.08258	3.57873	1.04999	-0.052661	0.22165E-03
0.700	0.474	0.05369	0.08311	3.14877	0.95643	-0.044458	0.24175E-03
0.750	0.507	0.04685	0.08343	2.73061	0.87106	-0.037911	0.26101E-03
0.800	0.541	0.04123	0.08354	2.32432	0.79130	-0.032522	0.27915E-03
0.850	0.574	0.03657	0.08344	1.92997	0.71634	-0.028053	0.29589E-03
0.900	0.607	0.03266	0.08313	1.54767	0.64510	-0.024302	0.31066E-03
0.950	0.641	0.02934	0.08260	1.17758	0.57667	-0.021118	0.32410E-03
1.000	0.674	0.02650	0.08186	0.81992	0.51018	-0.018385	0.20103E-03

CJR = 0.70763E-03
SOLIDITY = 0.106
DISK LOADING (LBS/SQFT) = 15.25
THRUST (LBS) = 15518.14
CT = 0.01140

```
C       JET-FLAP ROTOR HOVER ANALYSIS
C       J C BALL          12/77
C       NAVAL POSTGRADUATE SCHOOL
C
        DIMENSION TH(19),PP(19),PD(19)
C
C       INPUT DATA
C
        READ (5,50) NB,C,R,VT
 50     FORMAT (I10,3F20.8)
        READ (5,60) CJR,DELTAJ,THETAT,THETAO,ASONIC,CLA,RHO,XIN,XOUT,
       *TREQ,XINBLD
 60     FORMAT(4F20.8)
C
C       DEFINE CONSTANTS AND INITIAL ASSUMED VALUES OF CJR AND THRUST
C
        TOL=.001
        LIMIT=40
        TTOL=.0005
        CJR1=.0001
        TT1=1.0
        NPRINT=1
        PI=3.14159
        NN=NB
        SIGTOT=(FLOAT(NN)*C)/(PI*R)
        SLOTX=XOUT-XIN
        DELTAJ=DELTAJ/57.3
        THETAO=THETAO/57.3
        THETAT=THETAT/57.3
        DX=(XOUT-XINBLD)/18.0
        CTREQ=TREQ/(PI*R**2*RHO*VT**2)
        AKSQRD=2.0*SIGTOT/CTREQ
        CJR2=1.0
        TT2=100000.
C
C       PERFORM ITERATIONS NECESSARY TO CONVERGE CJR
C
 80     DO 500 M=1,30
C
C       PRINT INPUT DATA
C
        IF (NPRINT.NE.2) GO TO 90
        DELTAJ=DELTAJ*57.3
        THETAO=THETAO*57.3
        THETAT=THETAT*57.3
        WRITE (6,70) NB,C,R,THETAT,XIN,XOUT,SLOTX,XINBLD,TREQ,VT,
       *DELTAJ,THETAO,ASONIC,CLA,RHO
 70     FORMAT (/,1X,'BLADE GEOMETRY'//5X,'NO. BLADES =',I3/
```

```
     *5X,'CHORD (FT) =',F8.3/5X,'RADIUS (FT) =',F8.3/
     *5X,'WASHOUT (DEG) =',F8.3/5X,'INNER SLOT LIMIT =',F8.3/
     *5X,'OUTER SLOT LIMIT =',F8.3/5X,'SPANWISE EXTENT OF SLOT =',F8.3/
     *5X,'BLADE INNER LIMIT =',F8.3///1X,'OPERATING CONDITIONS'//
     *5X,'DESIRED THRUST (LBS) =',F10.2/5X,'TIP VELOCITY (FPS) =',F10.3/
     *5X,'JET DEFLECTION ANGLE (DEG) =',F10.3/
     *5X,'PITCH AT .75R (DEG) =',F8.3/5X,'SONIC VELCCITY (FPS) =',F10.3/
     *5X,'LIFT CURVE SLOPE (1/RAD) =',F8.3/
     *5X,'AIR DENSITY (SLUGS/FT3) =',E12.5)
      DELTAJ=DELTAJ/57.3
      THETAO=THETAO/57.3
      THETAT=THETAT/57.3
      WRITE (6,75)
 75   FORMAT (///6X,'STATION',7X,'MACH NC.',11X,'CJX',9X,'VX/VT',10X,
     *'ALPHA',13X,'CL ',12X,'CD ',10X,'TH(I)')
C
CC    PERFORM CALCULATICNS AT BLADE STATIONS
C
 90   DC 700 I=1,19
      II=I-1
      X=(FLOAT(II)*DX)+XINBLD
      THETAX=THETAO+THETAT*(0.75-X)
      KCUNT=0
C
CC    ASSUME ANGLE OF ATTACK AND CALCULATE RESULTANT ANGLE OF ATTACK
C
      ALPHAX=0.05
 10C  CCNTINUE
      IF (KOUNT.GT.LIMIT) GO TO 700
      KCUNT=KCUNT+1
      PHIX=THETAX-ALPHAX
      VXVT=TAN(PHIX)
      VX=VXVT*VT
      UX=SQRT(VX**2+(VT*X)**2)
      AMACH=UX/ASCNIC
      CLO=(5.73*ALPHAX)/(SQRT(1-AMACH**2))
      CDC=.008+.0C93*CLO**2
      UDIM=UX/VT
      CJX=2*CJR/(SLOTX*SIGTOT*UDIM**2)
      IF ((X+.0005).LT.XIN) CJX=0.0
      ANG1=ALPHAX+DELTAJ
      ANG2=THETAX+DELTAJ
      CL=CLO+CJX*SIN(ANG1)+3.0*SQRT(CJX)*SIN(ANG1)
      CD=CDO-CJX*COS(ANG1)-CJX*(1.0-COS(ANG1))
      AN1=(SIGTOT/16.0)*CLA
      AN2=(X*SIGTOT/8.0)*(CLA*THETAX+(CJX+3.0*SQRT(CJX))*SIN(ANG2))
      VXVT1=-AN1+SQRT(AN1**2+AN2)
      PHIX1=ATAN(VXVT1)
```

```
      ALPHA1=THETAX-PHIX1
C
C     CHECK CONVERGENCE OF ASSUMED AND CALCULATED ANGLE OF ATTACK
C
      FDIF=ABS(1-(ALPHAX/ALPHA1))
      IF (FDIF.LT.TOL) GO TO 300
C
C     IF NOT CONVERGED, ASSUME NEW ANGLE OF ATTACK AND RECALCULATE
C
      ALPHAX=(ALPHAX+ALPHA1)/2.0
      GO TO 100
  300 CONTINUE
C
C     IF CONVERGED, STORE ELEMENT CONTRIBUTION TO THRUST AND POWER
C
      IF ((I.EQ.1).OR.(I.EQ.19)) TH(I)=(VXVT1**2)*X*(DX/2.0)
      IF ((I.NE.1).OR.(I.NE.19)) TH(I)=(VXVT1**2)*X*DX
      IF (I.EQ.19) TH(I)=TH(I)*0.6
      IF ((I.EQ.1).OR.(I.EQ.19)) PD(I)=(VXVT1**3)*X*(DX/2.0)
      IF ((I.NE.1).OR.(I.NE.19)) PD(I)=(VXVT1**3)*X*DX
      IF (I.EQ.19) PD(I)=PD(I)*0.6
      IF ((I.EQ.1).OR.(I.EQ.19)) PP(I)=C*CDO*(X**3)*(DX/2.0)
      IF ((I.NE.1).OR.(I.NE.19)) PP(I)=C*CDO*(X**3)*DX
      ALPHA9=ALPHA1*57.3
      IF (NPRINT.NE.2) GO TO 700
C
C     IF FINAL RUN, PRINT BLADE STATION DATA
C
      WRITE (6,200) X,AMACH,CJX,VXVT1,ALPHA9,CL,CD,TH(I)
  200 FORMAT (/7X,F5.3,9X,F5.3,11X,F8.5,5X,F8.5,7X,F8.5,8X,F8.5,6X,
     *F9.6,4X,E12.5)
  700 CONTINUE
C
C     INTEGRATE OVER BLADE FOR TOTAL THRUST AND POWER
C
      THR=0.0
      PISUM=0.0
      PPSUM=0.0
      DO 800 I=1,19
      THR=THR+TH(I)
      PISUM=PISUM+PD(I)
      PPSUM=PPSUM+PP(I)
C
C     CALCULATE OUTPUT DATA
C
  800 CONTINUE
      TT=4.0*PI*R**2*RHO*VT**2*THR
      CT=TT/(PI*R**2*RHO*VT**2)
```

```
      DL=TT/(PI*R**2)
      PIND=4*PI*(R**2)*(VT**3)*RHO*PISUM
      PPRO=0.5*FLOAT(NN)*R*RHO*(VT**3)*FPSUM
      PTOT=PIND+PPRO
      OMEGA=VT/R
      Q=PTOT/OMEGA
      CQ=Q/(PI*(R**3)*RHO*(VT**2))
      CQSTR1=CQ*AKSQRD/(2*SIGTOT)
C
C     IF FINAL RUN, PRINT OUTPUT DATA
C
      IF (NPRINT.NE.2) GO TO 870
      WRITE (6,825) CJR
  825 FORMAT (//5X,'CJR =',E12.5)
      WRITE (6,830) SIGTOT
  830 FORMAT (5X,'SOLIDITY =',F8.3)
      WRITE (6,850) DL,TT,CT
  850 FORMAT  (5X,'DISK LOADING (LBS/SQFT) =',F10.2/
     *5X,'THRUST (LBS) =',F10.2/5X,'CT =',F10.5)
  860 FORMAT (5X,'CQSTAR =',F10.6)
C
C     CHECK THRUST CONVERGENCE WITHIN TOLERANCE
C
  870 TT3=TT
      CJR3=CJR
      IF (TT3.LE.TREQ) CJR1=CJR3
      IF (TT3.GE.TREQ) CJR2=CJR3
      TDIF=ABS(1-(TT3/TREQ))
      IF (NPRINT.EQ.2) GO TO 950
C
C     IF THRUST CONVERGED, MAKE FINAL RUN THROUGH PROGRAM FOR PRINT
C
      IF (TDIF.LE.TTOL) GO TO 900
C
C     IF THRUST NOT CONVERGED, ASSUME NEW CJR AND RESTART
C
      CJR=(CJR1+CJR2)/2.0
  500 CONTINUE
  900 NPRINT=2
      GO TO 80
  950 CONTINUE
      END
```

LIST OF REFERENCES

1. Poisson-Quinton, P., Introduction to V/STOL Aircraft Concepts and Categories, AGARDograph 126, May 1968, pp. 3-48.

2. Korbacher, G.K. and Sridhar, K., A Review of the Jet Flap, UTIA Review No. 14, University of Toronto, May 1960.

3. Dorand, R. and Boehler, G.D., "Application of the Jet-Flap Principle to Helicopters," Journal of the American Helicopter Society, v. 4, no. 3, July 1959, pp. 26-36.

4. Kretz, M., Fields of Application of Jet Flapped Rotors, AGARD-CP-121, February 1973.

5. Fiorini, V., "Study of a Jet Propelled Helicopter with Jet Flap," Journal of the American Helicopter Society, v. 6, no. 1, January 1961, pp. 34-41.

6. Evans, W.T. and McCloud, J.L. III, Analytical Investigation of a Helicopter Rotor Driven and Controlled by a Jet Flap, NASA TN D-3028, September 1965.

7. Gray, R.B. and Hubbartt, J.E., Rotor Jet Power Alternate Systems, Georgia Institute of Technology, GITAER 69-1, March 1969.

8. McCloud, J.L. III, Evans, W.T., and Biggers, J.C., Performance Characteristics of a Jet-Flap Rotor, NASA SP-116, 1966.

9. Fischer, C., Research and Development on Rotors with Tip Reaction Drive in Germany, AGARD-CP-121, February 1973.

10. Hirsch, H., The Hot Cycle Jet Helicopter, paper presented at the 14th Annual Forum of the American Helicopter Society, April 1958.

11. Morain, P.H.L., "Cold Jet Cycle Helicopters," Journal of the American Helicopter Society, v. 3, no. 4, October 1958, pp. 12-19.

12. Velkoff, H.R., "An Evaluation of the Jet Rotor Helicopter," Journal of the American Helicopter Society, v. 3, no. 4, October 1958.

13. Deckert, W.H. and McCloud, J.L. III, "Considerations of the Stopped Rotor V/STOL Concept," Journal of the American Helicopter Society, v. 13, no. 1, January 1968.

14. Carlson, R.M., Stopped/Folded Rotor Vehicles, Helicopter Developments, AGARD-CP-7, January 1966.

15. Reichert, G., Basic Dynamics of Rotors: Control and Stability of Rotary Wing Aircraft; Aerodynamics and Dynamics of Advanced Rotary-Wing Configurations, Helicopter Aerodynamics and Dynamics, AGARD-LS-63, March 1973.

16. Stepniewski, W.Z., Basic Aerodynamics and Performance of the Helicopter, Helicopter Aerodynamics and Dynamics, AGARD-LS-63, March 1973.

17. Yaggy, P.F., The Role of Aerodynamics and Dynamics in Military and Civilian Applications of Rotary Wing Aircraft, Helicopter Aerodynamics and Dynamics, AGARD-LS-63, March 1973.

18. von Gerichten, R.L., Formulating Military Requirements, V/STOL Propulsion Systems, AGARD-CP-135, January 1974.

19. Lotz, M. and Bartels, F., Problems of V/STOL Aircraft Connected With the Propulsion System as Experienced on the DO31 Experimental Transport Aircraft, V/STOL Propulsion Systems, AGARD-CP-135, January 1974.

20. Katzenberger, G.F., A Note on Helicopter Configurations for Increased Range, Speed and Endurance, Helicopter Developments, AGARD-CP-7, January 1966.

INITIAL DISTRIBUTION LIST

		No. Copies
1.	Defense Documentation Center Cameron Station Alexandria, Virginia 22314	2
2.	Library, Code 0142 Naval Postgraduate School Monterey, California 93940	2
3.	Department Chairman, Code 67 Department of Aeronautics Naval Postgraduate School Monterey, California 93940	1
4.	Professor M. F. Platzer, Code 67Pl Department of Aeronautics Naval Postgraduate School Monterey, California 93940	5
5.	Professor G. H. Lindsey, Code 67Li Department of Aeronautics Naval Postgraduate School Monterey, California 93940	5
6.	Dr. H. J. Mueller, Code AIR-310 Naval Air Systems Command Washington, D.C. 20361	1
7.	Mr. Ray Siewert, Code AIR-320 Naval Air Systems Command Washington, D.C. 20361	1
8.	LT John C. Ball, USN 885 Grissom Street San Diego, California 92154	1